Characterizing the Geochemical Reactions in an Overburden Waste Pile: Syncrude Mine Site, Fort McMurray, Alberta, Canada

A thesis submitted to the College of Graduate Studies and Research in partial fulfillment of the requirements for the Degree of Master of Science in the Department of Geological Sciences

University of Saskatchewan

Saskatoon

by

Susan N. Wall

January 2005

Permission to Use

In presenting this thesis in partial fulfillment of the requirements for a Postgraduate degree from the University of Saskatchewan, I agree that the Libraries of this University may make it freely available for inspection. I further agree that permission for copying of this thesis in any manner, in whole or in part, for scholarly purposes may be granted by the professor or professors who supervised my thesis work or, in their absence, by the Head of the Department or the Dean of the College in which my thesis work was done. It is understood that any copying or publication or use of this thesis or parts thereof for financial gain shall not be allowed without my written permission. It is also understood that due recognition shall be given to me and to the University of Saskatchewan in any scholarly use which may be made of any material in my thesis.

Requests for permission to copy or to make other use of material in this thesis in whole or part should be addressed to:

Head of the Department of Geological Sciences
University of Saskatchewan
114 Science Place
Saskatoon, Saskatchewan
Canada
S7N 5E2

Abstract

Potential environmental risks of constructing waste piles from sulphide-bearing saline-sodic overburden include acid-mine drainage and salinization of surface soils. Acid-mine drainage may result from the production of sulphuric acid during the oxidation of sulphide minerals. Acid production during the oxidation of sulphide minerals may also increase the concentrations of SO_4 (from sulphuric acid), Ca (from dissolution of carbonates), and Na (from cation exchange with saline-sodic overburden) in surface soils. To identify and quantify these potential environmental risks, *in situ* SO_4 and Ca production rates were calculated using two different methods. Sulphide mineral oxidation rates were calculated using simple one-dimensional analytical modelling (assuming diffusive gas transport) of in situ pore-gas O_2 concentrations. Ca loading from carbonate mineral dissolution (resulting in CO_2 production) was also calculated using the simple one-dimensional modelling of measured pore-gas CO_2 concentrations. Mass balance calculations using solid sample chemistry (total S, soluble ion and TIC concentrations) were also used to quantify the rate of SO_4 and Ca production rates.

Geochemical and geotechnical parameters controlling acid production and salt loadings were measured by installing gas probes to a depth of 25 m (n = 34) for in situ pore-gas O_2, CO_2, CH_4 and N_2 concentrations, and $\delta^{13}C_{CO2}$ values), diviner tubes to depths of 1.6 m (n = 3; for shallow moisture contents), a neutron access tube to 25 m (for deep moisture contents), and a thermistor string to 20 m (for temperatures). Pore-gas O_2, CO_2, CH_4 and N_2 concentrations were measured using a field-portable gas chromatograph. Depth profiles of solid sulphur (samples stored in anaerobic chambers) and carbon concentrations and forms were measured and used for acid-base accounting.

Pore-gas chemistry showed that O_2 concentrations decreased from atmospheric to less than 13 % at 5 m depth. CO_2 concentrations increased from atmospheric (0.04 %) to less than 4 % at the same depth The $\delta^{13}C_{CO2}$ results suggested that at South Bison Hill CO_2 was derived primarily from an inorganic carbon source. The moisture content data indicated higher moisture contents between 0.5 and 2.5 m depth than at greater depths in the profile. The pore-gas chemistry in conjunction with solids chemistry suggested the presence of an oxidation zone (acid producing) in the top 3 m of the profile. However, the results suggested that the oxidation zone was limited to the top 3 m of the profile by the presence of a saturated shale zone. Acid-base accounting results suggested that the acid-producing potential of the shale only slightly exceeded the neutralization potential (NNP = -6.5). The rates of O_2 and CO_2 flux through the reclamation cover were estimated to be 0.07 moles $O_2/m^2/day$ and 0.03 moles $CO_2/m^2/day$. The corresponding SO_4^{2-} production and $CaCO_3$ dissolution rates were estimated to be 1.3 and 4.2 $g/m^2/day$ respectively. These results were in keeping with rates estimated from mass balance calculations. The results show that a current moisture content conditions, the waste pile was not at risk for acidification or salinization.

Acknowledgements

I would like to thank Jim Hendry for his guidance, patience and support throughout this research project. Dr. Hendry's emphasis on independent learning and meticulous research provided me with invaluable project skills for my future. I also thank Dr. Lee Barbour for his input into this project and his infinite supply of enthusiasm for scientific research. Both of these men provided me with great inspiration.

I would also like to thank Ray Kirkland for the technical expertise, and for always answering my frequent and often not-so-intelligent questions. Many thanks to Barry Goetz and Len Wassenaar for the use of the soil science and isotope labs and for their advice on analysis procedures, and to Tyler Birkham for his patient proof-reading of some very terrible first drafts.

Thank you to my family, especially my husband Chris, who answered all the complaining, frustration and tears with encouraging words and patience. This thesis would never have been completed without them.

Financial support for this research was provided by Syncrude Ltd. Canada, without whom, this research would not have been possible.

Most of all, thanks to God for allowing me to finish and teaching me so many lessons along the way.

"Whatever your hand finds to do, do it with all your might, for in the grave, where you are going, there is neither working, nor planning, nor knowledge, nor wisdom. *Ecclesiastes 9:10-12.*

TABLE OF CONTENTS

LIST OF APPENDICES

(CD in back pocket)

Appendix A: Control-1 Pore-gas and moisture content data
Appendix B: SBH moisture content and temperature data
Appendix C: SBH Sulphur results, carbon results and acid-base accounting
Appendix D: SBH ion chemistry, CEC results and multiple dilution procedure
Appendix E: SBH pore-gas chemistry
Appendix F: SBH $\delta^{13}C_{CO2}$, $\delta^{13}C_{TIC}$ and $\delta^{13}C_{TC}$ results
Appendix G: Flux rate calculations

LIST OF TABLES

LIST OF FIGURES

1 Introduction

The mining of oil sands in Alberta is growing rapidly with the world's increasing demands for energy. Consequently there is an urgent need for effective long-term reclamation techniques to re-forest the extensive mine waste piles produced in the surface mining of oil sands.

To meet Alberta Environment closure and reclamation standards, oil sand mining companies must reclaim all disturbed land to an equivalent land capability, to what it was prior to disturbance. However, once the land has been disturbed, the physical and mineralogical characteristics of the soil are altered due to physical and chemical weathering. If the soil contains sulphide minerals, exposure to oxygen creates the potential for sulphide mineral oxidation and subsequent acid mine drainage. Mining operations around the world have encountered problems of high acidity and toxic heavy metal concentrations in both their waste-piles and drainage water (known as acid mine drainage or AMD) as a result of sulphide mineral oxidation (Harries and Ritchie, 1981; Harries and Ritchie, 1985).

AMD has been extensively studied over the past few decades both in the laboratory and the field. Laboratory based sulphide mineral oxidation studies have been used to determine the mechanisms and controls on oxidation as well as to predict the rate at which the reactions occur (Singer and Stumm, 1970; Nicholson et al., 1988; Bennet et al., 2000; Hollings et al., 2001). Laboratory experiments predominantly involve humidity cells, kinetic cells and column tests. These techniques are effective, but can be time-consuming, expensive and difficult to transfer to the field scale for long-term predictions on the rate and extent of AMD. Sulphide mineral oxidation rates have been determined *in situ* using both pore gas sampling methods and analysis of soil chemistry (Gelinas et al., 1992, Eberling and Nicholson, 1996; Birkham, 2002).

Previous AMD research has focused on the mine-waste at base metal and uranium mines where the waste material is composed predominantly of crushed rock, sand or tailings material. To date, no investigations have been done on the effects of sulphide oxidation in saline-sodic overburden piles, which are constructed during oil sand mining in northern Alberta.

Up to 50 m of overburden materials (including surface muskeg, glacial soils and deep marine shale deposits) are excavated to access the oil sand. The muskeg or surface organic material and glacial till deposits are separated and stored for later reclamation, and the deep marine sediments are placed in mined-out pits or overburden waste piles. The deep marine sediments are composed primarily of clay minerals containing high concentrations of sodium and calcium as well as sulphide minerals. The mineralogy and physical properties of the overburden piles places them at risk for both soil acidification and soil salinization/sodification. Once exposed to atmospheric oxygen, the sulphide minerals present in the waste pile will oxidize, creating soluble sulphate and H^+ ions. The carbonate minerals present in the soil naturally buffer soil acidity. However, the release of Ca^{2+} during carbonate dissolution can exchange for Na^+ present on clay exchange sites, increasing the soluble Na^+ concentration in the soil (Hendry and Buckland, 1990).

The South Bison Hill (SBH) overburden pile on the Syncrude oil sand mine site was chosen to investigate the type(s) and rate(s) of geochemical reactions in a saline-sodic waste pile. This study is part of a larger watershed research program focused on soil, water and vegetation interactions at the South Bison Hill. The South Bison Hill project is a pilot research program that will be used to set reclamation precedents for the industry.

The objectives of this study were 1) to identify the dominant mechanism of chemical weathering in the South Bison Hill overburden pile, 2) to characterize the depths and rates of these reactions and 3) to estimate the rate of salt release as a result of these reactions. The objectives were investigated using *in situ* measurement of pore-gas O_2, CO_2, CH_4 and N_2 concentration-depth profiles, $\delta^{13}C_{CO2}$, temperature, and soil moisture and solids chemistry. Fick's first law of diffusion was applied to estimate the flux of O_2 and CO_2

across the shale surface. The rate of salt release was estimated from the O_2 consumption and CO_2 production rates and compared to the rate of salt release estimated from mass-balance calculations and the results from solid sample analysis.

2 Literature Review

2.1 Sulphide Mineral Oxidation

Sulphide mineral oxidation by O_2 and Fe^{3+} has been extensively studied in the literature (Garrels and Thompson, 1960; Harries and Ritchie, 1980; Pugh et al, 1984; Harries and Ritchie, 1985; Gelinas et al., 1992). Pyrite oxidized by O_2 can be expressed as:

$$FeS_2 + 7/2O_2 + H_2O \rightarrow Fe^{2+} + 2SO_4^{2-} + 2\,H^+ \qquad (2.1)$$

In reaction (2.1), S is oxidized from S (-1) to S (+6). Intermediate sulphur species can be produced from the oxidation of pyrite when pH is less than eight (Moses et al., 1987), and will rapidly oxidize to sulphate (Nicholson, 1994). The oxidation of Fe^{2+} produced in reaction (2.1) to Fe^{3+} is rapid and expressed by:

$$Fe^{2+} + \tfrac{1}{4}O_2 + H^+ \rightarrow Fe^{3+} + \tfrac{1}{2}H_2O \qquad (2.2)$$

The rate of oxidation of Fe^{2+} to Fe^{3+} is pH dependent (Moses et al., 1987). If conditions are acidic (pH < 3.5), a significant quantity of Fe^{+3} can be produced and remain in solution. Reaction (2.2) is accelerated by the microbial catalyst *Thiobacillus ferroxidans* (Singer and Stumm, 1970) at low pH conditions and in the presence of oxygen (>2 % by volume) (Hoagg and Webber, 1976). Pyrite oxidation by Fe^{3+} is fast relative to pyrite oxidation by O_2 and is expressed as:

$$FeS_2 + 14Fe^{3+} + 8H_2O \rightarrow 15Fe^{2+} + 2SO_4^{2-} + 16H^+ \qquad (2.3)$$

In addition to oxidants, the particle size distribution of pyrite also affects the rate of oxidation. Small pyrite particles such as framboidal pyrite (with a larger surface area) will oxidize more quickly than larger grains (with a smaller surface area) (Moses et al., 1987; Nicholson et al., 1988; Nicholson, 1994). Sulphide mineral grains can also become coated

with less reactive iron hydroxide, an oxidation reaction product. The sulphide particle becomes less reactive over time as the coating thickens, reducing oxygen availability to the unoxidized core. This phenomenon is known as the 'shrinking core' model (Nicholson, 1994).

2.2 Temperature

Temperature is important both as a rate-controlling oxidation parameter and as an indicator of sulphide oxidation. The temperature profile in a waste pile depends on the rate of heat production from pyrite oxidation, on ambient temperature changes at the surface of the dump and by heat diffusion (Ritchie, 1994). Sulphide mineral oxidation is an exothermic reaction. If temperatures significantly higher than ambient are measured within a waste pile, it can be assumed that sulphide oxidation is occurring rapidly. A lack of significant increase in temperature may suggest that rates of sulphide oxidation are low or that ambient temperature is dominating the system (Ritchie, 1994).

In a sulphide oxidation study at the Rum Jungle mine site, Harries and Ritchie (1985) measured high temperatures at depth within a waste pile, indicating that sulphide oxidation was occurring. The high temperatures in the pile resulted in thermal convection currents and an increased supply of oxygen from the sides of the waste pile. Thermal convection as a transport mechanism must be investigated if temperature differences are detected within a waste pile below the depth of typical seasonal temperature variations.

The activity of microbial catalysts is also affected by temperature. The optimal temperature for activity of *Thiobacillus ferroxidans* is between 23 and 30°C. Activity is generally very low below 10°C (Wallace and Wallace, 1992). *Thiobacillus ferroxidans* have been estimated to increase the rate of the reaction in Equation (2.2) by a factor of 10^5 (Singer and Stumm, 1970).

2.3 Carbonate Mineral Dissolution

Carbonate mineral dissolution (Reaction 2.4) may neutralize the acid produced by sulphide mineral oxidation (Pye and Miller, 1990; Germain et al., 1994). Carbonate mineral dissolution releases Ca^{2+} and CO_2, and consumes H^+ (increasing the pH of the pore water).

$$CaCO_3 + 2H^+ \rightarrow Ca^{2+} + H2O + CO_2 \quad (2.4)$$

Dissolution of CO_2 into the pore water will produce carbonic acid ($H_2CO_3^-$), causing further dissolution of carbonates (Pye and Miller, 1990). The reaction can be represented by:

$$CO_2 + H_2O \rightarrow H_2CO_3 \quad (2.5)$$

Carbonate dissolution may also result in the precipitation of gypsum, decreasing SO_4^{2-} concentrations in pore water (Speck et al., 1998). This reaction can be expressed by:

$$CaCO_3 + H_2SO_4 + H_2O \rightarrow CaSO_4 + 2H_2O + CO_2 \quad (2.6)$$

2.4 Microbial Respiration

Microbial respiration is the biochemical oxidation of soil organic matter. Common organic matter found in soils includes recognizable biomass particles (cellulose, chitin, lignin), phenols and hydrocarbons. A simple carbohydrate (CH_2O) undergoing oxidation occurs as:

$$CH_2O + O_2 \rightarrow CO_2 + H_2O \quad (2.7)$$

Where 1 mole of O_2 produces 1 mole of CO_2. More complicated organic particles such as hydrocarbons are oxidized in multi-stage processes and have variable O_2 consumption to CO_2 production molar ratios. For example, the degradation of an alkane (a component of crude oil) follows the process:

$$\begin{gathered} CH_3CH_2CH_2CH_2CH_2CH_3 + O_2 \rightarrow CH_3CH_2CH_2CH_2CH_2CO_2H \\ CH_3CH_2CH_2CH_2CH_2CO_2H + 3O2 \rightarrow CH_3CH_2CH_2CO_2H + 2CO_2 + H_2O \\ CH_3CH_2CH_2CO_2H + 3O2 \rightarrow CH_3CO_2H + 2CO_2 + H_2O \end{gathered} \quad (2.8)$$

In this three-step degradation process, 7 moles of O_2 are consumed and 4 moles of CO_2 are produced (molar ratio 1:0.57) (Fetter, 1993).

2.5 Methanogenesis

Methane occurs under anoxic conditions, which most often develop in saturated environments. Two pathways are generally recognized for methanogenesis: CO_2 reduction and acetate fermentation (Whiticar et al., 1986; Whiticar and Faber, 1986; Revesz et al., 1995). Substrates other than acetate are known to be important for methanogenesis, but acetate fermentation is considered the most common, accounting for approximately 70 % of all methane produced in freshwater environments (Whiticar et al., 1986). Acetate fermentation refers to the transfer of a methyl group (CH_3) from any substrate. The reaction can be represented by:

$$CH_3COOH \rightarrow CH_4 + CO_2 \tag{2.9}$$

The acetate can also be oxidized to CO_2 and H_2O followed by a metabolic reduction of CO_2 to CH_4, using H^+ as an electron source according to the following reaction:

$$CO_2 + 8(H) \rightarrow CH_4 + 2H_2O \tag{2.10}$$

CO_2 reduction has been hypothesized to dominate in marine environments (Whiticar et al., 1986; Happel et al., 1994) because marine sediments typically have higher sulphide content. Sulphate reducing bacteria present in marine sediments compete for organic substrate, limiting acetate fermentation (Whiticar et al., 1986). CO_2 and bicarbonate produced from sulphate reduction is available to be reduced by CH_4. Accumulations of methane are usually only measured in the absence of dissolved SO_4 (Whiticar et al., 1986). Dissolved SO_4 is the last available electron acceptor to be reduced, after microbes consume

the available O_2, Mn, NO_3 and iron oxides to break down organic matter. Once SO_4 has been reduced methanogenesis can proceed.

In the presence of O_2, CH_4 will oxidize back to CO_2 according to the equation:

$$CH_4 + O_2 \rightarrow CO_2 + H_2O \tag{2.11}$$

2.6 Stable Carbon Isotopes

When CH_4 is low in concentration or not present, stable carbon isotopes of pore gas CO_2 can be used to determine the contributions of organic respiration (Reaction 2.7) and carbonate dissolution (Reaction 2.4) to the CO_2 in a waste pile. The ratios of the concentrations of the two stable carbon isotopes, ^{12}C and ^{13}C, can be measured using mass spectrometry (Mason and Moore, 1982) and are typically compared to a standard ratio of belemnite from the Pee Dee Formation of South Carolina (PDB). Ratios are reported as a delta value (δ), with units of ‰ (per mil). Delta values are calculated by:

$$\delta = \left\{ \frac{R_{sample}}{R_{s\,\mathrm{tan}\,dard}} - 1 \right\} * 1000 \tag{2.12}$$

where R is the ratio $^{13}C/^{12}C$. Plant matter and organically respired CO_2 typically have δ ^{13}C values ranging from –20 to –25 ‰, because plants tend to preferentially fixate ^{12}C over ^{13}C (Smith and Epstein, 1971). Marine carbonates and atmospheric CO_2 typically have $\delta^{13}C$ values near 0 ‰ and –7 ‰ respectively (Craig, 1953). Secondary carbonates have $\delta^{13}C$ values between –10 and 0 ‰ (Craig, 1953). $\delta^{13}C_{CO2}$ values will be higher than $\delta^{13}C$ of the carbon source material by at least 4.4 ‰ as a result of diffusive fractionation. Because of their different masses, $^{12}CO_2$ will diffuse more quickly than $^{13}CO_2$ (Cerling et al., 1991).

$\delta^{13}C$ is also used for identifying methanogenesis and CH_4 oxidation pathways. $\delta^{13}C_{CH4}$ ranges between -50 and -100 ‰ for CH_4 produced in anoxic, aqueous environments with a mean $\delta^{13}C$ of -68 ‰ in marine and -59 ‰ in freshwater environments (Whiticar et al., 1986a). The consumption of CH_4 results in large carbon isotopic fractionations (Whiticar et al., 1986; Whiticar and Faber, 1986; Revesz et al., 1995). Methanotrophic bacteria preferentially consume the lighter C isotopes of CH_4, leaving the remaining CH_4 enriched in ^{13}C (more positive) and producing CO_2 relatively depleted in ^{13}C (more negative). CO_2 produced in conjunction with CH_4 from acetate fermentation should have a $\delta^{13}C$ similar to that of the organic material consumed. $\delta^{13}C$ values for most hydrocarbons range between -25 and -31 ‰ (Schoell, 1980; Hunt, 1996). To clearly determine the pathways of CH_4 production and consumption both H and C isotope analysis must be used (Whiticar and Faber, 1986, Revesz et al., 1991). The presence of CH_4 in pore-gas greatly complicates the C cycle, making $\delta^{13}C$ interpretation of pore-gases difficult.

2.7 Quantifying Reaction Rates Using Pore Gases

Sulphide mineral oxidation consumes O_2, depleting subsurface pore gases in O_2 relative to the atmosphere. Similarly, carbonate mineral dissolution produces CO_2, leaving subsurface pore gases enriched in CO_2 relative to the atmosphere. These changes in pore gas concentration create concentration gradients, the driving force for diffusive transport of gas through the soil (Eberling et al., 1993). Diffusion through soil pores during normal gaseous exchange is the dominant gas transport mechanism in clay, silt and fine sand materials (Jaynes and Rogowski, 1983; Jaynes et al., 1984; Nicholson et al., 1989; Pantelis and Ritchie, 1992; Eberling et al., 1993). If the concentration gradients and the rate of transport are known, the rate of O_2 consumption and CO_2 production can be calculated. Mass flux of a gaseous species by diffusion is proportional to its concentration gradient (Fick's First law), although gas advection may be important in some cases.

2.7.2 Diffusion

One-dimensional gas diffusion can be described using Fick's first Law, where a diffusion coefficient relates mass flux to the concentration gradient by:

$$J = -D\frac{\partial C}{\partial x} \tag{2.13}$$

where J is the mass flux of a gaseous species, D is the diffusion coefficient and $\partial C/\partial x$ is the concentration gradient. The direction of mass flux is from the area of greater concentration to the area of lower concentration. Gas diffusion through a porous medium is slowed by tortuosity and reduced area available for diffusion. Tortuosity is a factor that accounts for the increased length of the diffusion path around mineral grains. The presence of water in pore spaces will reduce the area available for diffusion and decrease tortuosity. An *effective* diffusion coefficient (D_e) is used to calculate diffusive flux through a porous medium (Fetter, 1993) because it takes into account both the effects of tortuosity and moisture content. De can be calculated using the methods of Fuller et al. (1966) and Millington and Quirk (1961) (Birkham 2002, Birkham et al., 2003):

$$D_e = \frac{n_a^{\frac{7}{3}}}{\theta^2}\left(\frac{T}{T_0}\right)^{1.75} D_0 \tag{2.14}$$

Where n_a is the air-filled porosity, θ is the total porosity; T is the temperature at which diffusion is being calculated, T_o is temperature of diffusion at D_o (the diffusion coefficient of a gas species in air).

For gaseous diffusion through an unsaturated porous medium, Equation 2.13 can be rewritten as:

$$J = -n_a D_e\frac{\partial C}{\partial x} \tag{2.15}$$

where n_a is the air-filled porosity. The inclusion of air-filled porosity in Equation 2.15 accounts for the reduction in cross-sectional area available for diffusive flux. Tortuosity and cross-sectional area of pore gas decreases (air-filled porosity decreases) as moisture

content increases. The degree of saturation is the dominant control of the rate of oxygen diffusion into soils (Eberling and Nicholson, 1993). The degree of saturation, S (%), is described as the percentage of void space that is occupied by water (Fredlund and Rahardjo, 1993).

$$S = \frac{V_w}{V_v} \tag{2.16}$$

Where V_w is the volume of water and V_v is the volume of voids (porosity). In a saturated soil, all of the void space is filled with water. In an unsaturated soil, the percentage of void space filled with water is somewhere between 0 (dry) and 100 % (saturated). The degree of saturation in a soil gives an indication of the percentage of air-filled voids remaining.

An example of the relationship between D_e and the degree of saturation is given by Reardon and Moddle (1985) for silty, unsegregated uranium tailings from the Sudbury region in Ontario. The results of the experiment show that for a degree of saturation greater than 85 %, D_e decreases by approximately 2 orders of magnitude while the air-filled porosity changes by 15 %. The relationship between the effective diffusion coefficient and degree of saturation is shown in Figure 2.1. The results of the experiment suggested that for degrees of saturation greater than 85 % the gaseous diffusive flux through porous media is essentially the same as the diffusive flux through saturated media.

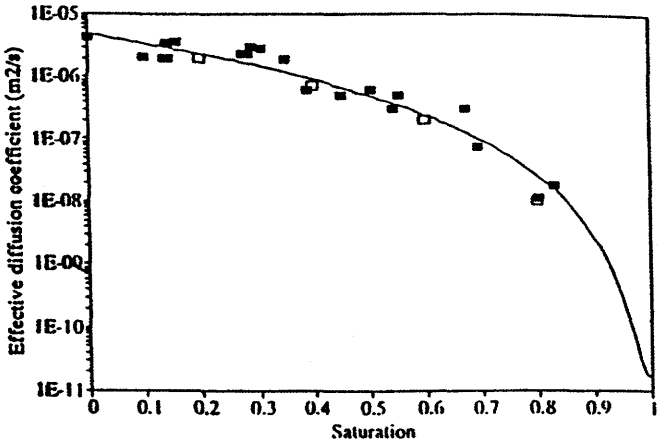

Figure 2.1: The relationship between the effective diffusion co-efficient for oxygen and the degree of saturation. Data points represent tailings studied by Reardon and Moddle (1985) and tailings studied by Eberling et al., (1993) (from Eberling et al., 1993).

2.7.3 Advection

Advection is the bulk transport of gas along a total pressure or density gradient. The advective mass flux of a gaseous species is proportional to its concentration and the volume of air flow produced by a pressure gradient. If a total pressure gradient exists, gas will flow from the area of higher pressure to the area of lower pressure (Massmann and Farrier, 1992). Total pressure or density gradients may develop as a result of changes in atmospheric pressure or subsurface reactions. For example, combining pyrite oxidation with carbonate dissolution, (Reactions 2.1 and 2.4), 3.5 moles of O_2 are consumed for every 1 mole of CO_2 produced:

$$FeS_2 + CaCO_3 + 3.5O_2 \rightarrow Fe^{+2} + Ca^{+2} + CO_2 + SO_4^{-2} \qquad (2.16)$$

This decrease in total gas volume creates a pressure gradient and results in the advective transport of gas. If both a concentration gradient and a total pressure gradient exist, then gas migration occurs both by diffusion and advection. When the concentration and total pressure gradients are in the same direction, the direction of the mass flux of a gaseous species is easy to determine. When the pressure and diffusion gradients are in different

directions, the direction of mass flux is difficult to determine (Massmann and Farrier, 1992).

The fluctuation of atmospheric pressure may also contribute to oxygen transport (Massmann and Farrier, 1992, Andersen et al, 2001). Changes in barometric pressure produce short-term pressure gradient changes resulting in atmospheric air being transported into or out of unsaturated zones. Although found to affect gas concentrations short-term, atmospherically-induced advection is likely insignificant when compared to long-term diffusive transport (Massmann and Farrier, 1992; Eberling and Nicholson, 1996).

To date, numerical and analytical models used to describe O_2 consumption in mine waste use one-dimensional vertical diffusion based on Fick's First law assuming homogeneous hydraulic and geochemical properties (Gerke et al., 1998). Although sulphide mineral oxidation in mine waste is a three-dimensional problem, it is generally accepted that it is possible to apply one-dimensional models for porous media (Eberling and Damgaard, 2001). As shown by Harries and Ritchie (1985), Pantelis and Ritchie (1991) and Eberling et al. (1993), the primary rate-controlling factor for sulphide mineral oxidation in a waste pile is the physical transport of O_2 into the material. Therefore the model used to describe oxidation does not need to take into account reaction kinetics at the mineral grain surface or the effects of bacteria (Gerke et al., 1998). Previous studies indicate that a simple, one-dimensional analytical model can be effective for determination of O_2 consumption and CO_2 production rates based on field-data (Cerling, 1984; Hendry et al., 1999). Further discussion of the analytical model used in this study is presented in Section 4.2.

2.8 Soil Salinization and Sodification

Salinity is a widespread and well-studied problem in the great plains of North America (Curtin and Mermut, 1985; Mermut and Arshad, 1987; Curtin et al., 1994; Van Stempvoort et al., 1994). Thousands of hectares of cultivated land in Saskatchewan and Alberta have been affected by salinity (Curtin and Mermut, 1985). Sulphate salts present in the soil are known to be the cause of salinity. The soil in these regions is derived at least in part, from pyrite-bearing Cretaceous marine shale (Curtin and Mermut, 1985; Van Stempvoort et al.,

1994). Studies have suggested that the weathering of pyrite in the shale was causing both the development of acid sulphate soil and the production of sulphate salts (Mermut and Arshad, 1987, Van Stempvoort et al., 1994). Once the weathering of pyrite produces sulphate, it can be precipitated as gypsum, transported by groundwater or reduced back to sulphide (Van Stempvoort et al., 1994). If evapotranspiration processes exceed precipitation, sulphate salts can accumulate within the shallow soil zone.

Salt-affected soils are classified as saline, sodic, or saline-sodic soils. The soil classification scheme for these types of soils was designed in order to implement soil remediation and management practices, primarily with respect to agriculture (US Salinity Laboratory Staff, 1954). The study of salt-affected soil has been expanded to include mine waste management to characterize the processes of salinization (RRTAC, 1990). Saline, sodic and saline-sodic soils possess different properties and require different remediation strategies.

Saline soils have an accumulation of dissolved salts great enough to impair plant productivity. Sodic soils have enough exchangeable sodium to decrease both plant productivity and soil quality. Saline-sodic soils contain high levels of both soluble salts and exchangeable sodium and exhibit properties similar to those of saline soils (Bresler, 1982). Salt-affected soils are most commonly found in arid and semi-arid regions where there is not enough rainfall to leach soluble salts out of the soil system, allowing salts to accumulate at surface or shallow depths (Sparks, 1995). An excess of ions in soil pore water can be toxic, causing osmotic effects and nutritional deficiencies in plants (Bresler et al., 1982). The most common ions contributing to soil salinity are Cl^-, SO_4^{2-}, HCO_3^-, Na^+, Ca^{2+}, Mg^{2+} and occasionally NO_3^- and K^+ (Bresler et al., 1982). The extent to which salt affects soil is dependent on several factors including the soil texture, the distribution of salts in the profile, the composition of the salt and the species of plant (US Salinity Laboratory Staff, 1954).

The Cretaceous marine sediments found in the South Bison Hill contain a large percentage of clay minerals. Clay minerals are layer silicates, made of alternating sheets of silicate tetrahedra and hydroxyl octahedra (Mitchell, 1979). Different stacking patterns and

interlayer cations characterize each clay mineral. A net negative surface charge on silica sheets is a result of cation substitution in the tetrahedral and octahedral sites (Mitchell, 1979). To satisfy this charge, clay minerals adsorb cations to their surface. The potential for this to occur varies between clay species and is described as the *cation exchange capacity* (CEC). The cations that are adsorbed to the surfaces are referred to as *exchangeable cations* because they can be exchanged for cations in the surrounding soil pore water (Mitchell, 1979; Dixon and Weed, 1989). The exchangeable cation concentration determined during CEC analysis indicates the amount of cations adsorbed to clay mineral surfaces and available for exchange.

Generally, Ca^{2+} and Mg^{2+} ions are present in greater concentrations in soil solution than Na^{+} and are much more readily adsorbed onto the exchange complex. At equivalent solution concentrations, the amount of Ca^{2+} and Mg^{2+} adsorbed is several times greater than the amount of sodium ions. When Na^{+} concentrations in solution approaches 50% of the total ions or greater (sodic soil), it will exchange for Ca^{2+} and Mg^{2+} on the clay surface (US Salinity Laboratory Staff, 1954). Na^{+} ions form bonds only half the strength of those formed by Ca^{2+} and Mg^{2+}, and due to its large size tends to attract large H_2O molecules around it further reducing attractive forces and causing swelling of clay particles. The clay particles separate from one another, separating the soil into even smaller component particles. This phenomenon is called soil dispersion, and is a common problem in sodic soils. The smaller soil particles can fill still existent macropores, decreasing water and gas movement and leading to 'waterlogging' of soil (Sparks, 1995).

2.8.2 Electrical Conductivity

The electrical conductivity (EC) is a measure of the resistance to electrical current by a solution. It is considered a quick, accurate method for estimating soluble salts in soil solutions (United States Salinity Laboratory staff, 1954). It is based on the concept that the electrical current under standard conditions will increase as the salt concentration in solution increases (Sparks, 1995). A sample solution is placed between two electrodes of known geometry and an electrical potential is applied across the electrodes. The resistance

(R) of the solution is measured between the electrodes in ohms (Bresler et al., 1982). The resistance of the solution is inversely proportional to the length of the conductivity cell holding the sample and the electrodes. In SI units the reciprocal of the ohm (resistance unit) is the siemen (S) which is multiplied by a 'cell-constant' having units of cm^{-1} (cm/cm^2). The standard EC measurement is reported as S cm^{-1} or μS/cm (Bresler et al., 1982).

2.8.3 Sodium Adsorption Ratio (SAR)

The SAR indicates the tendency of a solution to produce exchangeable sodium and is defined by:

$$SAR = \frac{[Na]}{\sqrt{\frac{[Ca]+[Mg]}{2}}} \qquad (2.17)$$

where $[Na^+]$, $[Ca^{2+}]$ and $[Mg^+]$ represent the molar concentration of each ion species in solution (meq/L). SAR is used for comparing the concentrations of soluble and exchangeable cations. Higher SAR values mean a higher percentage of exchangeable sodium is present, and therefore the soil is likely to have a lower hydraulic conductivity. Sodic and saline-sodic soils have an SAR of 13 or greater (Donahue et al., 1983).

The SAR is expressed in terms of ion concentrations rather than ion activities. Therefore, it does not take into account the effects of ion-pair complexes that result in a reduction of free-ion concentration (Sposito and Mattigod, 1977). The 'activity' of an ion is defined by the relation:

$$a = \gamma m \qquad (2.18)$$

where γ is the activity coefficient, m is the molal concentration and a is the activity.
The activity coefficient can be calculated using the Debye-Huckel Equation:

$$\log \gamma = \frac{-0.509 Z^2 \sqrt{\mu}}{1 + 0.330 \alpha \sqrt{\mu}} \tag{2.19}$$

where μ is the ionic strength of the solution and α is the distance of closest approach for the ion in question. μ can be calculated by:

$$\mu = \frac{1}{2} \sum m Z^2 \tag{2.20}$$

where Z is the ionic valence. Equations 2.19 and 2.20 show that the activity coefficient for divalent cations decreases more rapidly with increasing salt concentration than it does for monovalent cations (Bresler et al., 1982).

2.8.4 Exchangeable Sodium Percentage

The exchangeable sodium percentage (ESP) ESP is a convenient way to express the amount of exchangeable sodium as a percentage of the cation exchange capacity. The ESP is calculated as:

$$ESP = \frac{NaX}{CEC} * 100 \tag{2.21}$$

where NaX is the exchangeable Na^+ concentration expressed in meq/100 g soil.
The ESP value is used to define the physical and chemical properties of soil because exchangeable cations affect both these properties. A saline soil has an ESP of less than 15 whereas sodic and saline-sodic soil has ESP values exceeding 15 (US Salinity Laboratory Staff, 1954).

2.8.5 Soil pH

The pH value of an aqueous solution is the negative logarithm of hydrogen ion activity (US Salinity Laboratory Staff, 1954). Soil characteristics that are known to affect soil pH readings include: the types of exchangeable cations, the CEC of the clays, the types and

concentrations of soluble salts and the presence or absence of gypsum and alkaline-earth carbonates (US Salinity Laboratory Staff, 1954).

2.9 Summary

No previous studies known to the author have used soil pore gas concentrations and isotopic compositions to determine the rate and extent of sulphide oxidation and its control on the rate of salt release in saline-sodic overburden. Pore-gas concentrations and isotopic compositions combined with simple analytical rate calculations can indicate the types and rates of O_2 consumption and CO_2 production reactions occurring in the overburden. The clay surface exchange reactions, dissolved salt concentration in soil solution and even the physical properties of the soil are all related to the O_2 consumption/CO_2 production reactions identified in this section.

3 Description of Study Site

3.1 Site Location and Climate

The Syncrude oil sand mine is located 35 km north of Fort McMurray, Alberta, Canada (latitude: 56° 44' 45", longitude: 111° 22' 58") and approximately 900 km northwest of Saskatoon, Saskatchewan (Figure 3.1). The average precipitation at the Syncrude mine site is 338 mm/year and the average annual air temperature is 2°C (D. Chapman, personal communication). The average annual evaporation is about 575 mm/year (Alberta Environment Website, 2004)

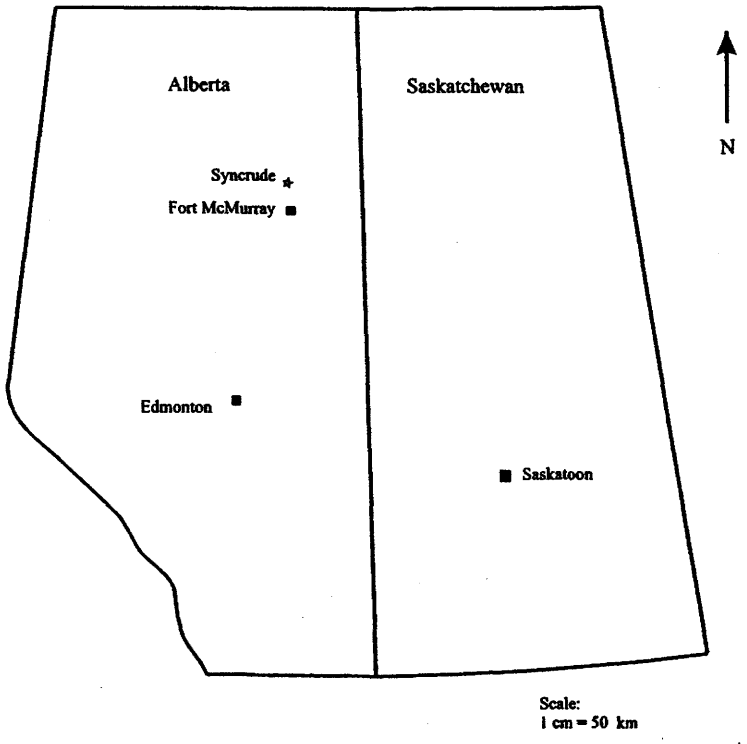

Figure 3.1: Location of the Syncrude mine site relative to Saskatoon, Saskatchewan and Edmonton, Alberta, Canada.

3.2 Mining History

The Syncrude oil sand mine began operation in 1978 and, as of 2001, the mine had produced 1 396 900 000 barrels of oil (Syncrude 2001 annual report). Syncrude is the largest holder of oil sand leases in Alberta with leases covering 101 960 ha and a potential 8.3 billion barrels of oil. There are enough oil sand reserves for Syncrude to continue mining operations for at least 40 years even if current production rates are doubled. The current rate of production is 247 000 barrels a day. At present, the total land area disturbed by Syncrude is 20 655 ha. The total land area reclaimed to date covered 4 822 ha (Mark Wyllie (Syncrude), personal communication).

3.3 Soil Mineralogy/Geological History

Current mining activities are concentrated in the lower Cretaceous McMurray Formation. The McMurray Formation sediments are fine-grained siliceous sand and clay deposited in lacustrine, deltaic and alluvial environments. The sand ranges in thickness from 30 to 80 m and is impregnated with viscous bitumen. As much as 80 m of Cretaceous deep marine Clearwater Formation sediments overlie the McMurray Formation, however, mining is generally limited to those locations where the Clearwater Formation is equal or less than 50 m thick.

The South Bison Hill is composed predominantly of Cretaceous saline-sodic, uncemented mud and clayey silt sediments from the Clearwater Formation. The Clearwater Formation was deposited during the Lower Cretaceous (144 Mya) in the Western Canadian Basin. The Western Canadian Basin was an eperic seaway of continental proportions stretching from the Beaufort Sea to the Gulf of Mexico. Due to variations in sediment supply and water level, the Clearwater Formation is a marine interbedded sequence of sandstone and shale deposited in environments ranging from lagoonal to beach and offshore and from fluvial deltaic to tidal estuarine and flats (Stott and Aitken, 1993). The strong lateral continuity of the siltstone beds is characteristic of quiet shallow marine conditions (Dussealt et al., 1989). Clay minerals compose approximately 50 % of the Clearwater Formation sediments; the remaining 50 % is dominated by quartz with trace amounts of

feldspar (Mermut, 2000). The average clay mineral composition is 42 % illite, 27 % smectite, 17 % kaolinite and 14 % chlorite (Dusseault et al., 1989). The high smectite/illite gives the Clearwater Formation sediments their high swelling capacity.

The Clearwater Formation is underlain by the McMurray Formation oil sands and overlain by glacial till deposits. Figure 3.2 shows the regional stratigraphy of the Athabasca oil sands area.

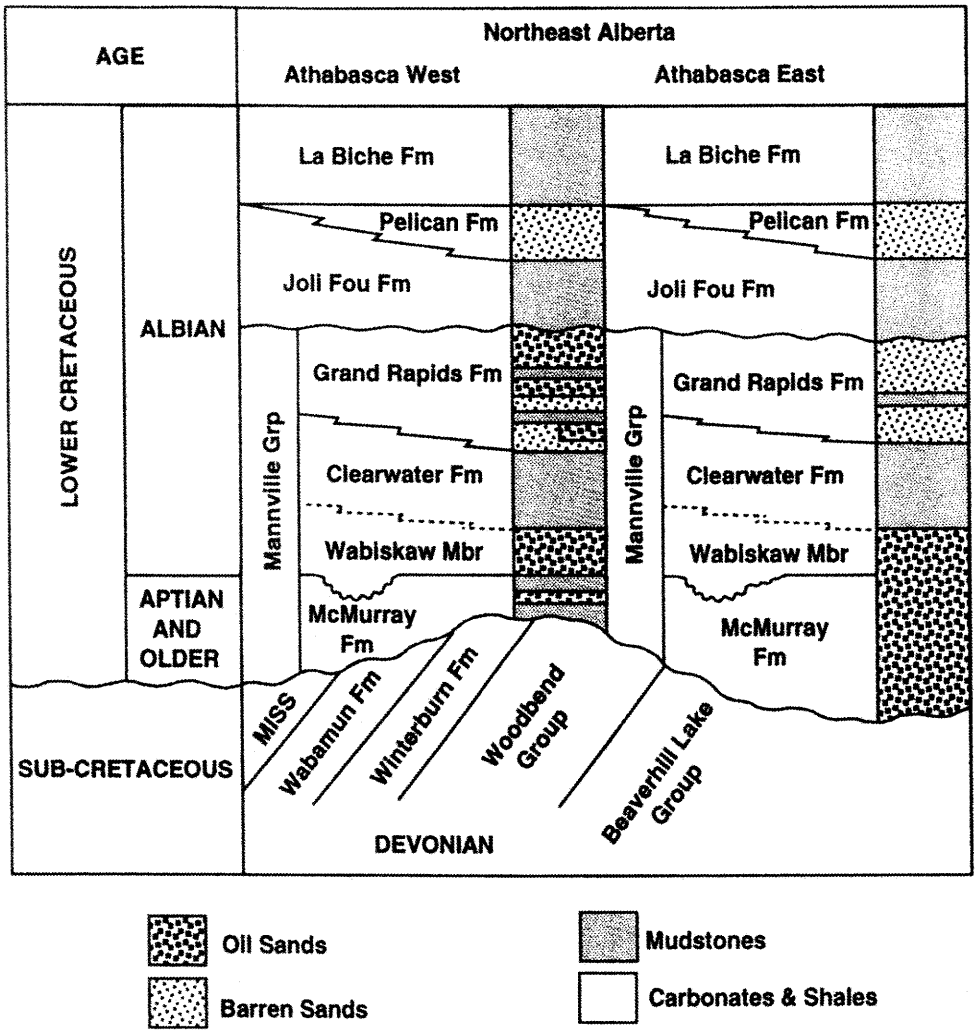

Figure 3.2: Regional stratigraphy of the Athabasca oil sands region (from Wrightman and Pemberton, 1997).

3.4 Location and Construction History

The SBH is located near the south shore of Base Mine Lake, on the south side of the North mine pit (Figure 3.3). The area chosen for the undisturbed control site is located southwest of SBH, on the west side of the southwest sand storage access road (Figure 3.3). A cross-section extending 1.5 km from the South Bison Hill access road (to the South) to the south shore of Base Mine Lake (to the North) (Figure 3.4) is presented in Figure 3.5. The South Bison overburden pile was constructed in four stages (D. Chapman, personal communication). The first stage was the construction of the S1 dump between 1980 and 1982 from glacial till (10% clay), placed on *in situ* undisturbed material beyond the mine lease area. The S1 dump was constructed in 2 m lifts by flattening formed benches with bulldozers.

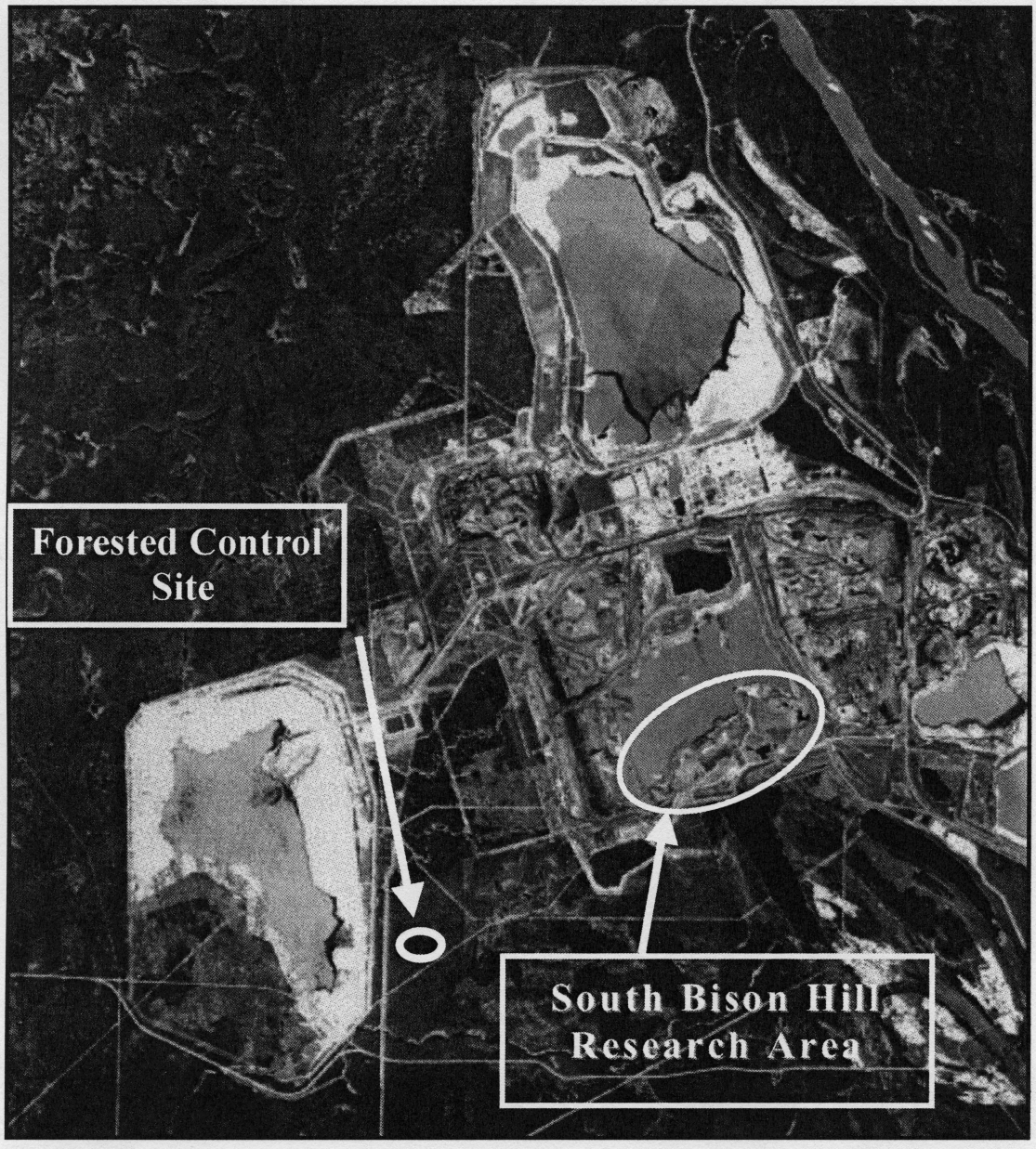

Figure 3.3: Aerial photograph of the location of the South Bison Hill research area with respect to the Syncrude mine site. Base Mine Lake is situated directly north of the research area. The undisturbed control site is located to the southwest.

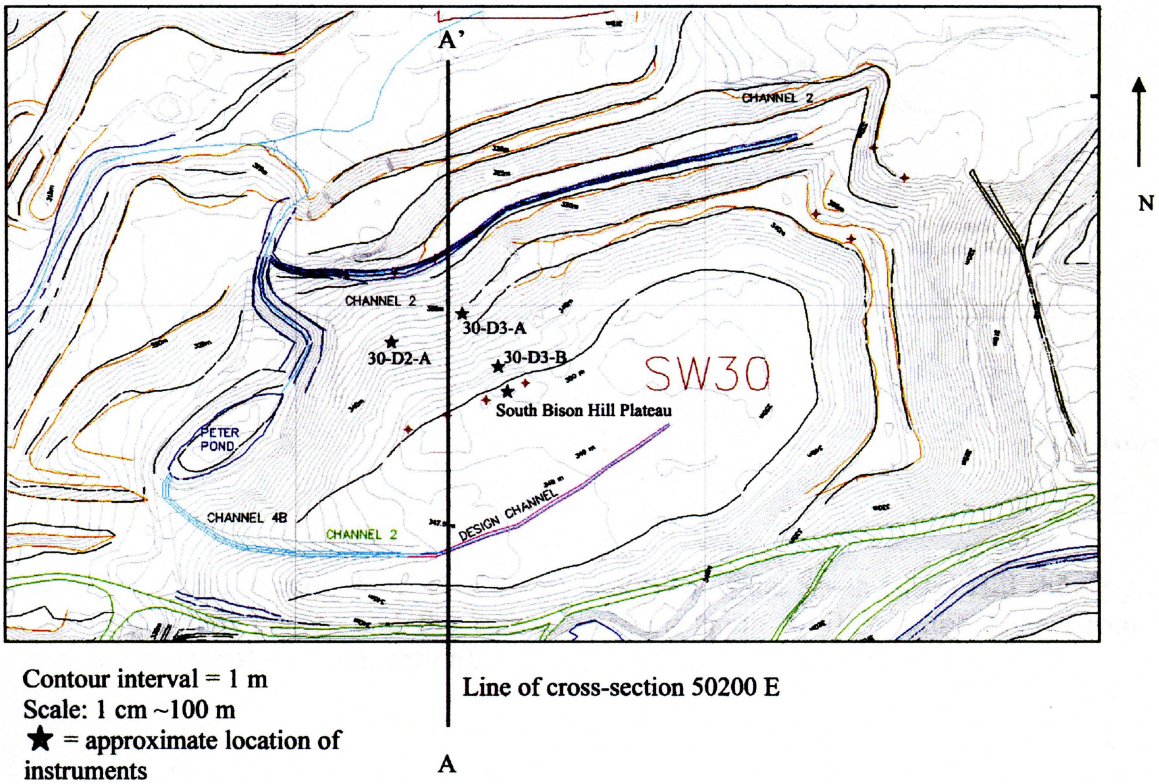

Figure 3.4: Topographic view of South Bison Hill. The location of cross section A-A' is indicated with respect to the study area.

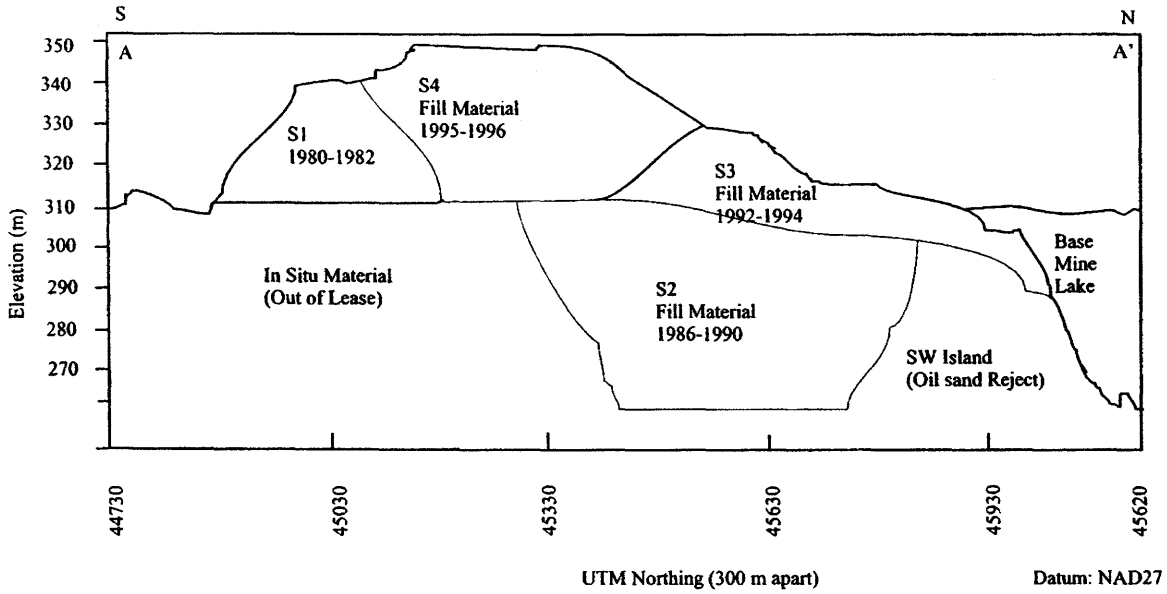

Figure 3.5: Cross-section A-A' (UTM line 50200 E) of the South Bison Hill showing the four construction phases and the approximate elevation of Base Mine Lake (from D. Chapman, personal communication).

The second stage (S2) was constructed from fill material placed between 1986 and 1990. This material was excavated from the same area as the S1 material. The clay content increased from 15 % on the east side of the dump to 25% on the west as the Clearwater Formation became thicker and surface muskeg content decreased. This stage was constructed by pushing the material into a 50-m deep pit between the *in situ* out-of-lease material and the Southwest Island (an oil sand reject pile present prior to construction). This construction technique resulted in a heterogeneous mixture of overburden material.

Stage S3 was constructed with fill material (containing 30 to 40% clays) between 1992 and 1994. Construction lifts were 10 to 20 m thick, by flattening formed benches with bulldozers. This method produced a structure similar to stage S1.

The SBH instrumentation for this study was located on stage S4, constructed between 1995 and 1996. The S4 material is highly heterogeneous, containing primarily clay material (up to 75 %), low-grade oil sands and small amounts of till and muskeg. This mixture includes

approximately 1 to 5 % by volume cobblestones and boulders (weighing between 1 kg and 100 kg). The 5-m construction lifts have a variable bulk density. The top 2 m of each lift is expected to have a higher bulk density compared to the underlying 3 m due to traffic compaction.

The slope of the final pile was designed to create a drainage system, including shallow swales and ridges for optimal drainage. Long-term subsidence was expected and incorporated into the design. The top of SBH is approximately 30 m above the original ground, with a water table approximately 60 m below the top of the hill.

3.5 Cover Treatments

Three different cover treatments were placed on the north slope of SBH to study their effects on plant growth, root penetration, air and water permeability, salt transport and moisture regimes. The cover treatments are identified in Figure 3.6. The D3 cover consists of 80 cm of glacial till capped with 20 cm of peat/mineral mix, the D2 cover consists of 20 cm of till capped with 15 cm of peat, and the D1 cover consists of 30 cm of till capped with 20 cm of peat/mineral mix.

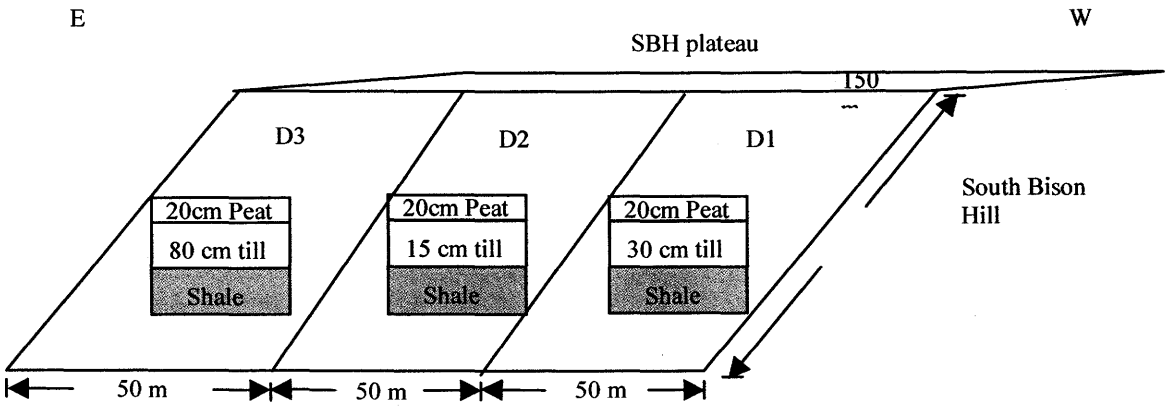

Figure 3.6: Schematic diagram showing the location of cover treatments on the North slope of South Bison Hill.

Cover treatments were placed during the winter of 1997. Vegetation on the North slope consists primarily of voluntary grasses (including sow thistle, foxtail, barley, fireweed, horsetail, alfalfa, sweet clover and dandelion) with planted native trembling aspen and white spruce trees. The top plateau, south and west slopes were seeded with barley in 2001 to reduce surface erosion and initiate the development of soil structure.

Boese (2003) measured the specific gravity (G_s) and in situ dry bulk density of the peat/mineral mix, till and shale on the north slope of South Bison Hill. The results of the in situ dry density of materials are presented in Table 3.1.

Table 3.1: Statistics for the in situ dry density of materials at South Bison Hill (from Boese, 2003)

Cover Material	# of samples	Kg/m^3			
		Max	Min	St. Dev	Mean
Peat/mineral mix	23	1403	200	310	920
Till	36	1640	929	206	1280
Shale	32	1735	980	196	1470

The results of the specific gravity testing conducted by Boese (2003) indicated that the specific gravity for the peat/mineral mix, till and shale were 2.62, 2.61 and 2.73 respectively. The in situ permeability was measured by Meiers (2002) using a Guelph permeameter. The mean hydraulic conductivities for the peat/mineral mix, till and shale (measured in 2002) were 1.3×10^{-4}, 2.0×10^{-5} and 2.0×10^{-7} m/s respectively. The grain size distribution for one shale sample collected from South Bison Hill was 30 % clay particles, 33 % silt and 37 % sand (Boese, 2003).

4 Materials and Methods

4.1 Instrumentation Overview

The South Bison Hill was instrumented with gas probes, a neutron access tube, three Diviner access tubes, and two shallow water wells. In addition, three gas probes and two Diviner access tubes were installed in an undisturbed, natural forest control site located on the southwest corner of the mine (Control-1; see Figure 3.3).

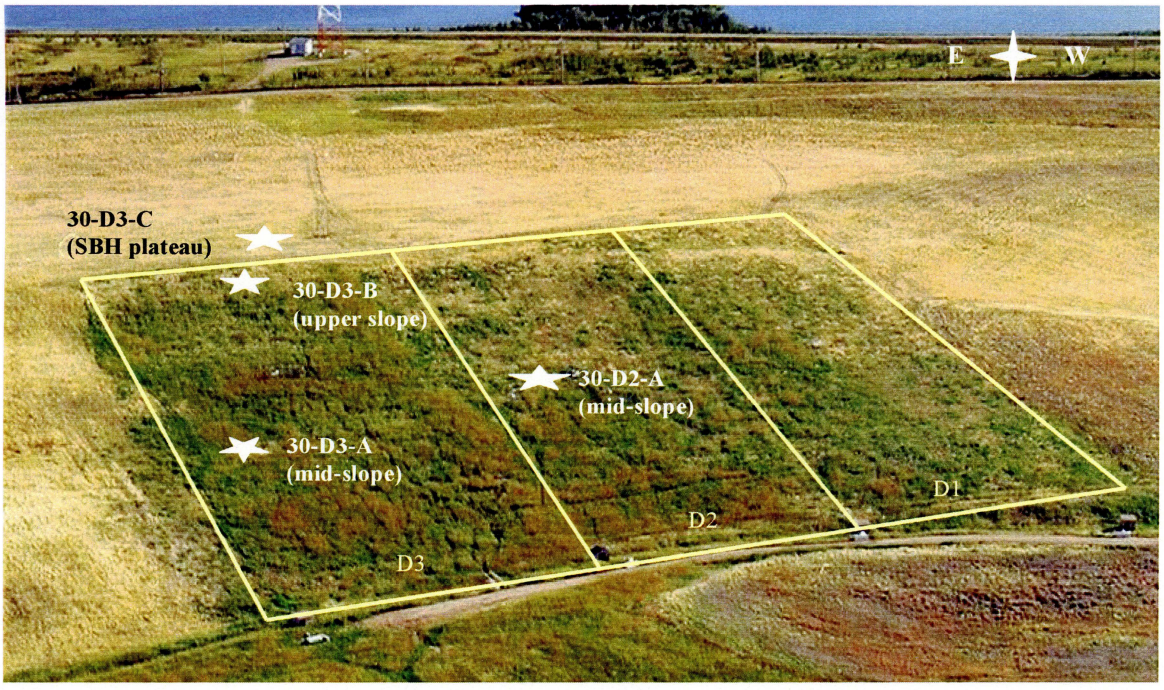

Figure 4.1: Location of instrumentation sites on the north slope of South Bison Hill.

4.1.2 Pore-gas Chemistry

A total of 35 gas probes to measure pore-gas O_2, CO_2, CH_4 and N_2 concentrations and collect gas samples for isotopic analyses were installed at four locations on the North slope

of SBH (30-D3-A, 30-D3-B, 30-D3-C and 30-D2-A, Figure 4.1). In addition, three gas probes were installed at the control site. The gas probes were installed November 2000 and June 2002. Details of the installations are presented in Table 4.11. On the SBH, locations were chosen to compare results from different slope positions and two cover treatments (Table 4.1).

Table 4.1: Dates, locations and installation depths of pore-gas sampling probes installed on the North slope of South Bison Hill and at the undisturbed Control site.

Location	Slope Position	Cover treatment	Depths (m) Below ground	Installation Date
30-D3-A	Mid-slope	D3	0.45, 1.05, 1.40, 2.45, 3.05, 4.05	November 6 2000
30-D3-B	Upper-slope	D3	0.55, 1.05, 1.55, 2.15, 2.65, 3.3, 4.45	November 6, 2000
30-D3-C	Top of hill (Plateau)	D3	3, 5, 7, 9, 11m, 13, 15, 17, 19, 21, 23, 25 0.35, 0.65, 0.85, 1.52, 1.87, 2.70	April 12, 2001 July 11, 2002
30-D2-A	Mid-slope	D2	0.25, 0.45, 0.78, 0.95, 1.5, 1.68, 1.90	June 30, 2001
Control			0.45, 1.15, 2.35	November 5, 2000

All gas probes were constructed of 6.4 mm high-density polyethylene tubing with screened filters fitted on the down-hole end. The screened filters were constructed of chain-saw oil filters pushed directly into the tube end and covered with window screen. Holes less than 5-m deep were hand augered with a 50 mm diameter auger head. Five centimeters of coarse clean drilling sand was placed in the bottom of the augered hole and the screened filter attached to the tubing was placed on this sand. The hole was then backfilled with

another 5 cm of sand, followed by bentonite pellets to the surface. Above ground surface, the tubing was fitted with a plastic three-way valve. A 50 mm diameter PVC pipe was placed over the exposed portion of tubing for protection. Holes for 30-D3-C gas probe installations were augered using a truck-mounted auger drill rig (Layne Christenson Canada Ltd.). The OD of the auger was 200 mm and the diameter of the auger stem was 100 mm. A spit-spoon sampler was used every 0.45 m to collect solid samples. The 6.4 mm tubing was fastened to the outside of a 25 mm ID PVC pipe, and the PVC pipe was placed down the hole. The annular space around the probes was backfilled with sand and 1.0-m thick bentonite plugs were placed between each probe.

O_2 and CO_2 concentrations were measured using a GasTech portable gas analyzer (Model #72-6208-04) in the field between February 2001 and October 2002. Concentrations were measured throughout the field season and once during the winter (2001: Feb 21, Apr 12, May 10, May 30, Jun 25, Jul 17, Sep 18. 2002: Feb 20, May 08, Jun 14, Jul 17, Aug 28, Oct 30). The GasTech analyzer drew the gas to the surface with a small internal pump. The gas passed over an electrochemical cell to measure O_2 concentration and past a non-dispersive infrared sensor to measure CO_2 concentration. The reported accuracy of the measured concentrations was ± 0.5 % by volume for the O_2 cell and ± 10 % of the measured reading for the CO_2 sensor. The detection range of the O_2 cell was 0 to 30 %, and 0 to 20 % for the CO_2 sensor.

The GasTech gas meter was calibrated in the lab before every field sampling period. The O_2 sensor was calibrated using natural air (20.9 %) and 100 % N_2 as span gases. The CO_2 sensor was calibrated using a gas standard (11.6 % ± 5 % of concentration) and natural air drawn through a CO_2 scrubber. Performance of the gas meter was checked before and after every sampling period using a gas standard containing 11.6 % CO_2 (± 5 % of concentration) and 3.05 % O_2 (± 5 % of concentration).

On the same occasions that the pore-gas concentrations were measured using the GasTech analyzer, gas samples were also collected for more precise O_2, CO_2, CH_4 and N_2 concentration analyses. The gas probe tubing was purged using a 50-ml plastic syringe.

The samples were collected in 250-ml evacuated glass serum bottles (Wheaton #2725), which were crimp sealed with a butyl blue septum (BellcoBiological Glassware, Vinland, NJ). The samples were transported to Saskatoon; where concentrations of O_2, CO_2, N_2 and CH_4 were measured using a Carle Special Series S model 311 analytical gas chromatograph (GC). The GC was equipped with Porapak and molecular sieve columns and automatic valve switching, as well as thermal conductivity and flame ionization detectors. The column did not separate O_2 from Ar.

In 2002, an M200 field-portable micro gas chromatograph was purchased from Agilent Technologies. This GC was equipped with 2 channels and used both He and Ar as carrier gases. The use of a carrier Ar gas ensured separation of O_2 from Ar. The lower detection limit for all gases was less than 200 ppm, varying slightly depending on gas species. Repeatability was <1 % at constant temperature. Pore-gas O_2, CO_2, N_2 and CH_4 concentrations were measured at the same locations on the following dates: May 15 2002, June 8 2002, July 4 2002, August 26 2002, October 30, 2002, February 20 2003, June 11 2003, October 6 2003. The micro GC was calibrated prior to each day of sampling using standards of air (20.9 % O_2, 78.1 % N_2), an ultra-high purity (UHP) gas mixture of 11.6 % CO_2, 3.05 % O_2 and 85.35 % N_2, and a UHP mixture containing 0.52 % CH_4, 1.58 % CO_2 and 10 % O_2 and 88.42 % N_2. The micro-GC was placed in an insulated, enclosed box on a single-axle cart for transport to each site on the South Bison Hill. Each gas port was purged using a 140-ml syringe with a three-way valve attached to the open end. A sample was collected in the syringe and immediately injected into the GC for analysis.

Gas samples were collected in evacuated bottles for $\delta^{13}C_{CO2}$ analysis using the sampling method described above. Samples were transported to Saskatoon and analyzed using a Micromass Optima dual inlet isotope ratio mass spectrometer coupled with a gas chromatograph located at the National Water Research Institute. Analysis error was better than 0.1 ‰ ± 0.2 ‰

4.1.3 Temperature

A thermistor string to measure temperature was installed on the SBH plateau (30-D3-C) in May 2002. The string was placed down the 1" PVC pipe that formed the center of the deep gas probe nest (3 to 25 m), at 30-D3-C (SBH plateau) installed in February 2001. Canola oil was poured into the pipe to provide thermal contact with the soil. One thermistor was left above ground, with the remaining thermistors installed at subsurface depths of 0.25, 1.25, 2.25, 3.25, 4.25, 5.25, 9.25, 14.25, and 19.25 m. Electrical resistance (kΩ) measurements were measured using a standard multi-meter approximately twice monthly during the 2002 field season. The thermistors were calibrated using an ice bath (~ 0°C) and ambient air temperature (~21°C). The resistance measured at each known temperature was used to develop the following equation:

$$T = T_o + mR \tag{3.1}$$

where T is the calculated temperature, T_o is the temperature at zero resistance, m is the slope of the calibration line and R is the measured resistance in kΩ.

4.1.4 Moisture Content

Gravimetric moisture contents were measured for all solid samples collected (n = 74). Samples were weighed when moist and after being oven dried at 100°C for 24 hours. Approximately 100 g of sample were used for each measurement. Soil samples collected in August 2002 (n = 20) were freeze-dried at the National Water Research Institute (NWRI) in a Labconco Freezone 12-L freeze-dry system to minimize exposure to oxygen during drying.

Three diviner access tubes were installed on top of South Bison Hill within a 3-m radius of the 30-D3-C gas probes in June 2002 to a depth of 1.6 m. Holes were hand-augered using a small auger head (50 mm diameter) and thin-walled 50 mm ID PVC tubes were pushed into the holes and a bentonite seal placed around the tube at the top of the hole. After installation the clay formation swelled, forming a tight seal with the PVC tubes. The tubes

were plugged at the bottom and capped at the top to prevent moisture from collecting in the tube. Solid samples were collected at 0.25 m intervals (n = 20) at the time of access tube installation for gravimetric moisture content analysis. Volumetric moisture contents were measured approximately twice monthly using a Sentek Diviner 2000 moisture probe and computer throughout the 2002 field season. At present, the Diviner 2000 system uses a default calibration supplied by the manufacturer based on sand, sandy loam and organic potting soil. The default calibration will not yield absolute volumetric moisture content measurements but will reflect relative changes in moisture content.

A neutron access tube was installed in August 2002 on the top of SBH approximately 5 m south from the 30-D3-C deep gas probe nest. The access tube extends to a depth of 20 m and is constructed of carbon steel PQ drill rods. The tube was installed using a hammerhead drill rig supplied by Beck Drilling Co. The drill hammered down a 125 mm diameter steel casing to 20 m, the 71 mm diameter PQ rods were pushed down inside the casing and the casing removed. The clay formation swelled forming a tight contact with the steel rods. A bentonite seal was placed at the top of the tube to prevent water from preferentially traveling along the length of the pipe. Neutron counts were measured using a CPN Model 503 DR Hydroprobe in October 2002. Neutron counts were converted to volumetric water content using a linear calibration equation determined by the Alberta Research Council using aluminum access tubes. Aluminum tubing has count efficiency (K) of 1.0 and is the best material for neutron probe measurements. Due to the depth of the access tube required at this site and the drilling procedure required for installation, a stronger, more durable carbon steel tube was necessary. The K for carbon steel is 0.87. Equations 3.2 and 3.3 were used to convert calibration coefficients calculated using aluminum tubing to carbon steel tubing. The equations are as follows:

$$A' = A\frac{C_h - C_0}{K(C_h - C_0)} \tag{3.2}$$

$$B' = B\frac{A'}{A} \tag{3.3}$$

where: C_h is the count in an aluminum tube in a high moisture standard,

C_0 is the count in an aluminum tube in a zero moisture standard,

K is the efficiency term for the new tube type from the above table,

A' is the new A coefficient,

A is the aluminum A coefficient (representing slope),

B' is the new B coefficient,

B is the aluminum B coefficient (representing offset).

The new coefficients are then applied to convert counts to volumetric moisture content via:

$$M = A(r) + B \tag{3.4}$$

where: m = moisture and

r = count ratio (counts recorded/standard count).

Two shallow water wells were installed at the 30-D3-C site in June 2002 to detect if standing water existed within the peat/till cover or across the cover/shale interface. The water wells were constructed of 50 mm PVC pipe with screened ends. The screen was made by cutting slits on either side of the pipe at 1 cm intervals. Holes were hand-augered into the soil using a 50 mm auger tip and the PVC tube pushed into the hole. Bentonite chips were placed around the top of the hole and watered (for faster expansion) to create a seal with surrounding soil. The exposed tube end was covered with 50 mm PVC caps. The first well used a 1.55 m of pipe with 0.36 m of screen pushed into a 1.10 m hole. The second well used a 1.10 m pipe with 0.14 m of screen pushed into a 0.51 cm hole.

4.2 Solids Chemistry

4.2.2 Sample Collection

Drill core from the top of SBH was collected at approximately 1-m intervals to 25 m using a split-spoon sampler at the time of the deep gas probe installation (February 2001). Samples (n = 13) were split and placed in Ziploc bags. Norwest Laboratories analyzed one

sample set for moisture content, texture, pH, EC, total inorganic carbon (TIC), total organic carbon (TOC) and soluble salts (including Na^+, Ca^{2+}, Mg^{2+}, K^+, SO_4^{2-} and Cl^-) using the same methods as described in Sections 4.2.2 and 4.2.6. The other sample set was taken to Saskatoon and refrigerated until May 2001 when the samples were analyzed for moisture content, TIC, TOC, total S, CEC, soluble salts (including Na^+, Ca^{2+}, Mg^{2+}, K^+, SO_4^{2-}, Cl^-), soil $\delta^{13}C$ (total carbon and total organic carbon), and sulphide forms (electron microprobe analysis). Solid samples were also collected at the time of shallow gas probe (0.25 to 2.8 m) installations at 30-D2-A (mid-slope, 0.35 m cover, n = 12) in June 2001 and 30-D3-C (SBH plateau, n = 7) in July 2002. Solid samples were collected at 30-D2-A (mid-slope, 1 m cover, n = 8) and 30-D3-B (upper slope, n = 7) for chemical analyses in June, 2001.

Soil samples (n = 30, approximately 30 g each) were collected from the SBH plateau at the time of neutron access tube installation (August 2002). The samples were collected at depths from 0 to 25 m (1-m intervals) using both auger stem and split spoon sampling. To minimize oxidation, the samples were immediately placed in portable anaerobic chambers (Difco Laboratories) and flushed with nitrogen. Anaerobic reaction packets were placed in each container to remove any O_2 still present after flushing. Samples were transported to Saskatoon where they were freeze-dried at the National Water Research Institute and ground with a Retsch ZM-1 centrifuge soil grinder fitted with a 1.0 mm screen. The samples were transferred to a Coy anaerobic chamber for storage and saturated paste preparation.

4.2.3 Soluble Salts

Saturated extracts were used to measure concentrations of soluble salts. A 100-g sample was mixed with deionized water to saturation. Saturation was defined by Rhoades (1982) to be when the soil paste glistens as it reflects light, flows slightly when the container is tipped, slides cleanly off a spatula and consolidates easily by tapping the container after a trench is formed in the paste with a spatula. The saturated pastes were covered with paper lids and allowed to stand for at least 12 hours. The paste pH was measured using an Orion

250A pH meter. Two different methods were used to extract the leachate from the saturated pastes. For soil samples collected in February, 2001, the saturated pastes were transferred to Buchner funnels fitted with a no.41 Whatman filter paper and connected to an air vacuum system in the Soil Survey lab, Department of Soil Science, University of Saskatchewan. The leachate was halved and placed in containers for analysis. For soil samples collected in August 2002, the saturated pastes were placed in centrifuge containers and the pore waters were filtered through Whatman no. 42 filter paper using a 4B countertop centrifuge (International Equipment Co.) set at 3000 rpm for 3 hours. The leachate was filtered again through Whatman Nuclepore 0.45 μm filter paper and halved. The two sets of soil samples (February 2001 and August 2002 were analyzed in the same manner. One half of the sample was diluted 100 times and then analyzed for SO_4^{2-} and Cl^- concentration using a Dionex 2000 ion chromatograph in the Department of Geology, University of Saskatchewan. The other half of the sample was acidified with a single drop of concentrated HNO_3, diluted 100 times and analyzed in the Dionex 2000 for Ca^{2+}, Na^+, K^+ and Mg^+ concentrations. Concentrations were reported in mg/L of solid in solution.

4.2.4 Cation Exchange Capacity

The exchange capacity of the soil samples was tested using the barium chloride method approved by the Soil Science Society of America (Sumner and Miller, 1996). A 5-g sample was mixed in a glass flask with 100 ml of 0.5 N $BaCl_2$ extracting solution at a pH of 8. Flasks were then shaken by hand and left to stand overnight. The contents of each flask was then transferred to a Buchner funnel fitted with a no. 41 Whatman filter paper and connected to an air vacuum system in the Soil Survey lab, Department of Soil Science, University of Saskatchewan. The samples were washed with $BaCl_2$ extracting solution to produce 200 ml of leachate, which was stored in 250-ml Nalgene bottles. Each sample was washed with approximately 100 ml of water to remove excess $BaCl_2$, and then washed again with 200 ml of 0.5 N ammonia acetate (NH_4OA_C), to produce 200 ml of leachate. The leachate was weighed to determine solution volume and placed in 250 ml Nalgene bottles.

The concentrations of total exchangeable cations and the CEC of the samples were determined using Atomic Absorption spectroscopy (AA) in the Department of Soil Science. The leachate in $BaCl_2$ solution was diluted once with a 2.9 g/L lanthanum solution (La_2O_3) and analyzed for Ca^{2+}, Mg^{2+} and K^+ concentrations. For Na^+ concentration, samples were diluted with a 5g/L KCl solution between one and ten times depending on the concentration of Na^+ in solution. The exchangeable cation concentration was determined by subtracting the soluble cations (determined using saturated paste extractions) from the total cation concentration for each species removed during CEC analysis.

Ba^{2+} concentration was measured from the NH_4OAc solution using atomic absorption (AA). CEC (meq/100g of soil) was calculated using:

$$CEC = \frac{\left|Ba^{2+}(mg/L)\right| * volume\ of\ BaCl\ solution(L)\ added}{(mass\ of\ soil(g)) * (equivalents\ Ba^{2+})} * 100 \qquad (3.5)$$

4.2.5 Gypsum Content

The concentration of gypsum in the solid samples was determined using the multiple dilution procedure (Loeppert and Suarez, 1996). Three samples were chosen to represent the soil profile: 0.5 to 0.9 m, 5.8 to 6.4 m and 22.2 to 22.7 m. Each ground and dried sample was weighed into three 25-g portions. A saturation extract was prepared as above for each sample using one 25-g sample and the water extracted via centrifuge. Two more 25-g portions for each sample were weighed into 100-ml and 1-L flasks. One hundred-ml and 1-L of deionized water was added respectively. A rubber stopper was placed on the flask and the flasks were put on a reciprocating shaker overnight. Each of the suspensions was filtered through Whatman no. 42 filter paper and the filtrate collected. The filtrate samples were analyzed for SO_4^{2-} concentration using an ion chromatograph. The gypsum content was calculated from Loeppert and Suarez (1996):

$$SO_4(mmol) = \left(\frac{SO_4(mmol)}{L}\right) * \left(\frac{L}{1000mL}\right) * (mL\ deionized\ water) \quad (3.6)$$

$$SO_{4(g)} = SO_{4(DE)} - SO_{4(SE)} \quad (3.7)$$

where $SO_4^{2-}{}_{(g)}$ is sulphate from gypsum (mmol),

$SO_{4\,(DE)}$ is sulphate in dilute extract (mmol),

$SO_{4(SE)}$ is sulphate in saturation extract (mmol).

4.2.6 Total Sulphur

Total S concentrations were measured using a LECO CNS-2000 elemental analyzer located in the Department of Soil Science at the University of Saskatchewan. The LECO-CNS combusts S in the sample to SO_2, then measures the SO_2 concentrations with an infrared absorption detector. The detection range for S is 0.020 to 100 mg of S with a precision of 0.01 wt %. To calibrate the machine, 0.2000 to 0.2100 g standards (n = 4) of S-bearing plant material (0.768 % S) were covered with LECO ComCat catalyst to ensure complete combustion of S in the standard. The four standards were analyzed, and a correction was calculated for the drift between the S content of the standards.

4.2.7 Carbon

The total inorganic carbon content (TIC) and total organic carbon (TOC) concentrations were measured using a LECO CR-12 Carbonator carbon system in the Department of Soil Science, University of Saskatchewan. The CR-12 Carbonator combusts carbon in the sample to CO_2 and measures the CO_2 concentration with an infrared absorption detector. Furnace temperature for total carbon is 1100°C and 840°C for organic carbon. TIC

concentrations were calculated by subtracting TOC from total C concentrations. The detection range was 0.01 to 99.99 wt % with accuracy of ± 1 % of the carbon concentration. Sucrose (42.10 wt % organic C) was used for organic carbon calibration. $CaCO_3$ (12 wt % inorganic C) was used to calibrate the machine for total C analysis. Four standards were weighed to 0.1 g, analyzed, and a calibration equation calculated by the Carbonator. A standard was run every tenth sample.

4.2.8 Soil Carbon $\delta^{13}C$

Stable carbon isotopes ($\delta^{13}C$) of solid samples (n=15) collected at the time of the deep gas probe installation (February 2001) were measured using a Tracer/20 Mass-spectrometer coupled to an ANCA g/s/l sample preparation unit (Europa Scientific of Crewe, England) in the Department of Soil Science, University of Saskatchewan. Precision was +/- 0.1 ‰. For each sample, the $\delta^{13}C$ for TC and TOC were measured. The TIC was dissolved for $\delta^{13}C_{TOC}$ analysis using acid-digestion to convert the TIC to CO_2. A small portion of sample was soaked in an excess of 3 M HCl at room temperature overnight. The samples were leached four times with deionized water through a 45 μm filter under vacuum to ensure all chloride was removed from the sample. After each rinse the filtrate was treated with a drop of silver nitrate solution and checked for precipitate. If a cloudy precipitate was detected, rinsing was repeated until no precipitate was seen upon addition of silver nitrate. The samples were then dried and weighed into tin cups for mass-spectrometer analysis. The $\delta^{13}C_{TIC}$ of the soil carbonate was calculated using:

$$\left(\frac{wt\%TOC}{100}\right)*\delta^{13}C_{TOC}+\left(\frac{wt\%TIC}{100}\right)*\delta^{13}C_{TIC}=\delta^{13}C_{soil} \qquad (3.8)$$

4.2.9 Electron Microprobe Analysis

Electron microprobe analysis (EMPA) is a technique that uses x-ray excitation by a focused electron beam to chemically analyze small areas of solid samples. Electron microprobe analysis was done using a JEOL JXA 8600 Superprobe located in the Department of Geology at the University of Saskatchewan. The analysis was useful for identifying the

dominant sulphide mineral(s) present, their crystal form and approximate distribution in the till and shale.

Samples (n = 10) were prepared using two different techniques. To create slides with a smooth polished surface, four- 2-g samples were placed into 2-cm diameter hollow plastic rings with a piece of packing tape across the bottom. Excess sample grains were gently tapped off leaving a thin layer of sample adhered to the tape. A 1-cm layer of clear plastic epoxy was poured over the sample and allowed to dry overnight before the sample surface polished flat. Each sample was carbon coated before being placed in the electron microprobe for analysis.

The other six 2-g samples were poured onto double-sided tape covering the surface of a glass microscope slide. These samples were coated with carbon using a carbon coating machine and put into the electron microprobe for analysis.

4.2.10 Acid-Base Accounting

Acid-base accounting (ABA) is a method for calculating the acid-drainage potential of a waste pile. ABA measures the balance between the acid-generating and acid-neutralizing components of a soil (Morin, 1990). The test involves the measurement of the total S concentrations or S forms expected to contribute to soil acidity and a measure of the inorganic carbon expected to contribute to acid-neutralization. ABA is conducted with the assumption that all S in the form of sulphide will contribute to acidification. This assumption allows for a fast, cost-effective method of determining the acid-generating potential of a waste pile (Morin, 1990). The S concentrations are converted to consistent units (e.g. kg $CaCO_3$/tonne of soil) and the neutralization potential is subtracted from the net acidification potential to yield the net neutralization potential (NNP) (Steffen, Robertson and Kirsten, 1989). The conversion factor used to convert S (wt %) to kg $CaCO_3$/tonne of sample is derived from the standard equation for pyrite oxidation which requires 2 moles of H^+ to reduce one mole of S (Reaction 2.1). Converted to a molecular weight ratio this becomes 3.125 % $CaCO_3$:1 % S, or 31.25 (Morin, 1990). A negative NNP

indicates that the acidification potential of the soil exceeds the acid-neutralization potential and the soil is declared acid producing. However, NNP values between –20 to 20 kg $CaCO_3$/tonne of soil do not clearly indicate the ability of a soil to generate acidity. This range of uncertainty is attributed to errors in converting the sulphur to acidity and analytical error (Steffen, Robertson and Kirsten, 1989).

4.2.11 Quantifying O_2 Consumption and CO_2 Production Rates

The rate of O_2 consumption was estimated using Fick's first law for one-dimensional gas diffusion. The method was based on the assumption that all of the O_2 consumption within the South Bison Hill overburden pile was occurring at the till/shale interface. This assumption is valid if the peat/mineral mix and till contain negligible concentrations of reduced S relative to the underlying shale. As a result, atmospheric O_2 will diffuse through the peat/till cover without being consumed by sulphide oxidation reactions. The rate of diffusion through the cover is equal to the rate of O_2 consumption below the till/shale interface. The primary direction of diffusive transport though the till is vertical. Diffusive transport in the horizontal direction was not expected because the site was relatively flat-lying and was not situated proximal to steep side slopes. Therefore a one-dimensional transport model was considered sufficient to estimate the rate of O_2 consumption in the shale.

Fick's first law (Equation 2.15) states that, the diffusive flux (J) is directly proportional to the change in gas concentration over some distance (x). Assuming an atmospheric concentration of 20.9 % for O_2 and a volume of 1 m^3, the initial concentration of gas (C_o) can be calculated using the Ideal Gas Law:

$$PV=nRT \tag{3.9}$$

where P is the standard pressure of 1 atmosphere (101, 325 Pa), V is the volume the gas occupies (1 m^3), n is the number of moles of gas present, R is the universal gas constant (8.3144 J/mol K) and T is the temperature (°K). The change in concentration of O_2 and

CO_2 through the peat/till cover was determined from the pore-gas chemistry measured at the upper slope site (30-D3-B).

The effective diffusion co-efficient (D_e) was calculated using Equation 2.14. The diffusion coefficient for O_2 in free air (D_o) was taken to be $1.54 m^2$/day at 0°C, at 0°C (Wood and Petraitis, 1984; Birkham, 2002). The total porosity (n) for each media was estimated by:

$$1 - \frac{dry\ bulk\ density\ (kg/m^3)}{specific\ gravity(kg/m^3)} = n \tag{3.10}$$

The range of dry bulk density values for SBH peat/mineral mix, till and shale presented in Table 3.1 were used to estimate a range of porosity values for each media.

The air-filled porosity was calculated as:

$$n_a = n - volumetric\ moisture\ content \tag{3.11}$$

The converted gravimetric moisture contents measured for the peat/mineral mix, till and shale were used to produce a range of air-filled porosity values for each media which were used to estimate De and subsequently a reasonable range of estimated O_2 consumption rates in the shale. Subsequent salt release rates were related to the flux of oxygen by conservation of mass and stoichiometric conversions.

For comparison, salt balance calculations were performed using the solids sample chemistry from the anaerobic samples (collected at the SBH plateau in August 2002) to estimate the rate of salt release in the upper 3 m of the SBH shale. This calculation was based on the assumption that the concentrations of soluble and reduced S in the shale were relatively constant with depth at the time of pile construction. The difference in soluble and reduced S concentrations between the shallow (0 to 3 m) and deep (5 to 25 m) zones at the time of measurement was attributed entirely to sulphide mineral oxidation. Thus the rate of oxidation was estimated over the time elapsed since pile construction.

5 Results and Discussion

The results and discussion of the data are presented in this section. To provide a comparison between the natural environment and the overburden pile, the conditions at the natural site (Control-1) are discussed at the onset. Subsequently, the conditions at SBH are presented and contrasted to those from the natural site. For the overburden pile, the data collected from the two sites with the most detailed instrumentation (i.e., 30-D3-B and 30-D3-C; Figure 4.1) are discussed because these sites were the primary focus of this research. After discussing these data, the results from the middle slope positions (i.e., 30-D3-A and 30-D2-A; Figure 4.1) are briefly discussed to provide a comparison for slope positions and cover treatment. Because 30-D3-B and 30-D3-C sites were the focus of this study, O_2 consumption/CO_2 production rate calculations, acid-base accounting and salt-release calculations were only determined for these sites.

5.1 Control-1

5.1.2 Geology

The geologic profile for Control-1 is relatively simple (Figure 5.1). It consists of approximately 0.1 m of peat/mineral mix overlying >2.5 m (maximum depth of investigation) of medium to dark brown silty-clay till. The thickness of peat/mineral mix at this site was less than that commonly observed in mining lease 17. Its thickness is typically between 0.15 and 0.90 m of peat, muskeg or mineral soil overlying glacial till (Regier, 1976). The till in this region is commonly divided into two units, the upper Pleistocene material and underlying older till and varies in thickness from 3.2 to 5.0 m (Lord and Isaac, 1989). The individual till units were not distinguished during this study. They are lithologically inconsistent, incorporating elements of the McMurray Formation oil sands and Clearwater Formation clay shales as well as soft, glacio-lacustrine clays, silts sand and gravel.

5.1.3 Moisture Content

The converted gravimetric and volumetric (Diviner 2000) moisture content depth profiles for Control-1 are presented in Figure 5.1 and Appendix A. The depth to the water table was >2.35 m (maximum depth of instrumentation). The moisture contents determined from gravimetric measurements (Figure 5.1 a) were converted to volumetric moisture contents for comparison with Diviner 2000 volumetric moisture content profiles (Figure 5.1 b and c). Samples for gravimetric moisture content measurements were collected at the Div-1 site at the time of Diviner access tube installation (June 2002). The conversion calculation used the mean dry bulk densities determined by Boese (2003). The gravimetric moisture contents were converted using the following formula (Gardner, Methods of soil analysis Part 1, 1965):

$$\theta_{vol} = \theta_{grav} * \frac{(soil\ bulk\ density)}{(water\ density)} \tag{5.1}$$

where θ_{vol} is the volumetric moisture content, θ_{grav} is the gravimetric moisture content and water density is 1000 kg/m^3. The accuracy of the calculated volumetric moisture content strongly depends on the accuracy of the dry bulk density of the soil as well as upon the gravimetric moisture content value (Gardner, 1965). Given the variability of soil density, some error in the estimation of dry bulk density can be expected. Gardner (1965) cites reported coefficients of variation of 17 and 20 % for gravimetric moisture contents from field samples. As a result, some error was expected in the estimated volumetric moisture content values presented in this study.

The volumetric moisture contents calculated from gravimetric measurements were constant with depth, ranging from 20 to 25 % with a mean value of 23 % (n = 13, standard deviation = 1.7). The Div-1 Diviner moisture content measurements ranged from 4 % at 0.1 m below ground surface to a maximum of 54 % at 1.6 m (Figure 5.1 b). The maximum moisture content (54 %) was an anomalous data point collected in November 2002. More typically, the moisture content at 1.6 m was between 10 and 13 %. This anomalous data

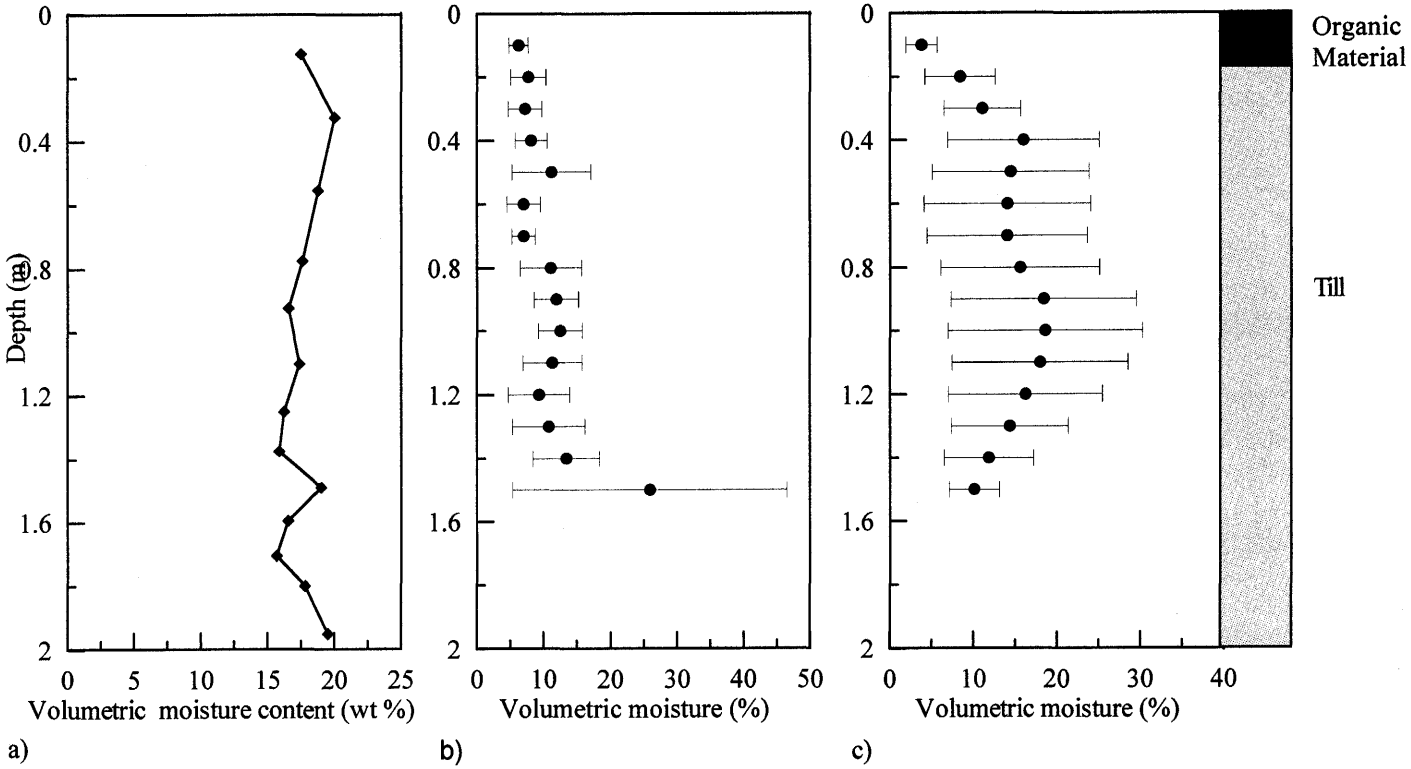

Figure 5.1: Control-1 moisture content profiles showing relatively constant moisture content with depth.
a) Volumetric moisture content profile from converted gravimetric data. b) Diviner 1 volumetric moisture content profile.
c) Diviner 2 volumetric moisture content profile. Circle symbols indicate mean values
+/- standard deviation (n=3). Depth to the water table was greater than 2.35 m
(maxiumum depth of instrumentation).

point might be the result of water present at the bottom of the access tube at the time of sampling. The mean moisture content for this profile was 11 % (n = 48, standard deviation = 4.6). The Diviner probe was approximately 10 % less than the converted gravimetric moisture content data. The difference between the Diviner data and the converted gravimetric data at this site was attributed to poor calibration of the Diviner 2000. As mentioned in Section 4.1.4, the Diviner probe was calibrated using a default factory calibration rather than specifically calibrated for the Control-1 soil profile. As a result, some discrepancy was expected between the converted gravimetric data and the Diviner probe data. The difference in moisture contents between the two sampling methods suggested that the Diviner probe overestimates moisture contents by approximately 10 %.

At Div-2, moisture contents ranged from 1 % at 0.1 m below ground surface to 34 % at 1.0 m. The mean moisture content was 14 % (n = 48, s.d. = 3.6). These results indicated that higher moisture conditions were present at Div-2 than at Div-1. Despite different moisture content values, both Div-1 and Div-2 moisture content profiles were constant with depth. The different moisture contents measured in Div-1 and Div-2 may be the result of natural heterogeneity at Control-1.

5.1.4 Pore gas O_2 and CO_2

The O_2 and CO_2 concentration depth profiles for Control-1 are presented in Figure 5.2 (a and b) and Table 5.2 (Appendix A). The O_2 concentrations varied between atmospheric (20.9 %) at surface and 19.4 % at 2.35 m below ground surface. The O_2 concentrations exhibited seasonal variations. Maximum O_2 concentrations occurred in July and August while minimum O_2 concentrations occurred in October and February. The seasonal variations measured in O_2 concentrations were even more pronounced in the CO_2 concentrations. Maximum CO_2 concentrations occurred in August and minimum CO_2 concentrations occurred in February. Concentrations ranged from 0.04 to 1.9 %. The greatest CO_2 concentrations generally occurred at 0.45 m depth and corresponded with the lowest O_2 concentrations.

Pore-gas O_2 and CO_2 concentrations measured at Control-1 were similar to those measured at an unsaturated clayey till site (Keller and Bacon, 1998) and an unsaturated sandy site (Hendry et al. 1999) located near Saskatoon, Saskatchewan. At the clay till site, the O_2 concentrations ranged from 20.9 and 19.5 % between surface and 2.5 m depth while CO_2 concentrations ranged from 0.04 and 1.0 % over the same depths. At the sandy unsaturated natural site CO_2 concentrations ranged between 0.04 and 1.2 % between 0.3 and 5.7 m below ground.

The seasonal variations observed in both O_2 and CO_2 concentrations at Control-1 were comparable to observations made by Hendry et al. (1999) and Keller and Bacon (1998). Gas concentrations at both of these sites exhibited similar seasonal variation. Maximum CO_2 concentrations were measured in July, while the minimum concentrations were measured in January. Seasonal variability observed at both of these sites was attributed to both root respiration and microbial activity. The similarity in seasonal variability at these sites and Control-1 provided additional support for suggesting that the gas trends at Control-1 were the result of root respiration and microbial activity.

5.1.5 $\delta^{13}C_{CO2}$

The $\delta^{13}C_{CO2}$ depth profile for Control-1 is presented in Figure 5.2(c) and Appendix A. The $\delta^{13}C_{CO2}$ at this site ranged from -17 and -21 ‰. No seasonal variability was observed in this data set (n = 5). Typically, the $\delta^{13}C_{CO2}$ from an organic source ranges from -26 to -20 ‰ (Craig, 1953). As a result, these data suggested that the pore gas CO_2 at Control-1 was derived primarily from an organic source. The slightly more positive $\delta^{13}C_{CO2}$ measured at 2.35 m below ground (-17 ‰) was attributed to CO_2 contributions from an inorganic carbon source.

The $\delta^{13}C_{CO2}$ results in this study were comparable to those of Hendry et al. (1999) and Keller and Bacon (1998) at natural unsaturated sites in central Saskatchewan. Hendry et al. (1999) measured a mean $\delta^{13}C_{CO2}$ of –23 ‰ (n = 14, s.d. = 0.24) on CO_2 collected from gas

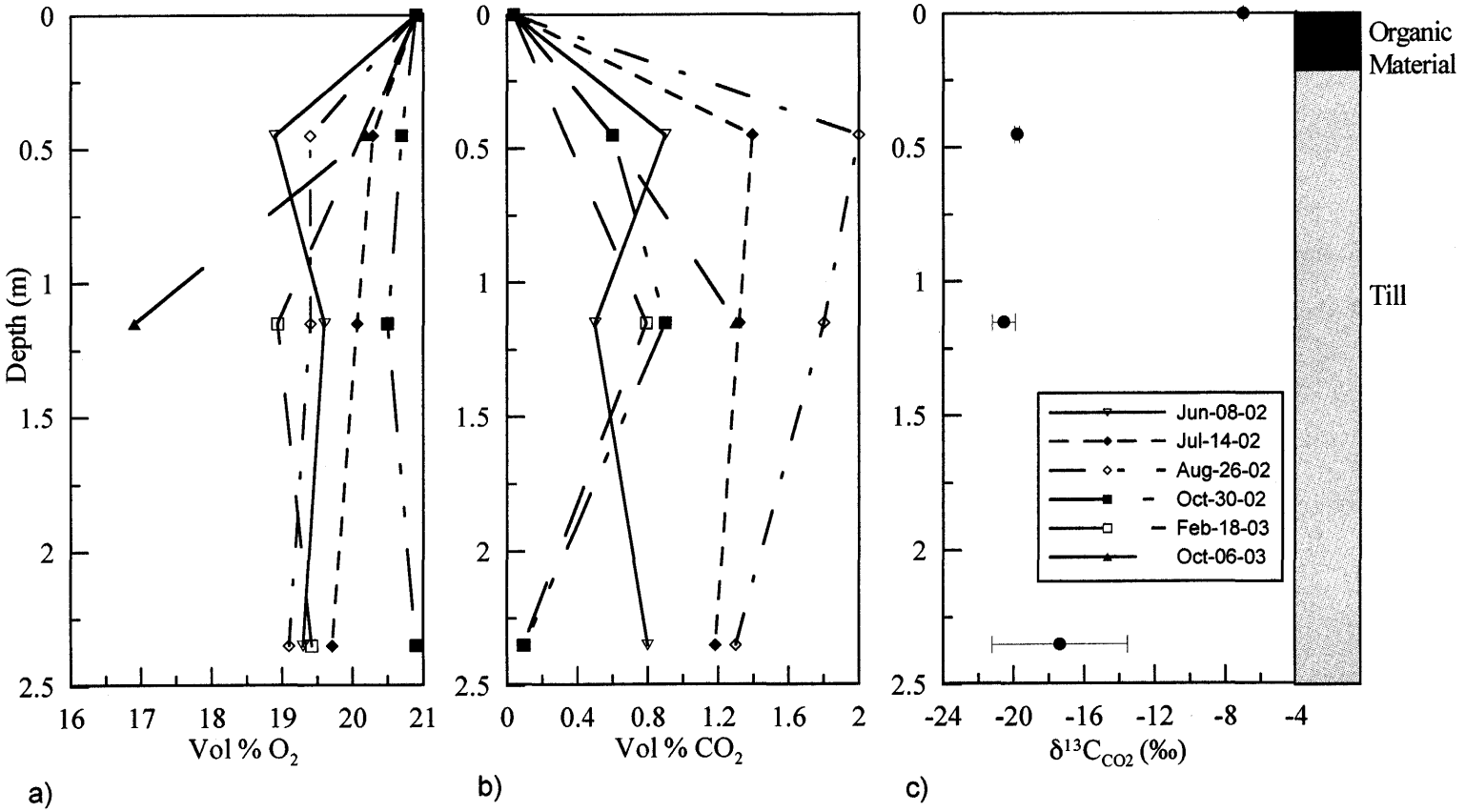

Figure 5.2: Control-1: a) O_2 concentration with depth. b) CO_2 concentration with depth. c) $\delta^{13}C$ profile with depth. Circle symbols represent mean values +/- standard deviation.

probe nests installed in a sandy unsaturated zone. The $\delta^{13}C_{CO2}$ measured at this site were determined to be in keeping with microbially produced and root-respired CO_2 (Hendry et al., 1999). Keller and Bacon (1998) measured $\delta^{13}C_{CO2}$ ranging from –21 to –20 ‰. Neither author observed seasonal variations in $\delta^{13}C_{CO2}$ values. In summary, moisture content, pore-gas concentrations and $\delta^{13}C_{CO2}$ results collected at Control-1 are in keeping with data collected at other natural sites (Hendry et al., 1999; Keller and Bacon, 1998).

5.2 South Bison Hill Plateau and Upper Slope Sites

5.2.2 Geology

The geology at the 30-D3-B (upper slope) and 30-D3-C (plateau) sites was described in detail in Section 3.3. The geological profile is presented in Figure 5.3. Both sites were treated with 0.8 m of glacial till followed by 0.2 m of peat/mineral mix. The peat/till reclamation cover was underlain by Clearwater Formation shale. Clearwater Formation shale was the primary overburden waste component in South Bison Hill.

5.2.3 Moisture Content

Moisture content data was collected using three different methods: gravimetric moisture content measurements on solid samples, neutron probe measurements and Diviner probe measurements (Appendix B). The results from each method are described and compared in this section. As noted in Section 3.3, the depth to the water table was approximately 30 m below ground surface.

The gravimetric moisture content profile was converted to a volumetric moisture content profile to allow comparison with neutron probe data (Figure 5.3 a and b). Two different gravimetric data sets were combined to produce one complete moisture content profile. The shallow moisture content data (0.0 to 1.65 m) were measured in June 2001, at the time of shallow gas probe installations (Figure 5.3 a). The deep moisture content data (0.75 to 22 m) were measured on soil samples collected at the time of neutron access tube

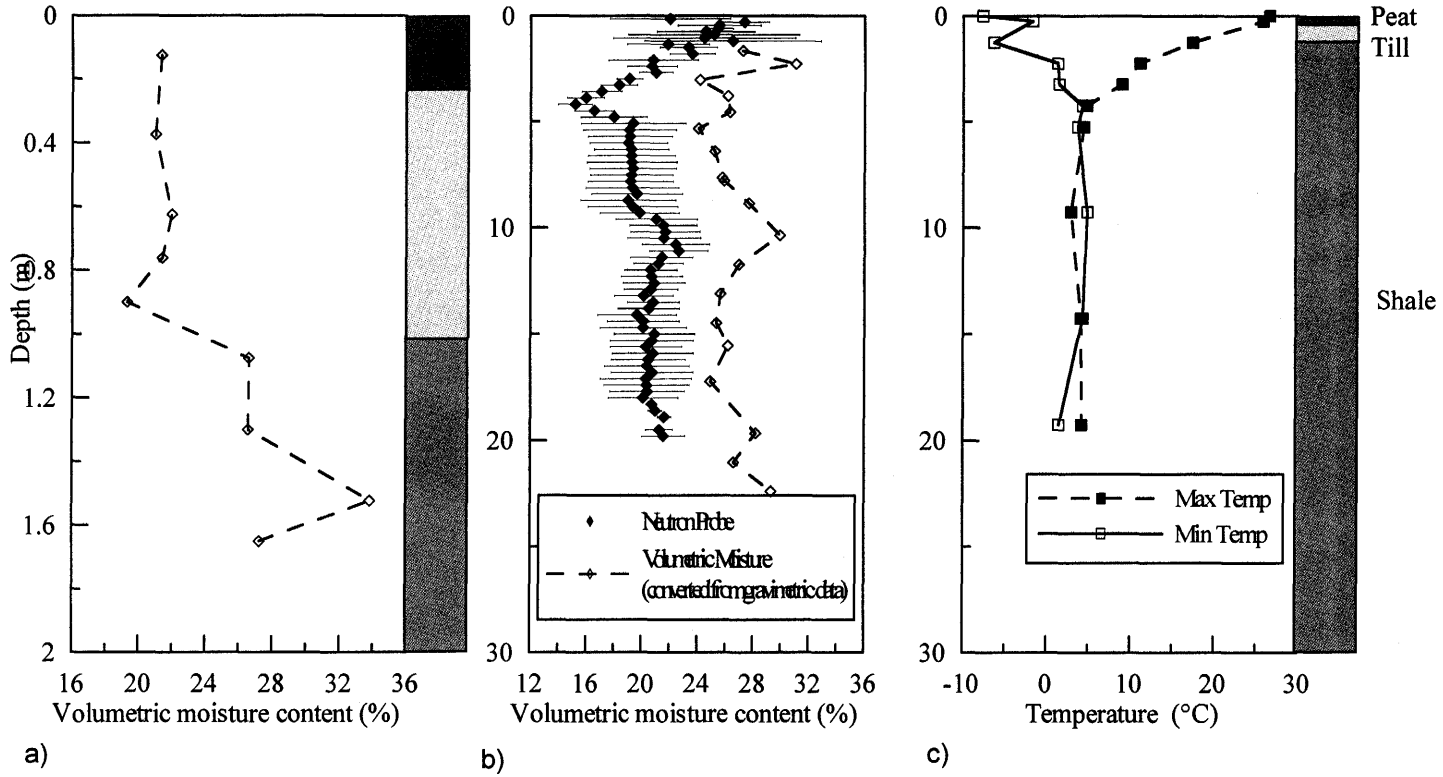

Figure 5.3:30-D3-C (SBH plateau) moisture content versus depth profiles. a) Shallow volumetric moisture content profile from samples collected June 2001. b) volumetric moisture content (n = 1) converted from gravimetric measurements indicating two distinct moisture content zones. The neutron probe depth profile indicated three distinct moisture content zones (n = 10). Diamond symbols represent mean values =/- standard deviation. c) Maximum and minimum temperature profiles measured between June 2002 and June 2003 (n=5). The inverted triangle represents the location of the water table (D. Chapman, personal communication).

installation (August, 2002). The use of two different data sets was necessary because detailed shallow (0 to 1.5 m) moisture information could not be collected during neutron tube installation. Therefore, the moisture data set from the previous summer (2001) was used.

Two different moisture content zones were observed in the converted gravimetric moisture content profile (Figure 5.3 b). Moisture contents ranged from 23 to 31 % in the till and upper shale (0.40 to 2.3 m below ground surface). Below 2.3 m, moisture contents ranged between 24 and 29 % to a depth of 22 m. The mean converted gravimetric moisture contents for the peat/mineral mix and till were 21 % (n = 1), and 22 % (n = 5, s.d. = 2.4) respectively. The mean converted gravimetric moisture content in the shallow shale profile (1.1 to 2.3 m) was 30 % (n = 4, s.d. = 3.0). Below 2.3 m (3.0 to 22.4 m), the mean converted gravimetric moisture content in the shale was 26 % (n = 21, s.d. = 1.6). The observed moisture content increase in the shale below the till/shale interface (1.0 to 2.3 m) may be attributed to the low hydraulic conductivity of the shale relative to the till. If this was the case, rainwater could percolate through the peat/till reclamation cover, but infiltration into the shale would occur much more slowly, resulting in a thin zone of increased moisture content directly below the cover/shale interface.

The volumetric moisture content depth profiles (n = 10) from neutron probe measurements for the deep profile (0 to 21 m) on the SBH plateau (30-D3-C) are presented in Figure 5.3 b. The volumetric moisture contents measured with the neutron probe exhibited no seasonal trends. The neutron probe data showed three distinct moisture content zones. Between ground surface and 2.1 m depth, moisture contents ranged from 22 to 27 %. Between 2.1 and 4.8 m below ground surface, moisture contents decreased from 20 to 15 % and below 4.8 m moisture contents remained constant at approximately 20 %. The presence of three distinct moisture content zones as indicated from the neutron probe data was attributed to the different soil media (peat/mineral mix, till, shale) in the shallow zone (0 to 4.8 m) as well as the effects caused by differing degrees of soil compaction. The mean volumetric moisture contents measured in the peat/mineral mix, till and shale with the neutron probe were 22 %, 25 % and 20 % respectively.

Compared to the converted gravimetric moisture content data, the volumetric moisture contents measured with the neutron probe were 4 to 9 % lower. The difference was attributed to two possible sources of error. First, the error induced from using assumed bulk density values for the peat/mineral mix, till and shale to calculate volumetric moisture contents may have affected the converted gravimetric moisture contents. Secondly, the limited sensitivity and difficult installation of the steel neutron access tube may have resulted in less accurate neutron moisture measurements. Steel is a less efficient media for neutron measurements than aluminum (the most commonly used tube type). Although a correction formula for steel was applied (Section 4.1.4), error in the measurements was still possible. The access tube must be in good contact with the soil throughout its length. The 125 mm bore hole required for the installation of the tube may have been larger than the swelling capacity of the shale. As a result, consistent contact between the tube and the soil over its length was not ensured. The major difference between the gravimetric and neutron probe data was that the neutron probe suggested three different moisture content zones were present (0 to 2.1 m, 2.1 to 4.8 m and 4.8 to 21 m), whereas the gravimetric data suggested two different zones. The difference between the gravimetric and neutron probe moisture content profiles may be indicative of sampling technique. The neutron probe measurements, collected every 0.3 m throughout the profile, yielded a much more detailed profile than that of the gravimetric data. Thus it is possible there were not enough data points in the gravimetric profile to detect the subtle difference in moisture content over the short distance of approximately 2 m.

The mean porosities calculated for the peat/mineral mix, till and shale from data collected by Boese (2003) were 64 %, 50 % and 46 % respectively. Using the volumetric moisture content data and these porosities, it was possible to estimate the degree of saturation in each media throughout the profile for both the neutron probe and the converted gravimetric data sets.

The neutron probe data in this study indicated that on average, the peat/mineral mix layer was approximately 34 % saturated and the till was 50 % saturated. Between 1.05 and 1.80

m, the average moisture content data indicated that the shale was 51 % saturated. Below 1.80 m (1.8 to 19 m), the average degree of saturation in the shale was 44 %. These results suggested that elevated moisture content conditions existed in the shallow soil profile (0 to 1.80 m) for the duration of the study. The results also indicated that there was a higher degree of saturation present in the upper 0.8 m of shale than was present in the remainder of the soil profile. The converted gravimetric moisture content data indicated that the peat/mineral mix and till were 72 % and 57 % saturated respectively. The data also indicated that the shale was 77 % saturated between 1.1 and 2.3 m below ground surface. Below 2.3 m, the shale was 54 % saturated. Both the neutron probe and converted gravimetric moisture content data indicated a higher degree of saturation existed in the top 1 m of the shale profile (approximately 1.0 to 2.3 m). The converted gravimetric data indicated that the shale was at a higher degree of saturation throughout depth in the profile (70 % compared to 44 %) than the neutron probe data. Again, this discrepancy was likely a result of the different measurement methods.

Volumetric moisture content profiles (mean +/- standard deviation) versus depth profiles collected from the three shallow (0-1.6 m) Diviner access tubes at 30-D3-C are presented in Figure 5.4. As mentioned in Section 4.1.4, the Diviner 2000 probe was not calibrated for SBH media (the instrument was calibrated using a default calibration). These data exhibited no notable seasonal trends but did exhibit spatial variability over the short distance between the diviner access tubes (<3 m distance between tubes).

Mean Div-1 moisture contents (n = 14) ranged from 17 % at 0.2 m below ground surface to 55 % at 1.4 m depth. The Div-1 moisture content profile showed that moisture content increased with depth to the cover/shale interface (1 m below ground surface). Below 1 m, moisture contents remained constant to 1.6 m depth. The Div-2 moisture content profile did not show as distinct a moisture content increase within the shale as noted in Div-1. Div-2 moisture contents (n = 13) increased from 26 % at 0.2 m below ground surface to 54 % at 1.2 m depth. Below 1.2 m, moisture contents decreased to 31 % at the bottom of the tube

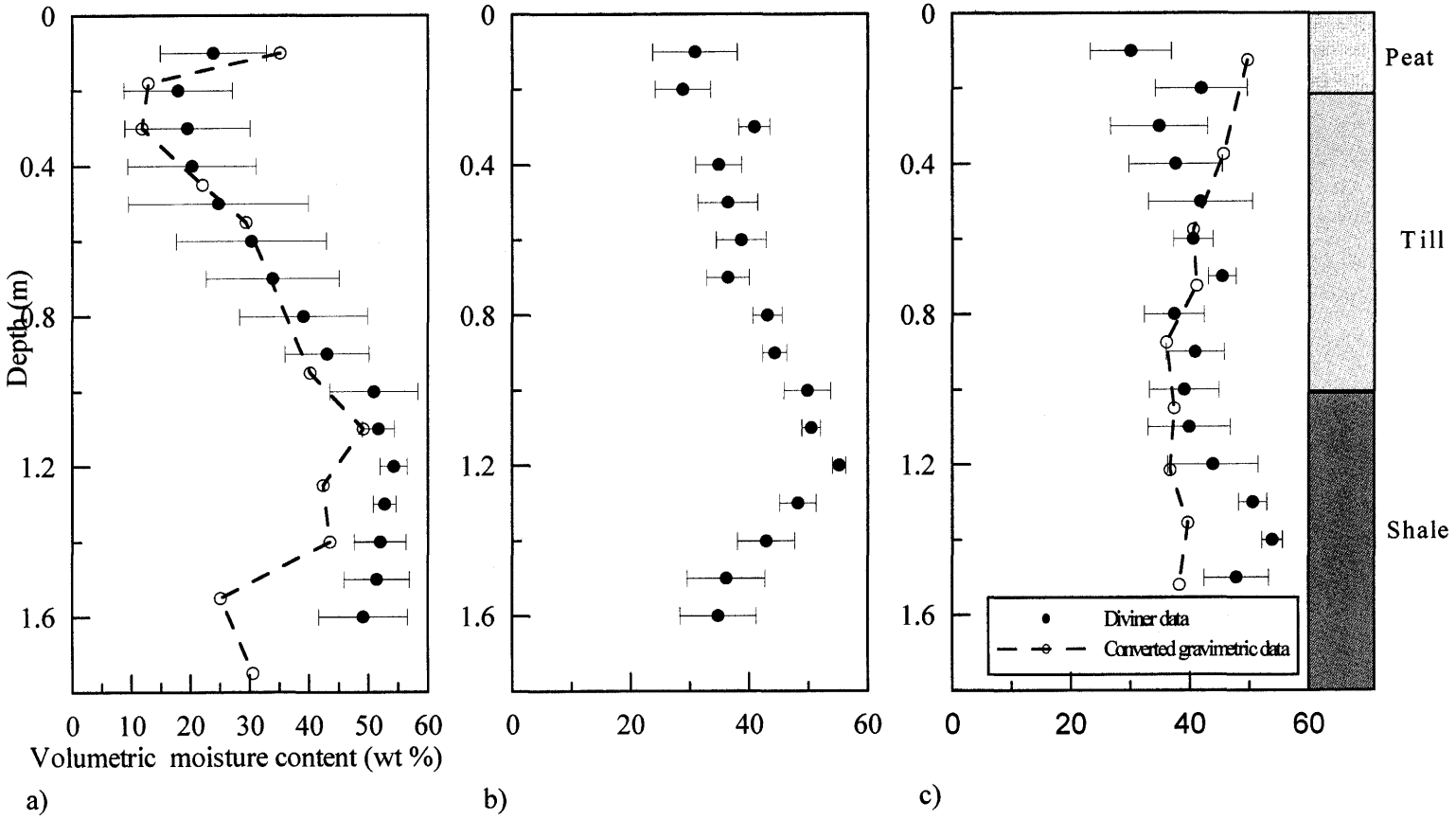

Figure 5.4: 30-D3-C: Volumetric moisture content profiles from Diviner data. a) Diviner access tube 1 (n = 14). b) Diviner access tube 2 (n = 13). c) Diviner access tube 3 (n = 14).

(1.6 m). In this profile, the maximum moisture content values occurred between 1 and 1.3 m below ground surface. The Div-3 profile yielded uniform moisture content measurements with depth. Values ranged from 25 to 52 %, with the greatest values occurring at 0.2 and 1.4 m (n = 14). The Div-3 profile showed the moisture content in the till (0.25 to 1.0 m) to be constant and only a slight moisture content increase was measured in the shale (1.0 to 1.6 m). The spatial variation exhibited by the three different Diviner moisture content profiles was attributed to soil heterogeneity and varying degrees of soil compaction. All three Diviner profiles showed a moisture content increase from the till to the shale (to maximum depth of 1.6 m). The increase in moisture content at 1.0 m (the cover/shale interface) was not observed at the control site. At Control-1, the Diviner profile indicated constant moisture content with depth, with the exception of the reading at 1.6 m. The increased moisture at 1.6 m was attributed to water in the bottom of the access tube. These data indicated that there is a difference in moisture content profiles between the disturbed (30-D3-C) site and the undisturbed natural site (Control-1).

Gravimetric moisture content measurements were made on solid samples collected at the time of Diviner access tube installation (Div-1 and Div-3 only). The gravimetric moisture content depth profiles for Div-1 and Div-3 were converted to volumetric moisture content as described by equation (5.1) and are presented in Figure 5.4. The resulting volumetric moisture contents for Div-1 ranged from 12 % at 0.15 m to 47 % at the cover/shale interface, 1.0 m below ground surface. These data indicated that the Diviner probe measured moisture contents to be approximately 5 to 10 % higher than those calculated from gravimetric measurements. The volumetric moisture contents calculated from gravimetric measurements for Div-3 ranged from 11 % at 0.13 m to 38 % at 1.3 m. These data indicated that the moisture content at Div-3 was approximately 15 % less than measured with the Diviner probe. Both profiles showed that the converted gravimetric and Diviner moisture measurements were similar through the peat/till cover. Below 1 m depth, the Diviner measurements in Div-1 and Div-3 are significantly different than the converted gravimetric measurements. These results indicated that it was not possible to estimate the calibration error in the Diviner probe by comparison with converted gravimetric measurements. The Diviner 2000 is a capacitance probe. It detects changes in soil dielectric properties. As a result, the measurements are sensitive to changes in both

temperature and salinity. The small sphere of influence of the Diviner probe requires that the outer walls of the access tube be in very good contact with the soil and can result in erratic data points. The difference between the Diviner probe and converted gravimetric moisture content in the shale was attributed to the effect of salinity on the Diviner probe measurements.

The shape of the volumetric moisture content profiles produced from the gravimetric measurements were similar to profiles produced from the Diviner 2000 data. The discrepancy between Diviner and calculated volumetric moisture contents may be attributed to calibration error, error in the estimation of dry bulk density values or the presence of salts in the soil solution. The results suggested that the default calibration used with the Diviner probe might either overestimate or underestimate actual soil moisture content depending on the salt concentration in the pore water. Diviner and gravimetric data collected at Control-1, indicated an underestimation of moisture content by the Diviner probe by approximately 10 % compared to converted gravimetric data. These results are similar to those of Div-3 on the SBH plateau. Thus Diviner data collected at all sites could not be used to represent actual moisture contents and must be viewed as relative data only.

Diviner moisture content measurements from Div-1, Div-2 and Div-3 indicated that the shale was 100 % saturated. The Diviner probe measurements indicated that the shale contained more water (45 % +) than the estimated 46 % of available void space. All three Diviner profiles indicated that the degree of saturation in the peat/mineral mix ranged from 38 to 65 % and the till ranged from 40 % to 100 % saturated. These results indicated a higher degree of saturation in the peat/mineral mix and till compared with the converted gravimetric and neutron probe data. Again, this result was probably a reflection of the errors induced by the factory calibration. Volumetric moisture contents calculated from gravimetric data also indicated that the peat/mineral mix, till and shale were saturated at the time of Diviner tube installation.

Visual observations made during solid sample collection as well as surface observations made throughout the field seasons on the top of the pile also indicated saturated conditions

in the shale. Solid samples collected at the time of diviner tube installation showed extremely variable moisture contents, ranging from near saturation (excess water on surface of soil sample) to dry and crumbly. The surface topography on the SBH plateau was gently undulating as a result of soil compaction. Accumulation of precipitation in topographic low areas was observed after precipitation events throughout the study. Thus it was suspected that the variation in moisture content observed in the Diviner data might be a result of soil compaction and surface topography.

Over the course of instrument installation and moisture content data collection it was observed that the moisture content varied considerably between 0 and 2.5 m. Although elevated moisture contents were measured gravimetrically as well as volumetrically between 1 and 3 m, it was difficult to determine the exact depth of the increased moisture zone. Variable moisture content data suggested that this zone of increased saturation was discontinuous. Each method of moisture content measurement used in this study to determine in situ moisture content exhibited limitations. The Diviner moisture probe data showed the potential effects of salinity. In addition, the small sphere of influence makes the Diviner data erratic and more sensitive to poor contact between the access tube and the soil than the neutron probe. The larger sphere of influence of the neutron probe measurements will result in smoother data and slightly less sensitivity to the tube/soil contact zone. However, the use of a steel access tube and the difficulty ensuring good contact of the neutron access tube with the soil create some uncertainty in the accurate representation of in situ moisture content. It will be assumed, for the purpose of this study, that the gravimetric moisture content data is most accurate because it is not dependent on instrument calibration and correct tube installation.

The moisture content in the shale (20 to 24 %) was similar to those measured by Lord and Issac (1989) on disturbed Clearwater Formation sediments. They reported gravimetric moisture content values ranging between 20 and 23 %. In addition, core samples collected from the shale at SBH in February 2001 and analyzed by Norwest Laboratories yielded a mean gravimetric moisture contents of 20 % (n = 16, standard deviation =3.2). Assuming a bulk density of 1650 kg/m^3 (Norwest Laboratories, 2001) for the shale, the mean

volumetric moisture content for these data was 33%. This value is also very similar to those measured in this study.

The SBH volumetric moisture content (typically between 21 and 30 %) was similar to other moisture measurements collected in unsaturated clay soils. Shaw and Hendry (1998) measured moisture contents between 20 and 27 % for clay in Southern Saskatchewan. Typically, in mine waste piles the range of moisture content is 5- 25 % (Ritchie, 1994), but these are typically very coarse materials and not comparable to the clay and till media present at SBH.

The two shallow water wells installed in June 2002 at 30-D3-C (0.51 m and 1.5 m) were observed to be full of water on the subsequent sampling date (July 2002) and remained full for the duration of the study (July 2002 to June 2003). The water levels were measured at 0.66 m and 0.25 m below ground in the deep and shallow wells. The presence of water in these wells throughout the study suggested that water may have accumulated at both the peat/till interface and across the cover/shale interface. The shallow gas probes installed at 30-D3-C in July 2002 (0.35 to 2.70 m) were plugged by August 2002 (with the exception of 2.70 m which was plugged immediately after installation). This suggested the accumulation of water at shallow depths. The water present in the shallow water wells was in keeping with the high moisture content below the cover/shale interface.

5.2.4 Temperature

The maximum and minimum temperature profiles measured at the 30-D3-C deep site (0 to 20 m) (n = 5) are presented in Figure 5.3c. Temperature fluctuations, attributable to seasonal temperature changes, were observed within the top 5 m of the profile. Below 5 m, the temperature remained relatively constant, ranging between 0 and 2°C.

The temperature results at 30-D3-C were similar to those measured by Hendry et al. (1999) at a natural site near Saskatoon, Saskatchewan. Thermistors installed between 0.75 and 7.2 m depth (at approximately 1.5 m intervals) indicated that below 1.52 m, subsurface

temperatures did not go below 0°C. The greatest temperature fluctuations were measured between 0 and 1.52 m depth. Below 4.5 m, only small variations in temperatures were observed. The temperature profile at 30-D3-C was also similar to profiles measured at the Key Lake mine in Saskatchewan (Birkham, 2002) and at the Aitik mine in Sweden (Ritchie, 1994b). At both of these sites, sub-surface temperatures stabilized below 10 m between -1 and 6°C. These results imply that the 30-D3-C temperature profile was comparable to both natural and mine-waste sites located in the northern hemisphere.

5.2.5 Solid Sample Analysis

5.2.5.1 Sulphur

The production of salts in geologic deposits is closely linked to the oxidation of reduced sulphur (Hendry et al., 1986; Mermut and Arshad, 1987; Curtin et al., 1994). To determine the mass of salts produced at SBH and the potential for additional salt generation, the total sulphur concentration and its forms were characterized. Three forms of sulphur are commonly determined: soluble sulphur (sulphate), sulfidic (pyrite), and organic (Bardsley and Lancaster, 1965). In the current study, soluble sulphur and total sulphur were measured. The difference between the two values was attributed to reduced S (organic S + sulfidic S). This approach is commonly used in the literature (Wagner, 1982; Mermut and Arshad, 1985). To test for the presence of sulphide minerals, samples were also analyzed using EMPA.

Two sets of solid samples were collected at 30-D3-C (SBH plateau) for total S and sulphur forms. The first set of samples was collected in February 2001 and the second set of samples was collected in August 2002. The same sampling method (split spoon sampling) was used in both cases, however, the storage and drying of the samples differed (see Section 4.3.2 for details). During the collection of the first set of samples, no attempt was made to maintain the samples under anoxic conditions. They were collected and stored in Ziploc bags at 4°C for four months prior to being oven-dried, ground and analyzed. Total S was determined using a LECO CNS analyzer in the Soil Science department (University of Saskatchewan). Sulphate concentrations were determined using the saturated paste extract

method. Saturated pastes were prepared and left to stand overnight in the laboratory. Pastes were then transferred to Buchner funnels and extracted using a countertop air-vacuum system in the Soil Survey lab (University of Saskatchewan). In contrast to this set of samples, the second set of samples was immediately placed in portable anaerobic chambers in the field. Once they were in the laboratory, they were immediately frozen to -60°C. Samples were then freeze-dried, ground and placed in a Coy anaerobic chamber. Total S concentration was determined using a LECO CNS analyzer in the Soil Science department (University of Saskatchewan). Saturated pastes were prepared in the anaerobic chamber, placed in sealed centrifuge containers and removed from the chamber for extraction in a 4B countertop centrifuge. Sulphur concentrations in the paste extracts were conducted as described above.

Sulphur results from the first set of samples are presented in Figure 5.5 a and Appendix C. Shale samples were collected between 1.74 and 24.25 m below ground surface. Total S concentration in the shale ranged from 4.1 to 12.8 g/kg, with a mean of 7.7 g/kg (n = 13, s.d. = 2.3 g/kg). The total S profile for this set of samples showed variable concentrations with depth. These variations in concentrations were most likely reflective of heterogeneity within the shale, with the exception of the sample collected at 24.25 m depth (0.33 g/kg S). The total S in this sample was an order of magnitude less than all other samples in the set. It was possible that an error in sample analysis occurred. At present, no explanation for this anomalously low S concentration is apparent.

The sulphur results measured from the second set of samples are presented in Figure 5.5 b and Appendix C. Total S concentration ranged from 4.5 to 12.8 g/kg in the shale. The greatest total S concentration was measured at 3 m below ground surface and S concentration increased between 1 and 3 m. Below 3 m, total S concentration in the shale remained constant at approximately 7 g/kg with depth to 25 m below ground surface. The mean total S concentration in the shale was 6.8 g/kg (n = 19, s.d. = 1.7 g/kg). Total S in the two till samples analyzed (0.61 and 0.99 m) were below instrument detection (<0.02 mg/g soil).

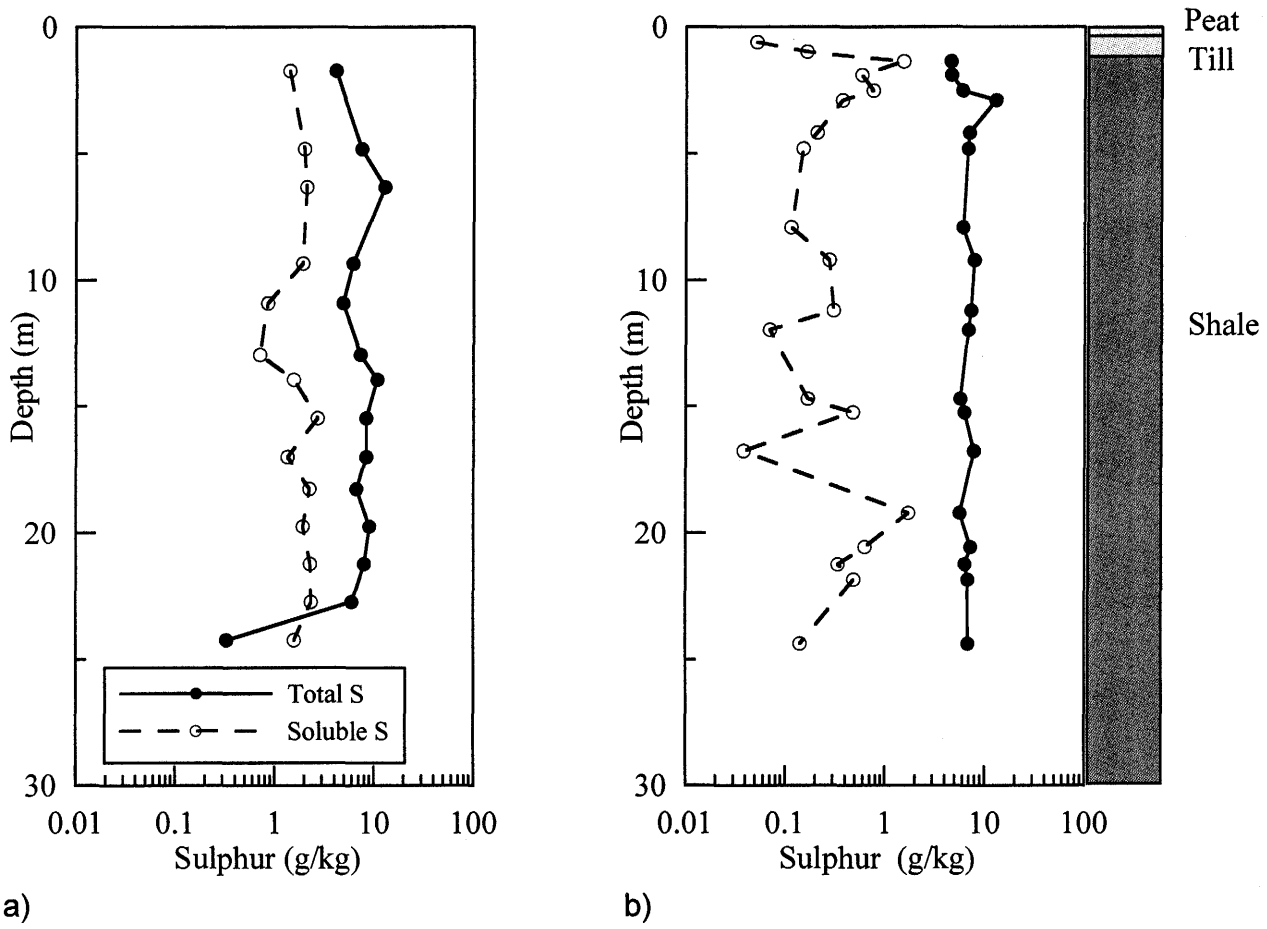

Figure 5.5: 30-D3-C (SBH plateau): Comparison of Total S and soluble S profiles with depth measured in two separate sets of soil samples. a) Total S and Soluble S concentration profiles for the first set of samples (collected February 2001). b) Total S and Soluble S concentration profiles from the second set of samples (collected August 2002). The soil samples collected in February 2001 were transported, stored and processed in atmospheric conditions whereas soil samples collected in August 2002 were transported, dried and processed in anaerobic conditions.

A comparison of total S concentrations in the two sample sets was done using Student's t-test (Appendix H). A comparison of the mean shale total S concentrations calculated from the two sample sets indicated that the two sample sets were statistically the same at a 0.05 level of significance. Mermut (unpublished data) reported Cretaceous marine shale in southern Saskatchewan to contain between 0.4 and 13.3 g/kg total S. The total S concentrations measured at 30-D3-C (SBH plateau) were within the range of these data. The total S concentration in Pleistocene till material in southern Saskatchewan was measured to contain between 0.6 and 16.2 g/kg total S (Mermut and Arshad, 1987). This study also found low S concentration (<2 g/kg) in the top 0.5 m of the 1 m thick till layer. Between 0.5 and 1.0 m, total S increased to 16 g/kg. The difference in S concentration in this study was attributed to sulphur relocation and oxidation (Mermut and Arshad, 1987). The total S profile with depth observed by Mermut and Arshad (1987) was similar to that observed on the SBH plateau (30-D3-C). At 30-D3-C, little or no S was measured between 0 and 1.2 m below ground surface. The greatest total S concentration occurred at 3 m depth.

Total S concentrations at 30-D3-C were less than the total S measured in typical mine waste piles. A typical mine waste pile is thought to contain approximately 25 g/kg (assuming an average bulk density of 1170 kg/m^3, Birkham 2002) pyritic S (not including other S forms) (Ritchie, 1994a). Total S concentrations in the SBH shale were comparable to S concentrations measured in gneissic waste rock (mean of 5 g/kg) at the Key Lake uranium mine in Saskatchewan (Lee et al., 2000). The difference between total S measured in the shale at the SBH plateau and typical mine waste piles was attributed to the different type of waste material. A typical mine waste pile investigated for AMD is composed of coarse grained gravel and rock (Ritchie, 1994; Birkham, 2002) whereas the SBH is composed of Cretaceous marine shale. The low total S values indicated that SBH shale should have a much lower acid-producing potential than the typical waste piles investigated for AMD.

The soluble S concentration versus depth profile for the first set of samples (Figure 5.5 b) was relatively constant with depth, ranging from 0.8 to 2. 7 g/kg. The mean soluble S concentration in this set of samples (n = 14, s.d. = 1. 65 g/kg) was 1.8 g/kg.

The soluble S concentrations for the second set of samples (Figure 5.5 b) ranged from 0.04 to 1.5 g/kg in the shale. The greatest soluble S concentrations were measured at 1.4 and 19.2 m below ground surface. Below 2.5 m, soluble S concentration was relatively constant with depth at approximately 0.4 g/kg with the exception of the sample collected at 19.2 m. This sample contained 1.7 g/kg soluble S. These results indicated that the reduced form of S dominated the shale throughout the soil profile, with the exception of the samples collected at 1.4 and 19.2 m. The elevated soluble S concentration at 1.4 m may represent sulphide oxidation that occurred in the shallow profile. The elevated soluble S concentration at 19.2 m may represent the location of a construction lift or a pause in construction of South Bison Hill. Either of these scenarios would have resulted in increased exposure to atmospheric O_2 concentrations (20.9 %), thus allowing near-surface oxidation of shale. The mean soluble S concentration in the second set of samples was 0.45 g/kg (n = 19, s.d. = 0.4 g/kg).

A statistical comparison of the two sets of soluble S data using Student's t-test indicated that the two sample sets were statistically different at a 0.05 level of significance (Appendix C). The difference in soluble S concentration profiles between the first and second set of samples was attributed to the differences in sample handling and storage. Studies have shown that extreme care must be exercise when sulphide mineral concentration in soil is to be determined (Bardsley and Lancaster, 1965) because some sulphides are easily oxidized to sulphate upon exposure to atmospheric oxygen. Freney (1958) found that sulphate concentration increased with air-drying. As a result, the second set of soil samples collected at 30-D3-C was handled to minimize oxygen exposure during sample collection and analysis. The soluble S results in this study suggested that sulphide oxidation had increased the soluble S concentration in the first set of samples to such an extent that the two sample sets must be considered different. These results were consistent with those of Freney (1958). The soluble S results from the first set of samples were important because

they showed that reduced S oxidizes to soluble S during sample storage and processing. The careful storage and handling of the second set of samples preserved the soluble S concentrations to as close to field values as possible. The S results from the second set of samples will be considered representative of field conditions for the purpose of this study.

The soluble S concentrations in the shale on the SBH plateau (3-D3-C) were similar to those reported by Mermut and Arshad (1987) for marine shale in southern Saskatchewan. Mermut and Arshad (1987) measured soluble S concentrations between 0.13 and 4.8 g/kg throughout an 8 m deep soil profile. The minimum soluble S concentrations were found to occur between 0 and 0.5 m below ground surface and the maximum concentrations occurred between 0.5 and 1.75 m (Mermut and Arshad, 1987). Below the oxidized zone (1.75 to 8.0 m), Mermut and Arshad (1987) measured a mean soluble S concentration of approximately 1.3 g/kg. The variation in soluble S concentration between 0 and 1.75 m was attributed to sulphide oxidation. All of the S present in this interval was in the form of sulphate, suggesting that sulphide had been oxidized to sulphate. Below the oxidized zone, the reduced S form was dominant (Mermut and Arshad, 1987).

The concentrations of soluble S measured in the second set of samples in this study were found to be less than those measured by Mermut and Arshad (1987) (0.4 g/kg compared to 1.3 g/kg below the oxidized zone). The difference in soluble S concentration was attributed to variation between the two different shale units studied. Clearwater Formation shale collected from the Syncrude mine site and analyzed by Mermut (unpublished data) contained between 0.02 and 2.2 g/kg soluble S. Thus, soluble S concentrations measured in this study were comparable with literature values for Clearwater Formation shale.

A geochemical investigation conducted by Regier (1976) on Syncrude overburden material indicated that peat/mineral mix and glacial till at Syncrude contained between 0.02 and 0.1 g/kg soluble S. A detailed soil profile (0.1 m increments) through the till layer (0.2 to 1.0 m) on the SBH plateau (S. Kessler, personal communication) indicated that the till contained an average of 0.14 g/kg soluble S. These results suggested that the reclamation

cover on SBH typically contained low soluble S concentrations and that the low concentration measured at 30-D3-C (0.6 m depth) was within literature values for the glacial till.

The reduced S concentration in the shale was calculated from total S and soluble S concentrations. This calculation was based on the assumption that any S not in the form of soluble S was in the form of reduced S (either sulphide mineral or organic S) (Wagner et al., 1982; Mermut and Arshad, 1987). A multiple dilution procedure was conducted to determine the gypsum concentration in the shale (Appendix D). This procedure eliminated the possibility of sulphate-S in the shale being present in the less soluble gypsum form. Sulphate-S incorporated in gypsum may not have been removed during saturated paste extraction and therefore would not be accounted for as soluble-S but would have been included in the total S measurement. In this case, the presence of significant gypsum would have produced an over-estimation of sulphide-S concentration. The results from the multiple dilution procedure for gypsum determination indicated that gypsum concentrations were negligible.

The reduced S concentration was calculated only for the second set of samples because this set was considered representative of *in situ* sulphur concentrations. The results are presented in Table 5.1. Reduced S concentrations in the shale ranged from 3.03 (1.4 m) to 12.43 g/kg (3.0 m), with a mean of 6.3 g/kg (n = 19, s.d. = 1.9). The reduced S concentration profile for sample set 2 was very similar to total S concentrations and indicated that the soil system at this site was dominated by the reduced- S form. This concentration was less than the 20 to 30 g/kg found in a typical mine waste pile (Ritchie, 1994a). However, less than 10 g/kg is still considered enough sulphide to produce acid in a waste pile (Ritchie, 1994a). Sulphide mineral concentrations measured in Cretaceous marine shale in Saskatchewan ranged from 0.1 to 11 g/kg soil (Mermut and Arshad, 1987). The reduced S concentrations measured at 30-D3-C (SBH plateau) were in agreement with the concentrations reported by Mermut and Arshad (1987).

Table 5.1: 3-D3-C (SBH plateau): Total S and soluble S concentrations measured in the second set of samples (collected August 2002). The reduced S concentration (organic + sulphidic S) was calculated by subtraction of soluble S from total S.

Depth (m)	g/kg		
	Total S	Soluble S	Reduced S
Till			
0.61	< 0.02	0.05	n/a
0.99	< 0.02	0.01	n/a
Shale			
1.37	4.53	1.52	3.03
1.91	4.58	0.58	4.01
2.52	5.91	0.75	5.17
2.90	12.80	0.37	12.43
4.17	6.99	0.21	6.80
4.80	6.79	0.15	6.62
7.93	6.04	0.11	5.93
9.22	7.87	0.28	7.60
11.20	7.26	0.30	7.03
11.97	6.83	0.07	6.76
14.71	5.68	0.17	5.51
15.24	6.25	0.48	5.35
16.77	7.77	0.04	7.74
19.21	5.63	1.71	4.40
20.58	7.21	0.63	6.52
21.27	6.32	0.34	6.00
21.88	6.74	0.48	6.23
24.39	6.83	0.14	6.64
Mean	6.78	0.46	6.32

EMPA analysis was used to determine the sulphide mineral assemblage present in the till and shale samples collected in February 2001. Pyrite was observed in trace quantities (<1 %) in the till and shale as finely disseminated framboidal grains (Figure 5.6 a and b). The one till sample analyzed was observed to contain less disseminated pyrite than the shale samples. Framboidal pyrite grains are a common occurrence in marine shale (Wilken and

Barnes, 1997). Framboids such as these are formed in an anoxic environment, in the presence of sulphate-reducing bacteria (Wilken and Barnes, 1997). The raspberry-like shape of the framboidal grains allows a larger surface area, thus enabling it to oxidize quickly (Moses et al., 1987; Nicholson et al., 1988; Nicholson, 1994). EMPA analysis confirmed that the principal sulphide mineral present in the till and shale was pyrite and that the pyrite is present as finely disseminated framboids (Table 5.2). Iron oxide minerals were also observed in the shallow shale samples (1.0 to 1.8 m), seen in many samples to coexist with pyrite. Concentrations of iron oxide minerals ranged from very trace (1 or two grains per sample) to equal abundance with pyrite (in shale sample collected between 1.0 to 1.14 m below ground). Iron oxide grains were not observed in samples collected deeper than 2 m below ground surface. These results were significant because they suggested that an oxidizing environment exists between 1 and 2 m in the shale.

Gypsum grains were also identified in trace amounts (<1 %) in the one till sample and four shale samples (Table 5.2, Figure 5.7). These observations were consistent with results from the multiple dilution procedure, which determined that gypsum was present in negligible quantities in the shale (Appendix D).

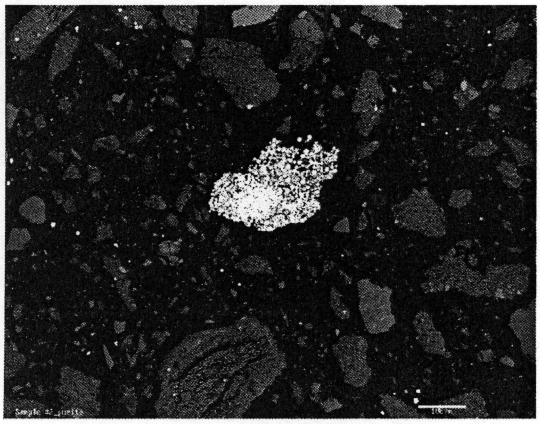

Figure 5.6a: Framboidal pyrite grain (centre, bright white) in a SBH shale sample collected between 16.7 and 17.2 m depth on the SBH plateau (February, 2001). Bright white grains in the peripheral show the average disseminated pyrite distribution in the shale.

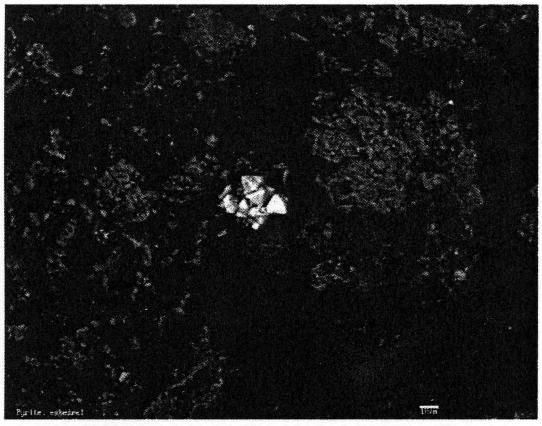

Figure 5.6b: A typical euhedral, framboidal pyrite grain (centre) within SBH shale. Sample was collected between 1.0 and 1.1 m depth on the SBH plateau (February 2001).

Figure 5.6c: Iron oxide grain (large white grain in centre of photo) seen in a shale sample collected between 1.2 and 1.6 m depth at the SBH upper slope site (June 2001). The bright white pyrite grains can be seen in the background.

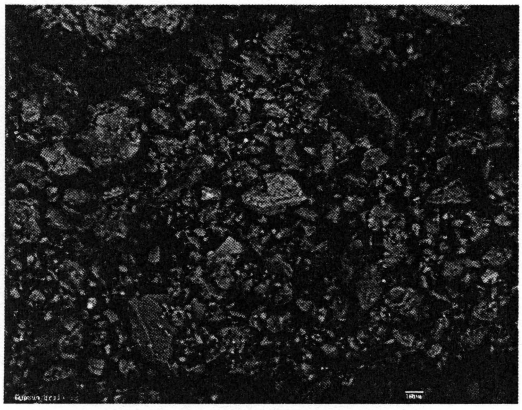

Figure 5.7a: Gypsum grain (large grey grain in centre of photo) seen in a shale sample collected between 1.75 and 1.95 m depth a t the SBH upper slope site (June 2001). The bright white pyrite grains can be seen in the background.

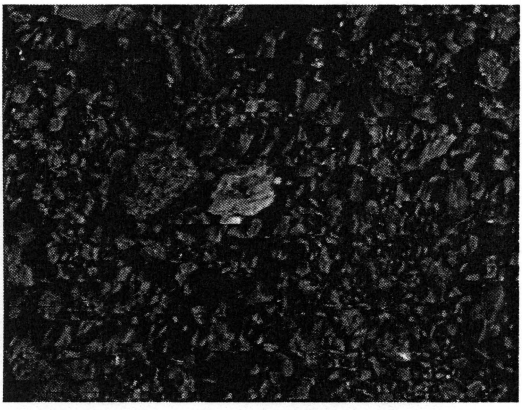

Figure 5.7b: carbonate grain (large grey grain in centre of photo) seen in a shale sample collected between 1.1 and 1.5 m on the SBH plateau.

Table 5.2: Key observations from EMPA for till and shale samples collected from the SBH plateau (30-D3-C) in February 2001 and 30-D3-B (SBH upper slope in June 2001.

Site	Sample depth (m)	Minerals observed
30-D3-C	0.25-0.5	Trace pyrite (less than observed in shale samples). Trace quantities of gypsum, iron oxides.
	1.05-1.1	Gypsum and pyrite abundant. Iron oxides slightly less frequent than pyrite.
	1.1-1.5	Iron oxides abundant. Less gypsum than in previous sample.
	1.57-1.75	Pyrite abundant and more frequent than iron oxides. Trace calcite, gypsum, and titanium oxide.
	16.80-17.23	Euhedral pyrite grains (more euhedral than at shallower depths). No iron oxide present.
	24.0-24.5	Little difference from previous sample. Evenly distributed, euhedral to subhedral disseminated pyrite grains. No iron oxides.
30-D3-B	1.0-1.14	Equal quantities of pyrite and iron oxides observed. Trace gypsum.
	1.14-1.5	Anhedral, subhedral and framboidal pyrite. Trace iron oxides, gypsum, and carbonate.

5.2.5.2 Carbon

TIC and TOC concentrations were measured on peat/mineral mix, till and shale samples collected at the time of the deep gas probe installations at 30-D3-C (February, 2001) as well as during the sampling campaign in August 2002. TIC and TOC was also measured on till and shale samples collected from the upper slope site (30-D3-B) in June 2001. For

simplicity, the detailed shallow TIC and TOC profile from the upper slope was combined with the deep soil samples (collected in February, 2001) to create one complete TIC and TOC profile (hereby referred to as the first set of samples). The depth profile of TIC and TOC concentrations for the peat/mineral mix, till and shale measured in the first set of samples is presented in Figure 5.8a. The depth profile of TIC and TOC from till and shale samples collected in August 2002 at 30-D3-C is presented in Figure 5.8b. TOC concentration in the shale remained constant with depth, ranging from 0.8 to 1.6 wt %. A statistical comparison of the TOC concentration in the two sample sets was conducted using Student's t-test. The results of the analysis indicated that the TOC concentration in the first and second sample sets (TOC data presented in Figure 5.8a and 5.8b) was statistically the same at a 0.05 level of significance. Therefore, the results of the two sample sets were combined. The TOC concentration in the peat/till cover of the first set of samples ranged from 0.5 to 3 wt %. Considerably more TOC was measured in the peat/mineral mix (1.3 to 3 wt %, n = 2) than in the till (0.5 to 0.6 wt %, n = 13).

The TOC concentrations measured in this study were comparable to concentrations reported in other soil investigations. The TOC in Syncrude shale overburden (Mermut 2000, unpublished data) ranged from 0.03 to 1.38 wt %. Marine shale studied at two natural sites in southern Saskatchewan contained TOC ranging from 0.3 to 6.2 wt % (Mermut and Arshad, 1987; Curtin and Mermut, 1985). At the two Saskatchewan sites the greatest TOC was measured between 0 and 0.25 m below ground surface, indicating that organic material had accumulated on the ground surface (Mermut and Arshad, 1987; Curtin and Mermut, 1985). The TOC in glacial till in southern Saskatchewan was reported to contain 0.55 wt % (Keller and Bacon, 1998), very comparable to till measurements at 30-D3-C. These results indicated that the TOC concentration present in SBH till and shale at 30-D3-C (SBH plateau) was within literature values for both disturbed and undisturbed sites composed of similar media.

A statistical comparison of means using Student's t-test was also conducted on the TIC results for the first set of samples and the anoxic samples (collected in August, 2002). The

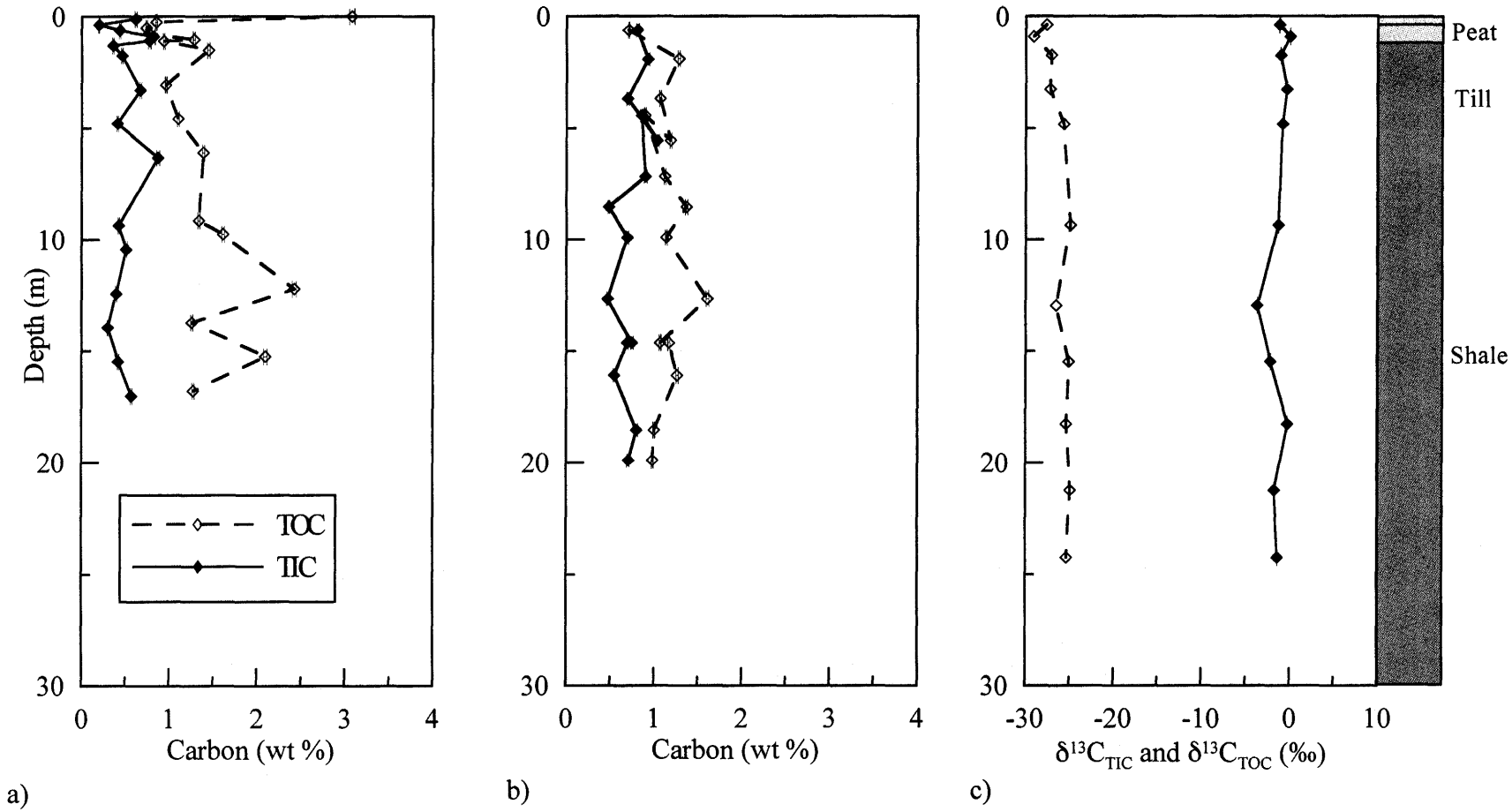

Figure 5.8: 30-D3-C (SBH plateau) TIC and TOC concentration profiles with depth. a) TIC and TOC concentration profiles measured in peat,till and shale samples collected February 2001 and June 2001. These samples were stored and processes in atmospheric conditions. b) TIC and TOC concentration profiles measured in till and shale samples collected in August 2002. These samples were stored and processes in anaerobic conditions. c) $\delta^{13}C_{TIC}$ and $\delta^{13}C_{TOC}$ (‰) measured on soil samples collected in August 2002.

results indicated that TIC concentrations in the two sample sets were statistically different at a significance level of 0.05. The difference was attributed to the differences in sample storage and handling. As mentioned in Section 5.2.3.1, exposure of soil samples to atmospheric conditions can result in the oxidation of reduced sulphur (Freney, 1958; Bardsley and Lancaster, 1965). The acid produced as a result of sulphur oxidation (Section 2.1) may be neutralized by carbonate mineral dissolution (Section 2.3). As a result, the TIC concentration in the soil samples exposed to oxygen for extended periods (4 months of storage) was less than the TIC concentration in the samples that were transported, stored and processed under anaerobic conditions. The TIC concentration in the first set of samples was not considered representative of field conditions and will not be used in this study.

The TIC concentration in the one till sample (collected August 2002) was 0.8 wt %. In the shale, TIC ranged from 0.4 to 0.8 wt % (n = 13) and remained constant with depth throughout the profile (1.9 to 19.9 m). Similar soil investigations at undisturbed sites by Mermut and Arshad (1987) and Shaw et al. (1998) reported variable TIC concentration in marine shale. Cretaceous marine shale in southern Saskatchewan was found to contain non-detectable amounts of TIC below 1.0 m in the 8.0 m deep soil profile studied (Mermut and Arshad, 1987). Shaw (1998) measured approximately 1.4 wt % TIC in Cretaceous clay material from southern Saskatchewan. The shale TIC concentrations measured in shale samples from the SBH plateau were between the two reported literature values. The one till sample collected compared well with the literature value of 0.02 to 0.5 wt % TIC measured in shallow glacial till (0 to 0.5 m depth) in southern Saskatchewan (Mermut and Arshad, 1987). The TIC results indicated that till and shale TIC concentrations measured at 30-D3-C (SBH plateau) were within reported literature values.

EMPA analysis identified inorganic carbon in shale samples (Table 5.2). Subhedral, rounded carbonate grains were a common occurrence in the shale, although concentrations were difficult to determine due to the grain similarity between gypsum, carbonate and feldspar (Figure 5.7 b and c).

5.2.5.3 Acid-base Accounting (ABA)

ABA calculations were conducted to evaluate the acid-generating potential of SBH overburden material. ABA measures the balance between the acid-generating and acid-neutralizing components of a soil (Morin, 1990). The ABA calculations are presented in Table 5.3. Pyrite concentrations calculated from total S and soluble S measurements (from the second sample set) were converted to kg $CaCO_3$ equivalent/tonne of soil based on the assumption that all S in the form of pyrite (i.e., reduced S) would be oxidized to SO_4 and the resulting acid neutralized by $CaCO_3$. The value of kg $CaCO_3$/tonne soil was determined from TIC analysis. The NNP in the shale ranged between -10 at 5.0 m and -3 at 13 m depth. The mean NNP was -6.3 (n = 16, s.d. = 1.8), within the inconclusive range of -20 and 20 (Steffen, Robertson and Kirsten, 1989). Within this range it cannot be clearly determined if a sample has an acidification or neutralization capability due to the errors and assumptions associated with this calculation. However, the negative NNP result in this study suggested that the acid generating potential may slightly exceed the carbonate buffering capacity in the shale.

Table 5.3: 30-D3-C (SBH plateau): Results from ABA on soil samples collected in August 2002. The Reduced S concentration (Table 5.1) was converted to kg/$CaCO_3$/tonne soil to be subtracted from measured $CaCO_3$ concentration. A negative NNP indicates the acid-generating potential of the waste pile has exceeded the carbonate-buffering potential. Mean and standard deviation are for shale samples only (samples collected between 1 and 20 m below ground surface).

Depth (m)	Kg $CaCO_3$ /tonne soil	Kg $CaCO_3$ equivalent /tonne soil	NNP
Till			
0.76	0.02	8.08	-8.06
Shale			
1.52	0.15	4.63	-4.48
2.29	0.20	9.26	-9.06
2.74	0.41	8.55	-8.14
3.05	0.23	6.71	-6.48
4.42	0.23	6.97	-6.74
5.03	0.20	10.36	-10.16
8.23	0.26	4.84	-4.58
9.45	0.24	6.91	-6.67
11.59	0.22	5.11	-4.89
12.20	0.19	4.69	-4.50
13.57	0.19	3.95	-3.76
14.94	0.20	6.90	-6.70
15.55	0.26	4.21	-3.95
17.23	0.19	5.68	-5.49
19.66	0.24	7.07	-6.83
Mean (shale)	0.23	6.39	-6.16
Std Dev (shale)	0.1	1.9	1.8

5.2.5.4 $\delta^{13}C_{TIC}$ and $\delta 13C_{TC}$

$\delta^{13}C_{TOC}$ and $\delta^{13}C_{TC}$ are presented in Figure 5.8c. The $\delta^{13}C_{TC}$ measured in the shale samples ranged between –18.5 and -23.6 ‰ (n = 9, s.d. = 1.8 ‰). After removal of inorganic C by acid digestion, $\delta^{13}C_{TOC}$ values in SBH shale material ranged between -24.9 and –27.2 ‰ (n = 9, s.d. = 0.86). The $\delta^{13}C_{TC}$ measured in the till samples ranged between –20.2 and –26.1

‰ (n = 2, s.d. = 3.0 ‰). After removal of inorganic C by acid digestion, $\delta^{13}C_{TOC}$ values in SBH till material ranged between –27.6 and –29.1 ‰ (n = 2, s.d. = 0.74 ‰).

$\delta^{13}C_{TOC}$ and $\delta^{13}C_{TC}$ for both the till and shale media were within the literature values of -30 to -24 ‰ found for most plant material (Clark and Fritz, 1997). $\delta^{13}C_{TIC}$ was calculated using mass balance and known TC and TOC concentrations for each sample (Section 4.3.7). The $\delta^{13}C_{TIC}$ in the shale ranged from -3.7 to 0.3 ‰, with a mean of -1.5 ‰ (n = 9, s.d. = 1.4 ‰). $\delta^{13}C_{TIC}$ in the till ranged from 0.07 to –1.2 ‰, with a mean of –0.5 (n = 2, s.d. = 0.6 ‰). These results showed a small variation in $\delta^{13}C_{TIC}$ within the SBH shale. The work of Craig (1953) and Hendry (2002) suggested that variation in $\delta^{13}C_{TIC}$ of carbonates was a result of fractionation by the shelly organisms forming the carbonate or the temperature at which carbonate is deposited.

The mean $\delta^{13}C_{TIC}$ in the shale was within the range of -5.9 to -0.4 ‰ measured in calcium carbonate from marine invertebrates (Craig, 1953) and the $\delta^{13}C_{TIC}$ values collected by Hendry (2002) on Jurassic carbonate cements (range -1.1 to +3 ‰). The mean shale $\delta^{13}C_{TIC}$ was within the measurable range of -6 to +6 for marine carbonate rock (Coplen et al., 2002).

5.2.5.5 Soluble Ions and Charge Balance Calculations

Soluble ion concentrations were measured on two different solid sample sets collected from the SBH plateau (30-D3-C). The first set of samples was collected in February 2001 and the second set of samples in August 2002 (Section 4.3.2). The soluble ion results collected from both sample sets are presented in Tables 5.4 and 5.5 and Figure 5.9. The TDS concentration in the shale from the first set of samples ranged from 3.98 to 12.33 g/kg and was variable with depth throughout the profile. The TDS concentration in the shale for the second set of samples ranged from 1.37 to 9.0 g/kg and was relatively constant at

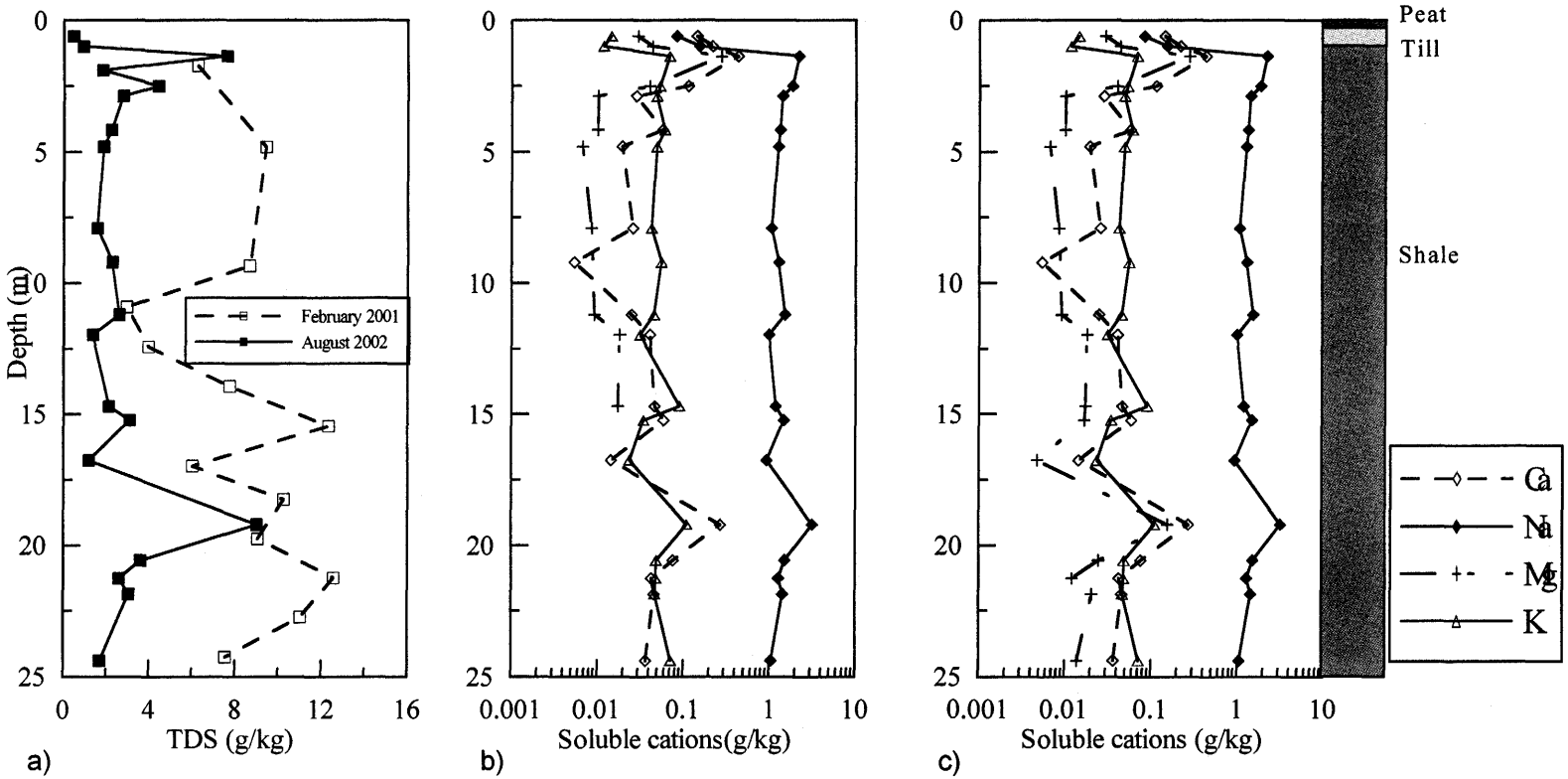

Figure 5.9: 30-D3-C (SBH plateau): Comparison of soluble cation and TDS concentrations in the soil samples collected in February 2001 (exposed to atmosphere) and August 2002 (processed under anaerobic conditions). a) TDS concentrations with depth for both sets of soil samples. b) Na, Ca, K and Mg concentrations with depth in samples collected February 2001. c) Na, Ca, K and Mg concentrations with depth in samples collected August 2002.

approximately 2.2 g/kg. The exceptions were samples collected at 1.4, 2.5 and at 19.2 m. The TDS in these three samples ranged from 4.4 to 9.0 g/kg. These results indicated that the TDS concentrations measured in the first set of samples were greater than the concentrations measured in the second set of samples. A Student t-test was used to statistically compare the means of the two data sets. The two sample sets were determined to be statistically different at a 0.05 level of significance (Appendix H). The difference was attributed to the different handling and storage techniques used with each sample set. This result supports the findings of reduced S and $\delta^{13}C_{TIC}$ presented in Sections 5.2.3.5 and 5.2.3.7. As a result, only the results from the second set of samples (those processed with minimal exposure to oxygen) will be considered representative of TDS concentrations at 30-D3-C (SBH plateau).

The soluble ion versus depth profiles (Figure 5.9) showed that Na^+ was the dominant soluble cation in the shale in both sets of samples. The Na^+ concentration in the shale measured from the first set of samples ranged from 1.04 to 3.60 g/kg. Concentrations varied with depth throughout the profile. In the second set of samples, the Na^+ concentration ranged from 0.9 to 3.2 g/kg in the shale. Na^+ concentrations were relatively constant throughout the profile, with the exception of two samples collected at 1.4 and 19.2 m. Na^+ concentrations in these two samples were 2.2 and 3.2 g/kg respectively, approximately 0.6 g/kg greater than those measured in the other shale samples. A Student t-test was conducted to compare the mean between the two sample groups. The two sets of samples were determined to be statistically different at a significance level of 0.05 (Appendix D). Similar to the TDS results, the difference was attributed to the different sample handling and storage techniques.

Two samples were collected from the till cover material (0.8 and 1.0 m) in August 2002. The Na^+ concentration in these two samples measured 0.08 and 0.15 g/kg respectively. The Na^+ concentration in the till cover was measured to be an order of magnitude less than in the shale.

The soluble Na^+ concentration measured at 30-D3-C (SBH plateau) was comparable to other literature values for unsaturated shale. A Cretaceous, interbedded shale and sandstone unit collected from a saline closed basin in northern Alberta contained between 0.5 and 4.0 g/kg Na (Miller et al., 1993). The maximum Na^+ concentration (4.0 g/kg) was measured at 0.19 m below ground surface. The elevated Na^+ concentration at this depth was attributed to upward salt migration (Miller et al., 1993).

Saturated paste results from shale collected in the first sampling period indicated that Ca^{2+} was the second most abundant cation. The Ca^{2+} concentration ranged from 0.04 to 0.44 g/kg. The Ca^{2+} concentration with depth profile indicated that concentration was greatest at 1.8 and 21.0 m. The significance of the elevated Ca^{2+} concentrations at these intervals was unknown. Shale from the same set of samples indicated Mg^+ and K^+ concentrations ranged from 0.01 to 0.3 g/kg. The depth profiles of soluble cations suggested that Mg^+ and K^+ concentrations were insignificant when compared to Ca^{2+} and Na^+. The Ca^{2+} concentration in shale samples collected at the second sampling period ranged from 0.02 to 0.43 g/kg, with a mean of 0.07 g/kg (n = 18, s.d. = 0.1). The greatest Ca^{2+} concentrations occurred at 1.4 m and 19.2 m depth, corresponding with elevated Na^+ concentrations. The Mg^+ and K^+ concentrations in the same set of shale samples ranged from 0.01 to 0.28 g/kg. The mean concentrations for Mg^+ and K^+ were 0.04 g/kg (n = 18, s.d. = 0.06) and 0.05 g/kg (n = 18, s.d. = 0.02). A statistical comparison of means for the two data sets was performed using Student's t-test. The results indicated that the Ca^{2+}, Mg^+ and K^+ concentrations were all different at a significance level of 0.05 (Appendix H). The difference between sample sets was attributed to the different methods of sample handling and storage.

Soluble ion results indicated that the samples collected at 1.4 and 19.2 m contained elevated soluble Na^+ and Ca^{2+} relative to the remaining shale samples in the profile. The elevated Na^+ and Ca^{2+} concentrations corresponded with the elevated soluble S concentrations at these depths. This suggested that elevated Na^+ and Ca^{2+} concentrations may have been the result of an oxidizing environment.

Two samples were collected from the till cover material (0.6 and 1.0 m) in August 2002 (sample set 2, Figure 5.6 b). Ca concentrations in these two samples were 0.14 and 0.22 g/kg respectively. The mean Mg and K concentrations were 0.04 g/kg (n = 2, s.d. = 1) and 0.01 g/kg (n= 2, s.d. = 7) respectively. These results indicated that the Ca^{2+} concentrations in the till were two times greater than the mean Ca^{2+} concentration in the shale. The Ca^{2+} concentrations measured in the till corresponded with the elevated Ca^{2+} concentrations at 1.4 and 2.5 m. The Mg^{+} concentrations in the till were comparable to those measured in the shale samples. The K^{+} concentrations measured in the till were less than half the minimum concentration measured in the shale samples. Thus, out of the four soluble cations analyzed (Na^{+}, Ca^{2+}, Mg^{+} and K^{+}), Ca^{2+} was the only cation present in greater concentrations in the till material than in the shale.

Table 5.4: 30-D3-C (SBH plateau): Soluble ion concentrations with depth measured from saturated paste extractions on shale samples. Samples were collected at the time of gas probe installation (February 2001), oven-dried and processed at atmospheric O_2 concentrations.

Average depth	**g/kg**						
(m)	**Ca^{2+}**	**K^{+}**	**Mg^{+}**	**Na^{+}**	**SO_4^{-2}**	**Cl^{-}**	**TDS**
Shale (SBH plateau)							
1.74	0.44	0.03	0.21	1.24	4.18	0.12	6.23
4.81	0.14	0.11	0.05	3.02	5.95	0.16	9.43
9.35	0.06	0.08	0.04	2.58	5.76	0.17	8.69
10.91	0.22	0.03	0.06	0.03	2.55	0.06	2.96
12.42	0.17	0.03	0.12	1.04	2.14	0.49	3.98
13.94	0.02	0.06	0.03	2.69	4.67	0.28	7.75
15.47	0.21	0.10	0.16	3.53	8.07	0.26	12.33
16.99	0.38	0.06	0.18	1.33	4.02	0.06	6.03
18.25	0.21	0.09	0.13	2.93	6.75	0.14	10.26
19.75	0.14	0.09	0.09	2.85	5.77	0.12	9.07
21.25	0.35	0.09	0.50	3.60	6.83	0.08	11.45
22.75	0.13	0.09	0.08	3.46	7.05	0.23	11.04
24.25	0.04	0.04	0.03	2.63	4.74	0.08	7.55
Mean	**0.22**	**0.08**	**0.12**	**2.49**	**5.27**	**0.18**	**8.22**

Table 5.5: 30-D3-C (SBH plateau): Soluble ion concentrations measured from saturated paste extractions on till and shale samples. Samples were collected in August 2002 and were transported, dried and processed under anaerobic conditions.

Average depth	g/kg						
(m)	Ca^{2+}	K^{+}	Mg^{+}	Na^{+}	SO_4^{2-}	Cl^{-}	TDS
Till (SBH plateau)							
0.61	0.14	0.01	0.03	0.08	0.15	0.02	0.47
0.99	0.22	0.01	0.04	0.15	0.49	0.01	0.93
Mean	**0.18**	**0.01**	**0.04**	**0.12**	**0.32**	**0.02**	**0.70**
Shale (SBH plateau)							
1.37	0.43	0.07	0.27	2.19	4.55	0.08	7.62
1.91	n/a	n/a	n/a	n/a	1.74	0.05	1.82
2.52	0.11	0.05	0.04	1.83	2.25	0.09	4.42
2.90	0.02	0.04	0.01	1.53	n/a	n/a	1.59
2.90	0.03	0.05	0.01	1.41	1.12	0.12	2.78
4.17	0.06	0.06	0.01	1.33	0.62	0.12	2.24
4.80	0.02	0.05	0.01	1.26	0.45	0.08	1.87
7.93	0.03	0.04	0.01	1.05	0.34	0.09	1.58
9.22	0.01	0.06	0.00	1.28	0.83	0.08	2.28
11.20	0.02	0.05	0.01	1.51	0.91	0.11	2.61
11.97	0.04	0.03	0.02	0.99	0.21	0.09	1.37
14.71	0.05	0.09	0.02	1.18	0.50	0.17	2.13
15.24	0.06	0.03	0.02	1.47	1.43	0.09	3.10
16.77	0.01	0.02	0.00	0.93	0.11	0.11	1.19
19.21	0.27	0.11	0.16	3.18	5.15	0.08	9.03
20.58	0.08	0.05	0.02	1.51	1.88	0.04	3.62
21.27	0.04	0.05	0.01	1.28	1.01	0.07	2.62
21.88	0.05	0.05	0.02	1.44	1.45	0.06	3.07
24.39	0.04	0.07	0.01	1.05	0.43	0.07	1.71
Mean	**0.08**	**0.05**	**0.04**	**1.47**	**1.37**	**0.09**	**3.05**

Ion balance calculations for the second set of soil samples are presented in Tables 5.6. A net positive charge was present throughout the soil profile, ranging between 20 and 50 meq/kg. The mean charge balance error (% CBE) was 40 %. The charge imbalance was attributed to bicarbonate ions (CO_3^{2-} and HCO_3^{-}), which were not measured in this study and are common ions in sodic soils (Bower and Wilcox, 1965; Wolt, 1994).

Table 5.6: Ion balance calculations on shale and till samples collected in August 2002. Results indicate that a net positive charge existed throughout the soil profile. The charge different was attributed to CO_3^2 and HCO_3, which were not measured in this study.

Average depth (m)	Total anions (meq/kg)	Total cations (meq/kg)	(Cations-anions)	% CBE
Till(SBH plateau)				
0.61	4.05	14.61	10.56	55
0.99	10.57	21.72	11.15	34
Shale (SBH plateau)				
1.37	96.96	144.90	47.94	19
2.52	50.16	92.68	42.52	28
2.90	27.50	67.87	40.36	40
4.17	17.17	66.32	49.16	57
4.80	11.67	59.82	48.16	66
7.93	9.65	52.48	42.83	68
9.22	19.72	60.64	40.92	50
11.20	21.95	71.97	50.02	52
11.97	6.84	49.69	42.85	75
14.71	17.20	62.23	45.03	54
15.24	32.29	71.87	39.59	36
16.77	5.36	45.19	39.83	77
19.21	109.51	174.47	64.96	22
20.58	40.26	75.69	35.43	30
21.27	24.96	64.05	39.10	43
21.88	31.98	69.61	37.63	36
24.39	11.38	52.56	41.18	63

5.2.5.6 Saturated Paste SAR and EC

Soil SAR was calculated for both the first and second set of samples. The SAR results are presented in Tables 5.7 and 5.8. The first set of samples contained only shale samples and the second set of samples contained both shale and till samples. Shale SAR values ranged between 15 and 60 in the first set of samples and did not show any trend with depth. Shale SAR values in the second set of samples ranged from 29 to 59. A statistical comparison of mean SAR values in the shale samples for the two sample sets was performed using

Student's t-test. Results indicated that the two sets of shale samples were statistically the same at a significance level of 0.05. Therefore, the SAR data from the two sets of samples were combined for further discussion.

The shale SAR results indicated that sodic conditions existed throughout the shale profile. As mentioned in Section 2.9.2, an SAR value of 13 or greater classifies a soil as sodic (US Salinity Laboratory Staff, 1954). The average SAR measured by Lord and Isaac (1989) on a Clearwater Formation soil sample collected from an overburden waste pile was 41. This value was similar to shale SAR values measured on the SBH plateau (site 30-D3-C).

Soil SAR was calculated for two till samples (0.6 and 1.0 m). The SAR in the till samples were 3 and 4 respectively, considerably less than that calculated in the shale. The limited data suggested that the sodic conditions observed in the shale did not extend to the till cover material.

Table 5.7: 30-D3-C (SBH plateau): Shale SAR calculations and EC and pH measurements from saturated paste extractions performed on the first set of soil samples (collected February, 2001). Soil pH was measured in the paste prior to extraction.

Average depth (m)	SAR	E.C. (dS/m)	pH
1.74	15	6.1	7.32
4.81	50	5.1	8.35
9.35	53	4.5	7.48
10.91	25	5.1	7.56
12.42	22	6.7	7.41
13.94	71	3.7	7.91
15.47	45	7.9	7.09
16.99	16	4.9	7.14
18.25	38	5.4	6.99
19.75	44	5.4	7.12
21.25	28	7.2	6.82
22.75	51	5	7.42
24.25	60	2.9	8.32
Mean	**38**	**5.4**	**7.5**

Table 5.8: 30-D3-C (SBH plateau): SAR calculated from the soluble cation results of saturated paste extractions performed on the second set of samples (collected August 2002). SAR was calculated for both till and shale samples.

Average depth (m)	SAR	ESP
Till (SBH plateau)		
0.61	3	1
0.99	4	
Mean	**3**	**1**
Shale (SBH plateau)		
1.37	29	9
1.91	n/a	
2.52	44	9
2.90	59	32
2.90	50	
4.17	32	15
4.80	46	20
7.93	37	
9.22	53	37
11.20	46	30
11.97	30	
14.71	29	33
15.24	40	
16.77	41	31
19.21	39	6
20.58	40	
21.27	38	
21.88	43	
24.39	31	27
Mean	**40**	**19**

The soil EC was determined from the saturated paste leachate. EC measurements were only made on the first set of samples (February, 2001). Results are presented in Table 5.7. These samples were oven-dried and processed in atmospheric oxygen concentrations. EC measurements for the shale ranged between 2.9 and 7.9 dS/m, with a mean of 5.4 dS/m (n = 13, s.d. = 1.3). The mean shale EC is within the range of EC defined by the US Salinity Laboratory Staff (1954) as saline (4 to 8 dS/m). As noted in Section 2.9, a saline soil

contains enough dissolved salts to affect plant productivity. The shale EC results in this study were similar EC other unsaturated shale EC values reported in literature. Curtin et al. (1995) measured EC ranging from 2.9 to 7.9 dS/m in irrigated shale in southwestern Saskatchewan. Mermut (unpublished data) measured EC on Clearwater Formation shale collected from the Syncrude mine site. EC in these samples ranged between 1 and 16 dS/m (Mermut, unpublished data). Mermut and Arshad (1987) reported EC values ranging from 1.3 to 10.9 dS/m in Cretaceous marine shale of southern Saskatchewan.

5.2.5.7 Saturated Paste pH

The pH of shale was also only measured in the first set of samples (February, 2001). The pH was measured in the saturated paste prior to extraction. Results are presented in Table 5.7. The shale pH ranged from 6.8 to 8.3 with a mean of 7.5 (n = 13, s.d. = 0.5). The pH was relatively constant with depth throughout the profile. These results were comparable with other unsaturated shale pH values determined from saturated paste analysis in literature. Mermut (unpublished data) measured pH ranging from 5.8 to 8.5 on Clearwater Formation shale collected from the Syncrude mine site. Mermut and Arshad (1987) measured paste pH ranging between 4.4 and 9.0 on Cretaceous marine shale collected from southern Saskatchewan. The pH on undisturbed Clearwater sediments measured by Regier (1976) ranged from 7.2 to 7.3. The saturated paste pH results from SBH shale did not indicate that acidic conditions were present within the soil profile.

5.2.5.8 CEC and exchangeable cations

The CEC and exchangeable cation concentration was determined for the till and shale samples collected in August 2002. This set of samples were transported, stored and processed with minimal exposure to oxygen. Detailed sample collection and preparation procedures are described in Section 4.3.1. The CEC and exchangeable cation data are presented in Table 5.9. The shale CEC ranged from 28 and 48 meq/100 g soil with a mean of 36 meq/100 g soil (n = 13, s.d. = 6.4). The CEC measured in the one till sample analyzed (0.61 m) was 22 meq/100g. The CEC of the till sample was approximately 6

meq/100 g soil less than the minimum CEC measured in the shale. The CEC measured in shale samples in this study were similar to those reported for unsaturated marine shale in literature. Mermut (unpublished data) reported CEC in Clearwater Formation shale collected from reclamation areas on the Syncrude mine site ranging between 22 and 48 meq/100g soil. Pratt et al. (1962) measured CEC in the surface horizon of uncultivated acid soil derived from marine sediment parent material. The CEC values ranged from 28 to 36 meq/100g.

The profile of exchangeable cation concentration with depth is presented in Figure 5.10. Exchangeable cation concentrations indicated that Na was the dominant exchangeable cation in the shale below 4.8 m depth, with the exception of the sample collected at 19.2 m. The exchangeable Na concentration below 4.8 m ranged from 2.0 to 14.1 meq/100g soil with a mean of 8.4 (n = 13, s.d. = 4.5). No explanation was determined for the anomalously low concentration (2.0 meq/100g soil) measured at 19.21 m. Ca was the second most abundant exchangeable cation, with concentrations ranging from 4.4 to 6.5 meq/100 g soil. Above 4.8 m (1.4 to 4.8 m below ground surface) both the exchangeable Na and Ca concentrations were extremely variable. Exchangeable Na ranged from 2.6 to 11.3 meq/100 g soil and exchangeable Ca ranged from 5.6 to 9.8 meq/100g soil. Mg and K concentrations remained relatively constant throughout depth in the profile, ranging from 1.5 to 5.3 meq/100 g. The one till sample analyzed (0.61 m) contained 10.22 meq/100g Ca and 0.22 meq/100g soil Na. Exchangeable Mg and K concentrations in the till were similar to those measured in the shale (1.5 and 4.5 meq/100 g respectively). The results from exchangeable cation analysis indicated that there was a difference in exchangeable cation distribution in the shallow shale profile (1.4 and 4.8 m) compared to the deep zone (4.8 to 24.3 m). These results suggested that the exchange reactions between Na and Ca may have occurred within the shallow zone (1.4 to 4.8 m).

The total exchangeable cation concentration in the shale was calculated to be approximately equal to half the measured CEC. This result suggested that either the total exchangeable cation concentration was under-estimated or the CEC of the shale was over-estimated. As

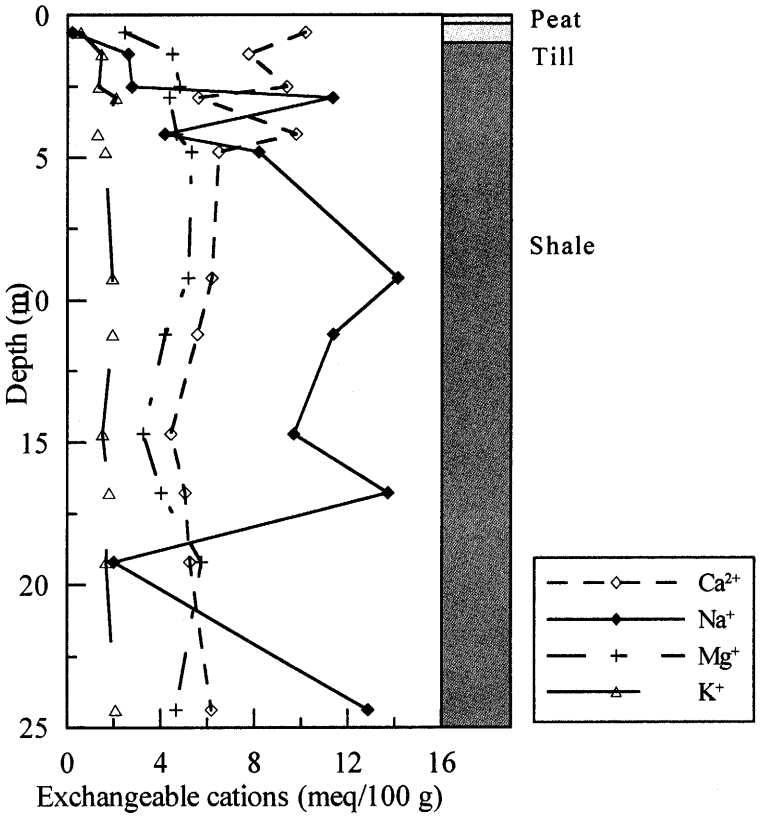

Figure 5.10: 30-D3-C (SBH plateau): a) Profile of exchangeable cations with depth measured on soil samples collected in August 2002 and processed under anaerobic conditions. Results indicated that Na and Ca are the dominant exchangeable cations between 1.4 and 4.8 m depth.

described in Section 2.8, the CEC of a soil the capacity of a soil to adsorb cations to charged clay surfaces. Therefore, the total exchangeable cation concentration should be approximately equal to the measured CEC of a soil. There are two common sources of error in CEC determination that may be applicable. Firstly, the replacement strength of Ba may not have been sufficient enough to replace the more strongly adsorbed Al and its hydroxyl forms (Rhoades, 1982). Secondly, dissolution of carbonate may have occurred during saturation, thus increasing the concentration of exchangeable Ca (Rhoades, 1982). Therefore, the corrected exchangeable Ca (soluble Ca – exchangeable Ca) would be artificially reduced. Although the exchangeable Al concentration was not measured in this study, Curtin and Mermut (1987) reported exchangeable Al concentrations from 9.2 to 28.1 meq/100 g soil in Cretaceous marine shale from southern Saskatchewan. Al is also a commonly a major ion in the soil solution of acid soils (Wolt, 1994). Therefore, it was likely that the difference between the CEC and exchangeable cation concentration was due to the presence of exchangeable Al.

Table 5.9: 30-D3-C (SBH plateau): Exchangeable cation concentration (determined by NH_4OH Ac extraction) in meq/100 g soil. The total exchangeable cation concentrations are approximately equal to one-half the CEC. CEC was determined using the method of BaCl replacement.

Average depth (m)	Exchangeable cations (meq/100g soil)				Total	CEC (meq/100g soil)
	Ca	K	Mg	Na		
Till (SBH plateau)						
0.61	10.18	0.58	2.46	0.22	13.44	21.97
Shale (SBH plateau)						
1.37	7.74	1.47	4.50	2.60	16.31	27.83
2.52	9.37	1.35	4.81	2.76	18.29	31.50
2.90	5.60	2.08	4.37	11.34	23.39	35.66
4.17	9.78	1.30	4.67	4.17	19.92	28.56
4.80	6.48	1.63	5.31	8.19	21.61	41.26
9.22	6.19	1.94	5.19	14.13	27.44	37.88
11.20	5.57	1.94	4.19	11.38	23.08	38.46
14.71	4.44	1.52	3.26	9.69	18.91	29.46
16.77	5.05	1.80	4.03	13.71	24.59	44.56
19.21	5.26	1.67	5.75	2.00	14.68	33.83
24.39	6.18	2.08	4.67	12.86	25.79	48.44
Mean	**6.51**	**1.71**	**4.61**	**8.44**	**21.27**	**36.13**

The ESP was calculated for the shale and till samples collected in August 2002. The results are presented in Table 5.8. The ESP ranged between 1 and 30 with a mean of 22.5 (n = 11, s.d. = 11.8). All shale samples collected from below 2.90 m had an ESP greater than 15, with the exception of the sample collected at 19.21 m. The shale sample collected at 19.2 m was measured to contain less exchangeable Na when compared to the other shale samples in the profile. As a result, the calculated ESP was also less than the mean ESP for the shale. The two shale samples above 2.9 m (1.4 and 2.5 m below ground surface) were calculated to have an ESP of 9. The minimum ESP in the soil profile (1.0) was calculated in the till sample (0.6 m). The soil classification scheme (US Salinity Laboratory Staff, 1954) defined sodic soil to have an ESP of 15 or greater. The ESP calculated in this study indicated that below 2.9 m, the shale was sodic. Between 1.4 and 2.9 m, sodic conditions were not present in the shale. The one till sample (0.6 m) could also not be defined as sodic.

5.2.6 Pore-gas and Stable Isotope Results

The depth profiles of pore-gas O_2, CO_2 and CH_4 concentrations at 30-D3-B (SBH upper slope) and 30-D3-C (SBH plateau) are presented in Figures 5.11 and 5.12. Pore-gas H_2S was not detected at these sites. Pore-gas concentrations were measured approximately monthly throughout the field season (May to October) and once during the winter months between 2001 and 2003 (for specific sampling dates and gas concentrations refer to Appendix E). The upper slope and plateau pore-gas profiles were presented together to depict both a detailed shallow pore-gas profile as well as the pore-gas profile to 25 m depth.

5.2.6.1 Pore-gas O_2 Concentration with Depth

On the SBH plateau (30-D3-C) the depth profiles of O_2 concentration showed an overall decrease in concentration from June 2001 to June 2003 in all gas probes. Although the O_2 concentrations were not observed to progressively decrease with each consecutive sampling period. The small variations in O_2 concentrations measured at the same depth were attributed to the high risk of atmospheric contamination during sampling as well as the slight changes of moisture content, temperature and microbial activity that were expected in a field setting. The O_2 concentrations decreased from atmospheric (20.9 %) at ground surface to values between 1 and 13 % at 5 m depth. Below 5 m, the O_2 concentrations ranged from 0.5 to 3 %. The O_2 concentrations remained relatively constant with depth below 5 m (5 to 25 m) on each sampling occasion. Anomalously high O_2 concentrations were measured in the 15, 19 and 21 m gas probes on August 26, 2002. These elevated O_2 concentrations were attributed to the installation of the neutron access tube on the SBH plateau. The installation of the neutron access tube occurred on the same day as the August 26, 2002 pore-gas sampling campaign. The installation included one failed attempt at rotary drilling with reverse air-circulation (at 100 psi pressure) followed by hammer drilling steel pipe 22 m into the ground. The neutron access tube was installed on the SBH plateau approximately 20 m west of the 30-D3-C (SBH plateau) gas probes. The use of air-circulation during drilling may have adversely affected pore-gas concentrations at the gas ports. The nearly immediate effect of the tube installation on gas-sampling results

suggested that lateral gas flow through the clay material probably occurred through relatively large interconnected voids. At the upper slope site (30-D3-B), the O_2 concentration profiles with depth were in keeping with those on the SBH plateau. The O_2 concentrations at the upper slope decreased from atmospheric at ground surface to between 1 and 6 % at 4.5 m depth.

The pore-gas O_2 concentrations measured at the upper slope and plateau sites were similar to those measured at other mine waste piles. Harries and Ritchie (1985) measured O_2 concentrations ranging from atmospheric (20.9 %) at ground surface to values less than 1 % at 2 m depth in slate and shale waste piles at the Rum Jungle mine site. At this site the pore-gas O_2 concentrations in the waste pile remained below 2 % to the bottom of the profile (30 m below ground surface). At La Mine Doyon in Quebec (Gelinas et al., 1992) pore-gas O_2 in the waste pile decreased from 20.9 % at ground surface to 3 % at 5 m depth. Below 5 m O_2 remained constant at 3 % to 30 m depth. The O_2 concentrations measured on SBH were considerably less than those measured at the forested control site (Section 5.1.3). At 2.35 m depth, the minimum pore-gas concentration at the control site was 19.4 % compared to 5 % at a similar depth on the SBH upper slope. These results suggested that oxidation reactions were occurring between 0 and 5 m depth at both sites on the SBH overburden pile.

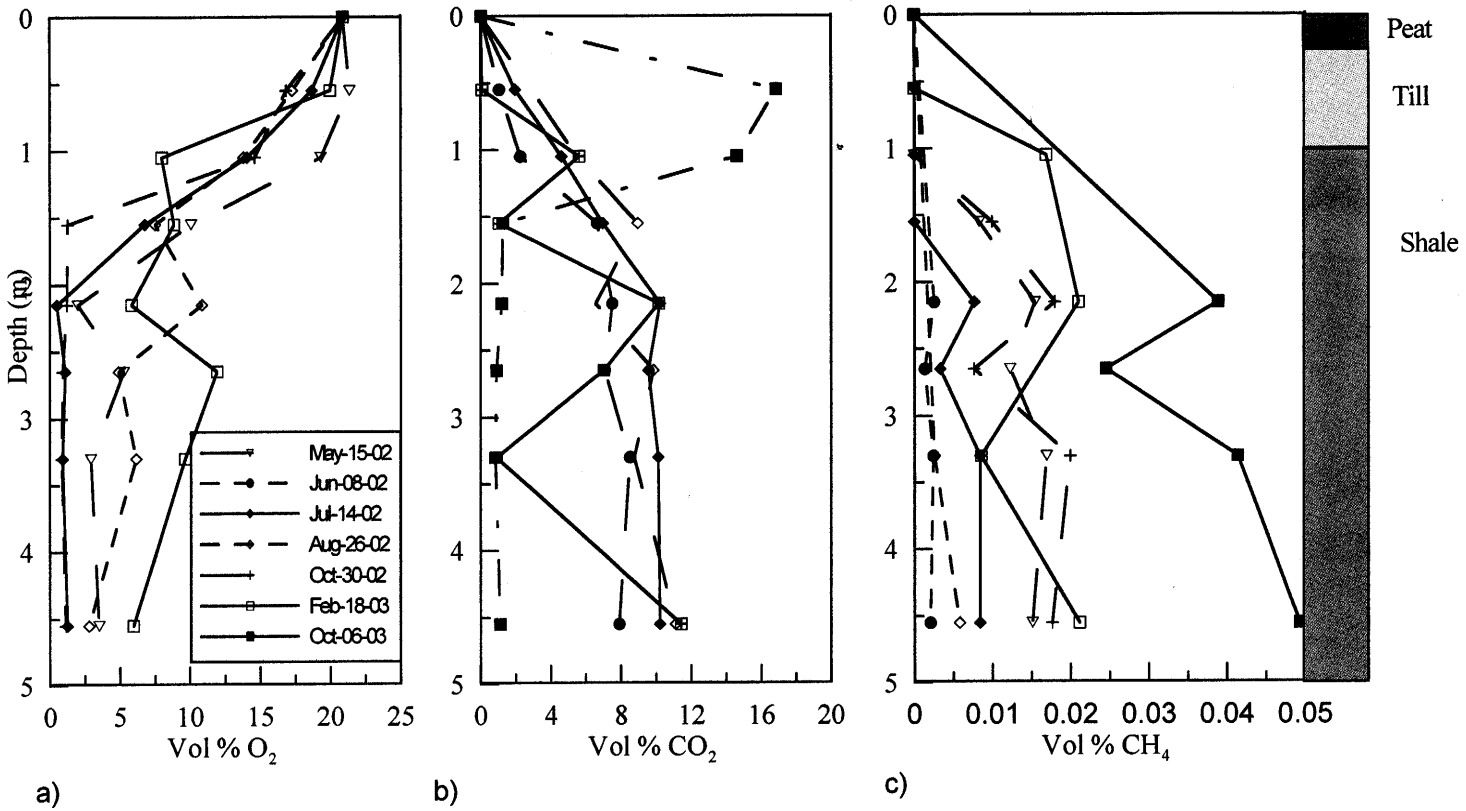

Figure 5.11: 30-D3-B (upper slope) pore-gas concentration profiles with depth for each sampling occasion. a) O_2 concentration profile depicting a decrease in O_2 with depth. b) CO_2 concentration profile depicting increasing CO_2 with depth. c) CH_4 concentration profile showing the presence of detectable CH_4 at shallow depths.

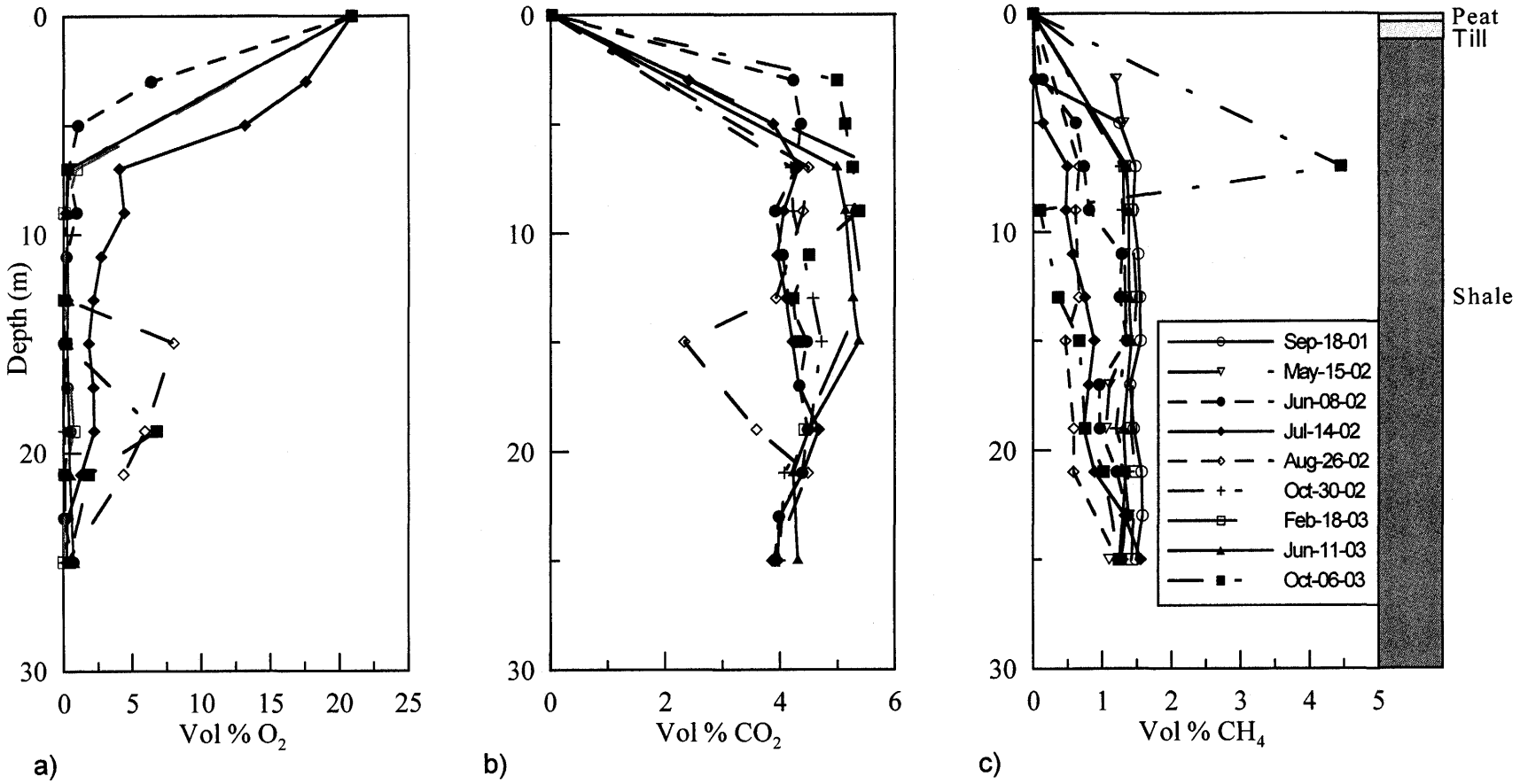

Figure 5.12: 30-D3-C (SBH plateau) pore-gas concentration profiles with depth for each sampling occasion. a) O_2 concentration profile depicting a decrease in O_2 with depth. b) CO_2 concentration profile depicting increasing CO_2 with depth. c) CH_4 concentration profile showing the presence of detectable CH_4 at shallow depths.

5.2.6.2 Pore-gas CO_2 Concentration with Depth

The depth profiles of pore-gas CO_2 concentration for each sampling occasion on the SBH plateau indicated an overall increase in concentration with time (from June 2001 to June 2003). The CO_2 concentrations at this site increased from atmospheric (0.04 %) at ground surface to 4 % at 5 m depth. Below 5 m, CO_2 concentrations remained constant with depth at approximately 4 % (to 25 m depth) on each sampling occasion. Similar to the O_2 concentration data, the CO_2 concentrations were not observed to increase with each consecutive sampling period, nor were they observed to vary seasonally. The small variations in CO_2 concentration at each sampling period were also attributed to changes in moisture content and temperature within the unsaturated zone, as well as the high risk of atmospheric contamination during sampling and analysis. No correlation between elevated O_2 concentration and reduced CO_2 concentration at a given sampling period was determined. At the upper slope site (30-D3-B), the CO_2 concentration increased from atmospheric at ground surface to between 8 and 13 % at 4.5 m depth.

The CO_2 concentrations measured at the upper slope site were greater than those measured on the SBH plateau. CO_2 concentrations at the SBH plateau ranged from atmospheric to approximately 4 % at 5 m below ground surface whereas concentrations on the upper slope reached values greater than 13 %. The difference may have in part been due to the mature vegetation present on the upper slope. The upper slope was vegetated with voluntary grasses since cover placement (1997) while the plateau was not planted with barley until August 2001. However, as noted in Section 5.1.3, the CO_2 contribution from root and microbial respiration would not be enough to account for the difference. The elevated CO_2 at the upper slope site may indicate a greater rate of carbonate mineral dissolution relative to the plateau. However, at present, no reasonable explanation for the difference in concentrations was determined.

The CO_2 concentrations measured at both the upper slope and plateau sites on SBH were considerably greater than those measured at natural unsaturated sites (Section 5.1.3).

However, SBH CO_2 concentrations were comparable to those measured at other mine waste piles. Harries and Ritchie (1985) reported CO_2 concentrations ranging from 4 to 8 % (at 5 m below ground surface) in waste piles composed of weathering slate and shale. Gelinas et al. (1992) reported similar CO_2 concentrations measured in meta-volcanic mine waste at La Mine Doyon in northern Quebec. The CO_2 concentrations increased with depth to a maximum of 7 % at 30 m below ground surface (Gelinas et al., 1992). In a black shale mine waste pile in Germany, Hockley et al. (1997) measured CO_2 concentrations ranging from 3 to 10 % at 5 m below ground surface. The CO_2 produced in all three mine waste piles was determined to be the result of carbonate mineral dissolution in response to acid neutralization (Harries and Ritchie, 1985; Hockley et al., 1997; Gelinas et al., 1992). These findings suggested that the elevated CO_2 concentrations (relative to Control-1) measured at SBH could be the result of carbonate mineral dissolution reactions occurring within the overburden pile in response to acid produced from sulphide mineral oxidation.

5.2.6.3 Pore-gas CH_4 Concentration With Depth

The depth profiles of pore-gas CH_4 concentration at the SBH plateau indicated that CH_4 concentration increased from atmospheric (18 ppm) to values between 3 000 and 15 000 ppm at 7 m depth. Below 7 m, the CH_4 concentrations remained relatively constant with depth (to 25 m) on each sampling occasion. The exceptions to this pattern were the CH_4 concentrations measured in the 23 and 25 m gas probes in July 2001, July 2002, and August 2002. In July 2001, the CH_4 concentration was observed to decrease from 8 000 ppm at 21 m to 400 ppm at 25 m. This result was attributed to atmospheric contamination during sampling. The CH_4 profiles for July and August 2002 showed that CH_4 increased from approximately 7 000 ppm at 21 m to values between 12 000 and 15 000 ppm at 25 m. At present, no explanation for these results is evident. At the upper slope site (30-D3-B), pore-gas CH_4 was consistently detected in the gas probes located deeper than 1.5 m below ground surface. Pore-gas CH_4 increased from atmospheric at ground surface to a maximum of 500 ppm at 4.5 m depth.

Pore-gas CH_4 concentrations for mine-waste piles were not reported in literature to the knowledge of the author. Revesz et al. (1995) measured pore-gas CH_4 concentrations in the unsaturated zone of a crude oil spill that ranged from 0 ppm at 0.5 m below ground surface to 115 000 ppm at 5.5 m. CH_4 concentrations at this site were up to two orders of magnitude greater than the CH_4 concentrations measured at SBH. The difference was attributed to the high concentration of volatile hydrocarbons (Revesz et al., 1995). In a temperate mixed hardwood forest in New Hampshire, the mean daily CH_4 concentration in soil gas was 200 ppm at a depth of 0.02 m (Crill, 1991). CH_4 concentrations at this site were observed to decrease with increasing depth and were attributed to CH_4 production in the leaf litter layer overlying the soil (Crill, 1991). The CH_4 concentrations measured at the SBH plateau were generally higher than those reported in literature. At the undisturbed control site, pore-gas CH_4 concentration was below instrument detection (<20 ppm). These results suggested that the pore-gas CH_4 measured on SBH was a result of reactions in the overburden pile. As mentioned in Section 2.5, CH_4 is generally produced in anoxic, saturated environments. However, CH_4 production may also occur in unsaturated media with very low gas transport characteristics. The <2 % O_2 concentrations measured below 5 m on the SBH plateau suggested that anaerobic or near-anaerobic conditions were present at depths greater than 5 m in the overburden pile. However, the production of CH_4 is also restricted to sediments that do not contain significant concentrations of dissolved SO_4 (Winfrey and Ward, 1983). The presence of significant SO_4 concentrations inhibits the production of CH_4. This is because in anoxic sediments, the processes of SO_4 reduction and CH_4 production compete for the consumption of H_2 and acetate (Winfrey and Ward, 1983). In soils containing significant SO_4, the reduction of SO_4 will dominate CH_4 production until no SO_4 is left remaining in the sediments (Winfrey and Ward, 1983). As presented in Section 5.2.3.1, significant concentrations of soluble SO_4 were present throughout the shale profile on SBH. The presence of SO_4 suggested that CH_4 production within the soil profile was inhibited. The results suggested that the pore-gas CH_4 was most likely produced at the water table or within the saturated capillary fringe was diffusing upwards in the waste pile.

5.2.6.4 Temporal Variations of Pore-gas O_2, CO_2 and CH_4

At the time of installation, the pore-gas chemistry at each gas probe was atmospheric as a result of the installation procedure. To determine the time required for the pore-gas chemistry to reach steady-state after installation, pore-gas O_2, CO_2 and CH_4 concentrations at each gas probe were plotted against the time elapsed (in months). The 7, 13 and 25 m gas probes at 30-D3-C (SBH plateau) and the 0.55, 1.05, 2.15 m and 4.45 m gas probes at 30-D3-B (upper slope) were selected as representative profiles for the two sites. The gas probes on the upper slope and plateau sites were installed on November 6, 2000 and April 12, 2001 respectively. The time versus pore-gas concentration profiles for the two sites are presented in Figures 5.13 and 5.14.

The concentration profiles with time for the SBH plateau showed O_2 concentrations decreasing with time until approximately May 15, 2002. The CO_2 concentrations appeared to increase with time until the same sampling occasion. After May 2002, the O_2 and CO_2 concentrations remained constant. The exceptions to this trend were the O_2 concentration spikes that occurred on July 14 2002 in the 7 and 13 m gas probes. Elevated O_2 concentrations were measured throughout the profile on this sampling occasion, however, a corresponding decrease in CO_2 concentration, which would be expected if the source of the O_2 was atmospheric air, was not measured. At present, an explanation for the elevated O_2 concentrations is not evident. The CH_4 concentration profile showed an increase of CH_4 with time until approximately September 18, 2001 and remained constant throughout the sampling program.

The pore-gas concentration versus time plots at the upper slope site showed that O_2 concentrations decreased with time until approximately September 18, 2001 while CO_2 increased until approximately the same sampling occasion. After September 2001, both the O_2 and CO_2 concentrations remained relatively constant. The exception was an O_2 concentration spike measured on August 26, 2002 in the 2.15 m gas probe. Elevated O_2 concentrations were measured in the 2.65, 3.3 and 4.5 m gas probes on the same sampling occasion. These anomalously high O_2 concentrations were attributed to the installation of the neutron access tube, which occurred on the same day at the August 26th sampling

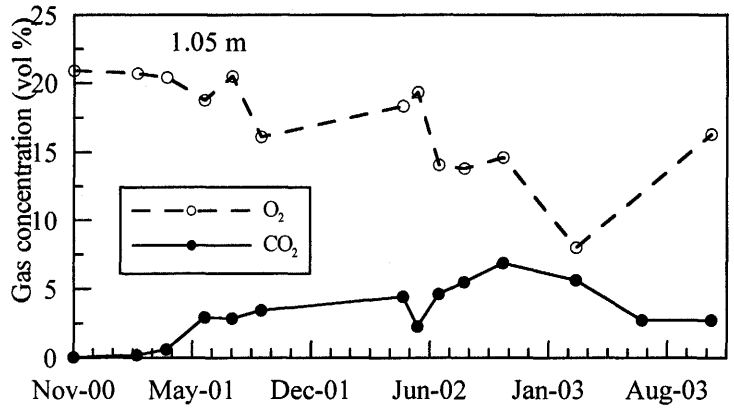

a)

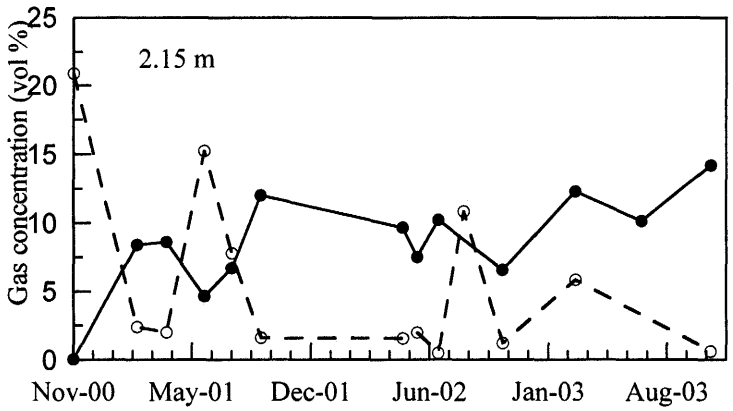

b)

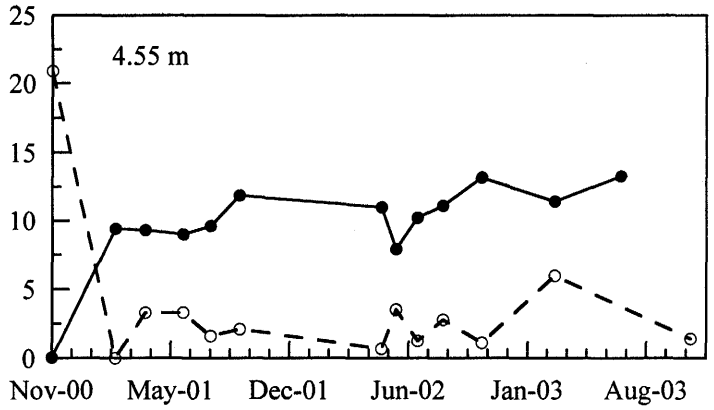

c)

Figure 5.13: 30-D3-B (upper slope) pore-gas concentrations profiles versus time at the 1.05, 2.15 and 4.55 m deep gas probes. The O_2 and CO_2 concentrations reached steady-state after September, 2001.
a) 1.05 m gas probe. b) 2.15 m gas probe. c) 4.55 m gas probe.

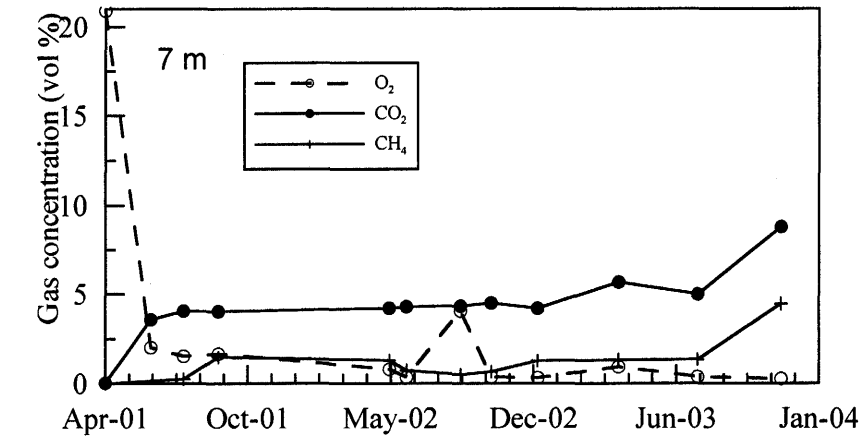

a)

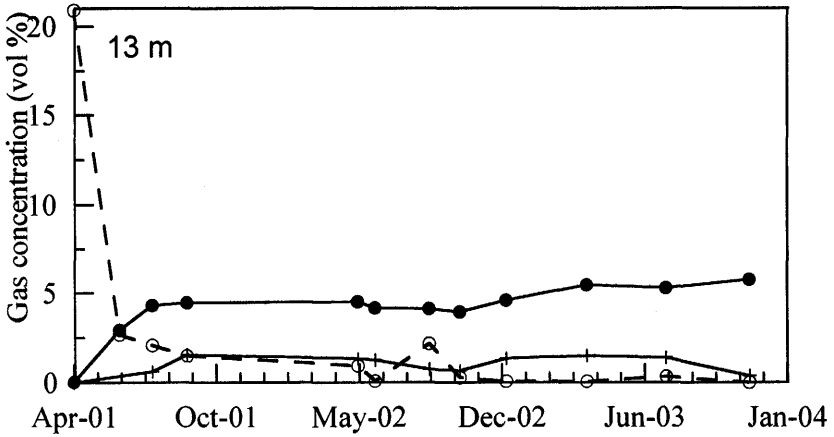

b)

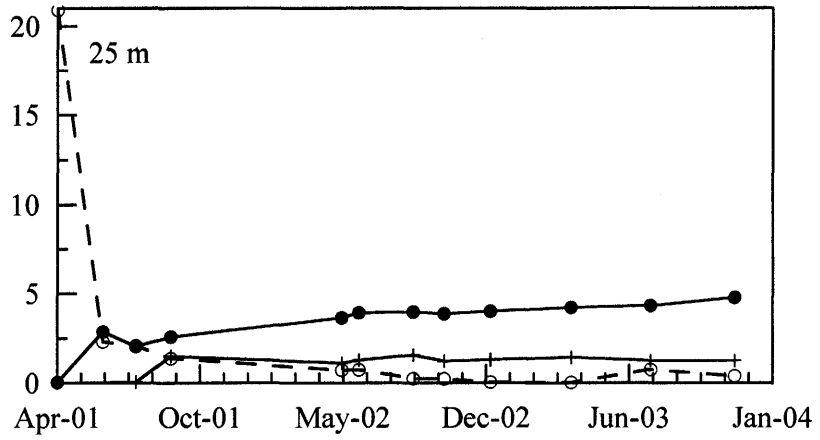

c)

Figure 5.14: 30-D3-C (SBH plateau) pore-gas concentrations over time at 7 m, 13 m, and 25 m depths. The O_2 and CO_2 concentrations reach steady-state after May 2002. The CH_4 concentrations reach steady-state after September 2001. a) 7 m gas probe. b) 13 m gas probe. c) 25 m gas probe.

campaign. A corresponding decrease in CO_2 concentration was not measured, with the exception of the 2.15 m gas probe. The shallow gas probes (0.55 to 3.3 m) displayed more variation in O_2 and CO_2 concentrations throughout the gas sampling program than the deeper (5 m to 25 m) gas probes.

Seasonal variations in O_2 and CO_2 concentrations were observed in the 0.55 and 1.05 m gas probes. The O.55 m gas probe showed a decrease in O_2 concentration and a corresponding increase in CO_2 concentration during the summer months of 2002. At the 1.05 m gas probe profile, O_2 concentrations were observed to decrease during the summer months of 2001 and 2002. A corresponding increase in CO_2 concentrations was also observed on the same sampling occasions. The seasonal variations in the 0.55 and 1.05 m gas probes on the upper slope site were in keeping with the O_2 results presented for Control-1 (Section 5.1.3) as well as for other natural, unsaturated pore-gas investigation sites. As noted in Section 5.1.3, the O_2 and CO_2 concentrations at Control-1 as well as those reported by Keller and Bacon (1998) and Hendry et al. (1999) exhibited seasonal variations. The pore-gas O_2 concentrations were least during the summer months and increased during the fall and winter months. Conversely, the pore-gas CO_2 concentrations were greatest during the summer months. These investigations reported minimum O_2 concentrations of 19.5 % at 2.5 m depth and maximum CO_2 values of 1.2 % at 2.5 m depth (Hendry et al., 1999). The O_2 consumption and CO_2 production was attributed to microbial and root respiration. The observed seasonal variations in pore-gas O_2 and CO_2 were a result of increased organic respiration during the summer months.

The gas concentration versus time profiles suggested that pore-gas O_2 and CO_2 in all the gas probes at the SBH plateau and upper slope sites required about one-year to approach steady state concentrations after the installation of the gas probes. On the plateau, pore-gas O_2 and CO_2 concentrations attained near steady-state after 400 days (about May, 2002). On the upper slope, the O_2 and CO_2 concentrations attained near steady-state concentrations after about 320 days (September, 2001). The CH_4 concentration profile suggested that CH_4 required less time to equilibrate than O_2 and CO_2. The CH_4 concentrations appeared to reach steady state concentrations about 160 days after the installation of the gas-probes.

Prior to reaching steady state concentrations, pore-gas chemistry may still have been influenced by atmospheric gas that was introduced during probe installation. As a result, pore-gas concentrations measured on the first four sampling periods for both the upper slope and plateau sites were not included in the calculation of the mean (and standard deviations) O_2, CO_2 and CH_4 concentration profiles. These data were also not incorporated into reaction-rate calculations (see Section 5.5). Isotope data corresponding to all non-steady state pore-gas concentrations were also not considered further. The calculated mean and standard deviations for pore-gas O_2, CO_2 and CH_4 concentrations for both the SBH plateau and upper slope sites are presented in Table 5.10 as well as Figures 5.15 and 5.16.

Table 5.10: Mean pore-gas concentrations calculated from steady-state O_2, CO_2 and CH_4 data for the SBH plateau (n = 6) and the upper slope (n = 7). Gas concentrations are presented as % volume.

Site	Depth (m)	O_2	standard deviation	CO_2	standard deviation	CH_4	standard deviation
SBH plateau (30-D3-C)	3	12.0	5.6	5.1	2.7	1.2	1.7
	5	6.4	5.0	4.9	1.2	0.7	0.5
	7	1.0	1.3	4.8	0.6	1.0	0.4
	9	1.0	1.5	4.6	0.5	1.0	0.4
	11	1.5	1.3	4.2	0.3	1.1	0.4
	13	0.4	0.7	4.6	0.5	1.2	0.3
	15	1.7	2.9	4.3	1.0	1.2	0.3
	17	1.2	0.9	4.3	0.0	1.1	0.2
	19	2.4	2.6	4.3	0.3	1.0	0.4
	21	1.2	1.5	4.4	0.2	1.1	0.4
	23	0.2	0.1	4.0	0.0	1.4	0.1
	25	0.3	0.3	4.0	0.2	1.3	0.1
Upper slope (30-D3-B)	0.55	18.7	1.5	1.4	0.9	0.000	0.0
	1.05	14.3	3.4	4.6	1.6	0.004	0.0
	1.55	6.9	3.0	7.1	3.6	0.006	0.0
	2.15	3.5	3.8	10.1	2.6	0.017	0.0
	2.65	4.2	3.9	9.9	2.5	0.010	0.0
	3.3	3.5	3.4	9.3	4.3	0.016	0.0
	4.55	2.7	1.7	11.2	1.8	0.019	0.0

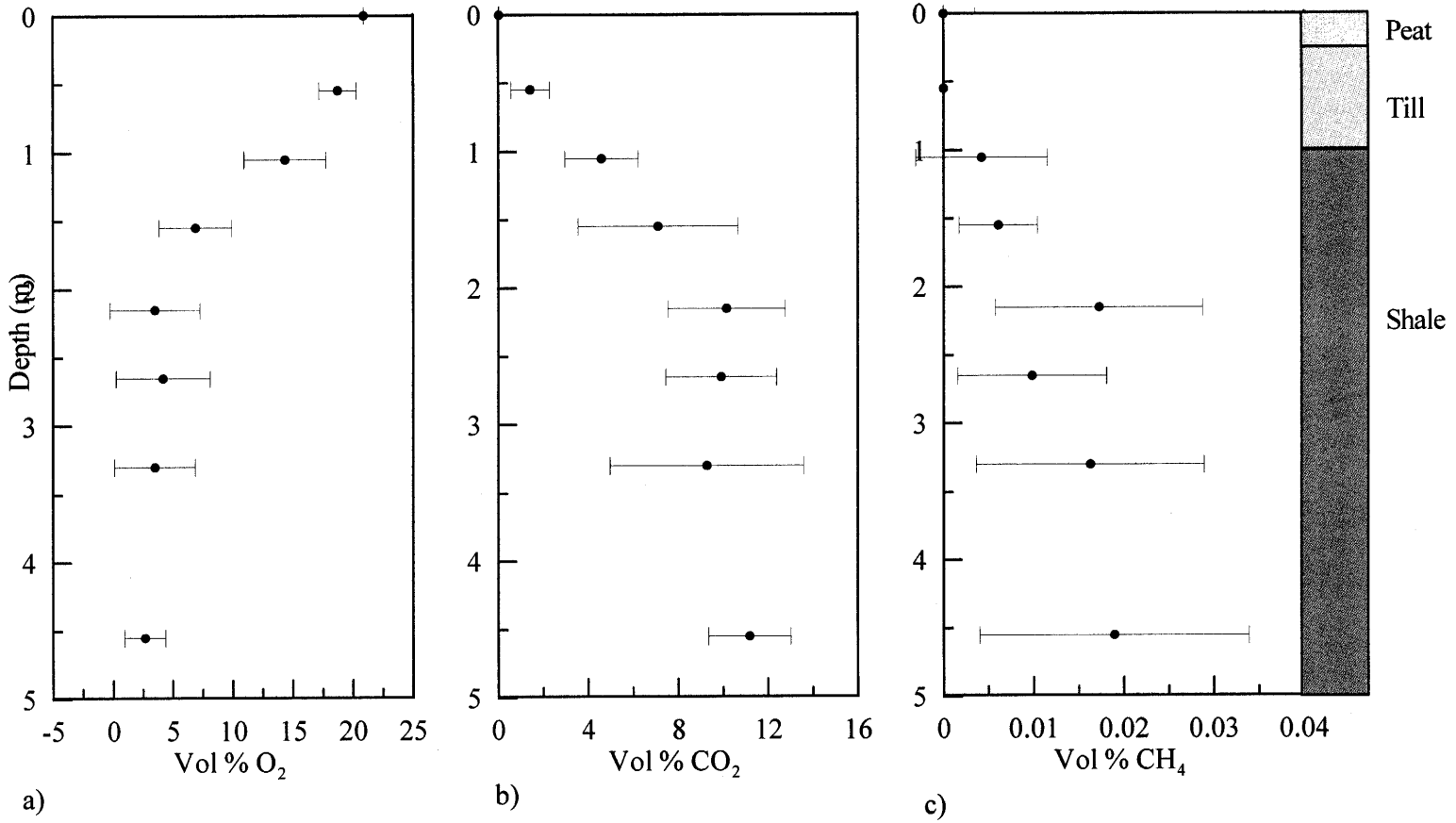

Figure 5.15: 30-D3-B (upper slope): Mean pore-gas concentrations with depth. a) O_2 concentration profile. b) CO_2 concentrations. c) CH_4 concentration profile. Circle symbols represent mean +/- standard deviation.

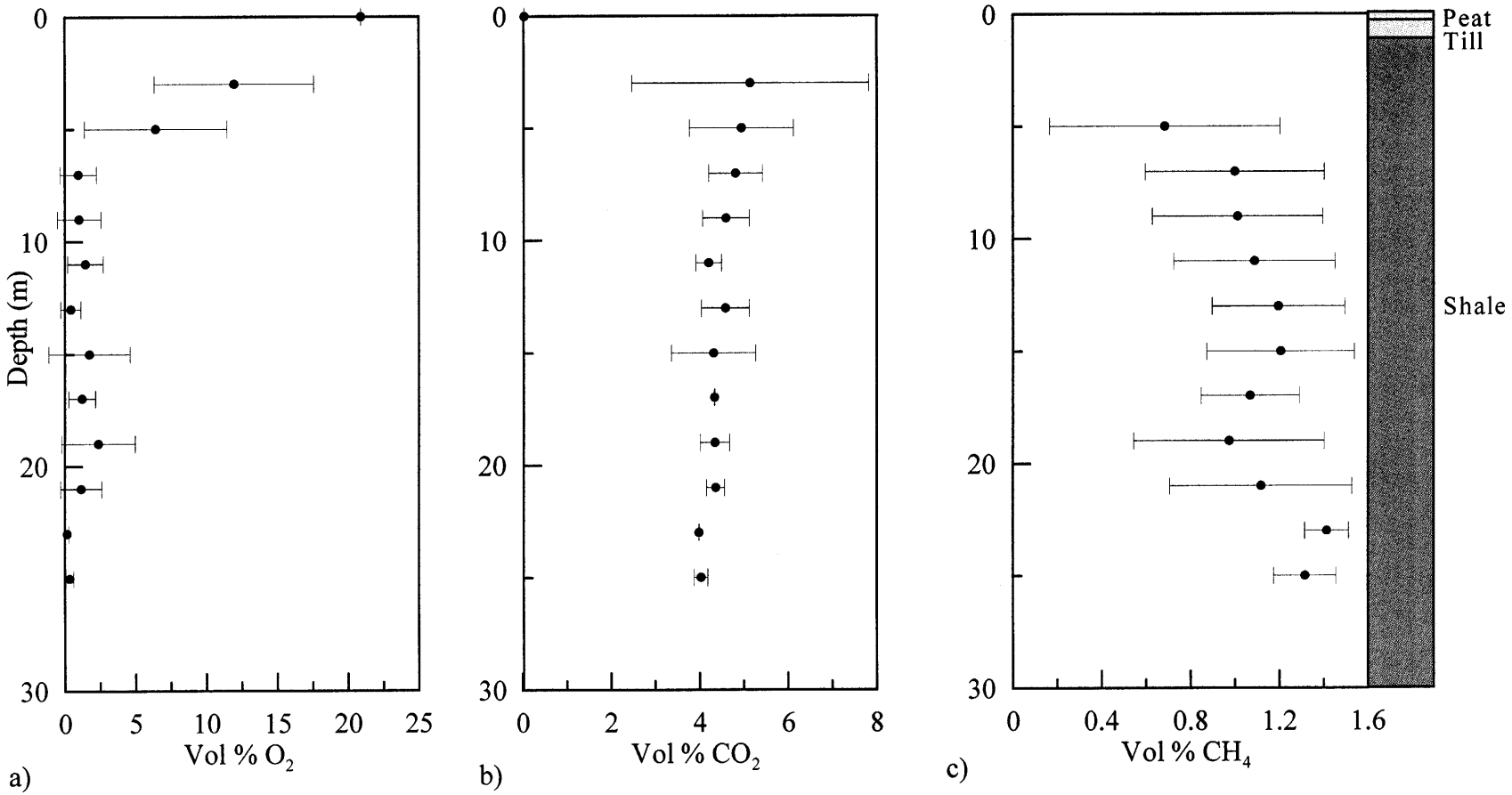

Figure 5.16: SBH plateau (30-D3-C) mean pore-gas concentrations with depth. a) O_2 concentrations with depth. b) CO_2 concentrations with depth. c) CH_4 concentrations with depth. Circle symbols represent mean values +/- standard deviation.

5.2.6.5 Correlation Between O_2, CO_2 and CH_4 Concentrations

The pore-gas concentrations versus time plots were useful for identifying any pore-gas interactions occurring within the overburden pile. On the SBH plateau, each gas probe typically showed that where O_2 concentrations increased above 2 %, CH_4 concentrations decreased. The greatest CH_4 concentrations were measured on occasions where O_2 concentration was less than 1 %. Conversely, as CO_2 concentrations increased, CH_4 concentrations increased. These results suggested that a relationship existed between CH_4 and O_2 and between CH_4 and CO_2. As noted in Section 2.5, CH_4 production is restricted to anaerobic environments. In addition, CH_4 will oxidize to CO_2 in the presence of O_2. Therefore, the relationship between CH_4 and O_2 concentrations suggested that CH_4 was either being oxidized to CO_2 or that CH_4 production was inhibited in the presence of increased O_2. Because CO_2 concentrations increased with increasing CH_4, it seemed likely that increased O_2 concentration was inhibiting CH_4 production. The coexistence of CO_2 and CH_4 in the soil suggested that CH_4 was probably not being produced from CO_2 reduction. Furthermore, the correlation in CO_2 and CH_4 concentrations suggested that some fraction of the CO_2 concentration was produced from the same source as the CH_4. As noted in Section 2.5, acetate fermentation produces equal concentrations of CH_4 and CO_2. The greater concentration of CO_2 with respect to CH_4 was attributed to other CO_2-producing reactions such as carbonate mineral dissolution and organic respiration occurring within the soil profile.

5.2.6.6 Pore-gas $\delta^{13}C_{CO2}$

$\delta^{13}C_{CO2}$ were measured at both the upper slope and plateau sites throughout the sampling program (for specific dates and sampling results refer to Appendix D). As noted in Section 5.2.4.1, approximately one year was required for the pore-gas chemistry to reach steady-state after gas probe installation. As a result, the pore-gas and $\delta^{13}C_{CO2}$ data collected prior to steady-state were not incorporated in the calculation of mean values presented in this section; however, $\delta^{13}C_{CO2}$ values from the complete data set did not vary seasonally. The mean $\delta^{13}C_{CO2}$ values were calculated from the data for May 15 and June 8, 2002. The

mean $\delta^{13}C_{CO2}$ profiles with depth for the upper slope and plateau sites are presented in Figure 5.17. The mean $\delta^{13}C_{CO2}$ on the SBH plateau ranged from +1 to -7 ‰ with the most positive values occurring between 11 and 15 m. The most negative values were measured at 25 m. At the upper slope site, the mean $\delta^{13}C_{CO2}$ ranged from -3 to -4 ‰ throughout the profile. As noted in Section 2.6, CO_2 produced from marine carbonates typically has a $\delta^{13}C_{CO2}$ ranging from 0 to -3 ‰. Atmospheric CO_2 has a $\delta^{13}C_{CO2}$ of approximately -7 ‰ (Craig, 1953). The $\delta^{13}C_{TIC}$ results (Section 5.2.3.7) indicated that the inorganic carbon present in the SBH shale has a mean $\delta^{13}C_{TIC}$ of – 5 ‰. Therefore, pore-gas CO_2 produced from the inorganic carbon in SBH should have a mean $\delta^{13}C_{CO2}$ of approximately -1 ‰. The increase in $\delta^{13}C_{CO2}$ by approximately 4 ‰ relative to the carbon source is attributed to diffusive fractionation (Craig, 1953, Cerling, 1991). Thus, the $\delta^{13}C_{CO2}$ results from the upper slope site suggested that the pore-gas CO_2 was derived primarily from an inorganic carbon source.

At the SBH plateau, $\delta^{13}C_{CO2}$ data suggested that the CO_2 between ground surface and 15 m (ranged from +1 to -6 ‰) was also derived from an inorganic carbon source. From 15 to 25 m $\delta^{13}C_{CO2}$ data suggested that the pore-gas CO_2 was produced from both organic and inorganic carbon sources. The more negative $\delta^{13}C_{CO2}$ measured at these depths (ranged from -7 to -8 ‰) may have been related to the presence of >1 % pore-gas CH_4 below 15 m. Whiticar et al. (1986) measured $\delta^{13}C_{CO2}$ values ranging from 0 to -20 ‰ in saturated, anoxic soil environments where acetate fermentation was occurring and both pore-gas CO_2 and CH_4 were present. These results suggested that the more negative $\delta^{13}C_{CO2}$ measured below 15 m on the SBH plateau may be related to either CO_2 produced during acetate fermentation or CH_4 oxidation. Whiticar et al. (1986) also noted that anaerobic oxidation of methane has shown to be possible using sulphate as oxidant. It was more likely that the more negative $\delta^{13}C_{CO2}$ values at depth were a result of CH_4 oxidation if the pore-gas CH_4 was produced at the water table and diffusing upwards through the waste pile.

The $\delta^{13}C_{CO2}$ results from the SBH upper slope and plateau sites were more positive that those measured at Control-1 and other natural soil profiles (Section 5.1.4). At the natural

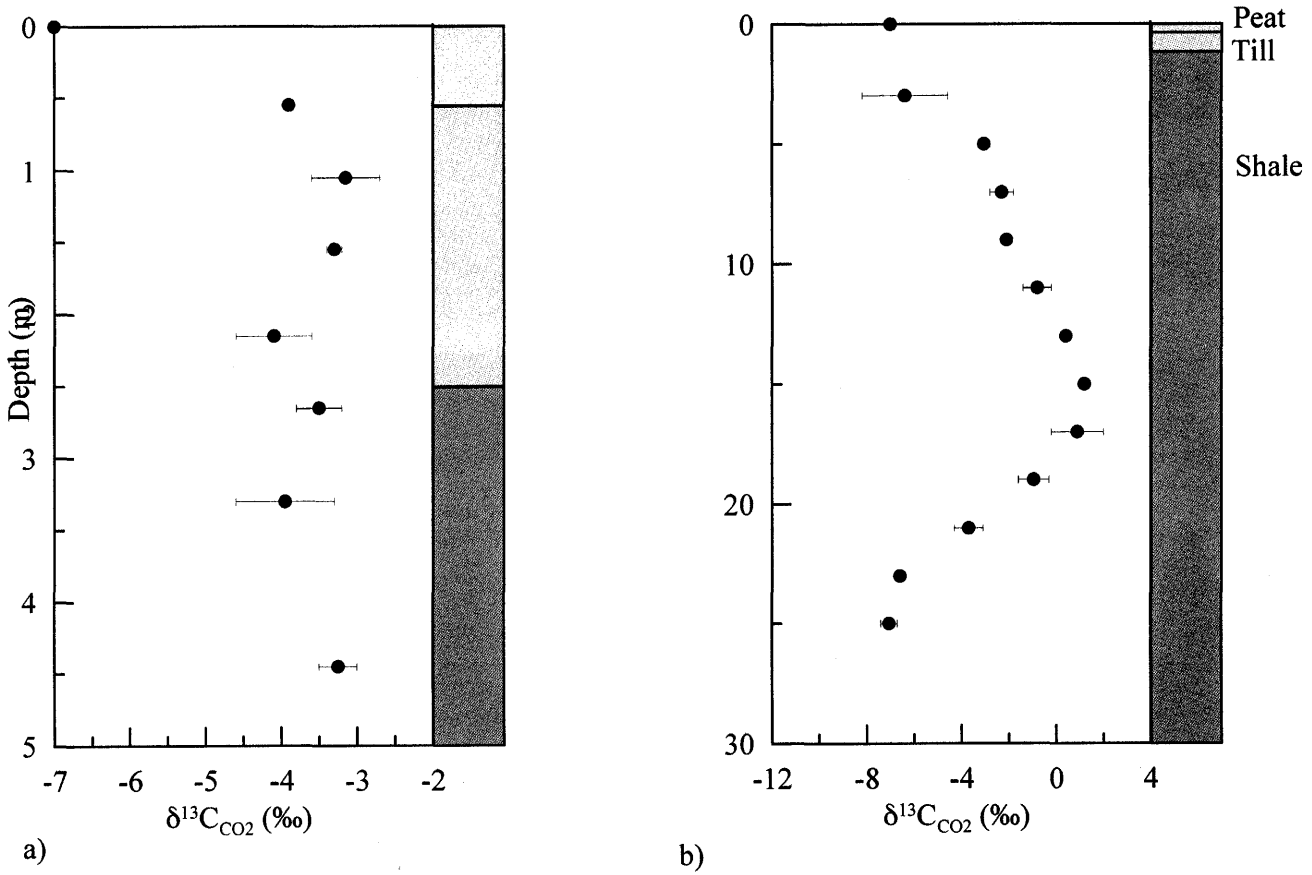

Figure 5.17: SBH upper slope (30-D3-B) and plateau (30-D3-C) $\delta^{13}C_{CO2}$ results with depth.
a) SBH uppper slope $\delta^{13}C_{CO2}$ profile with depth. b) SBH plateau $\delta^{13}C_{CO2}$ profile with depth. Circle symbols represent mean values +/- standard deviation.

unsaturated sites, the $\delta^{13}C_{CO2}$ ranged from -23 to -17 ‰. The pore-gas CO_2 at these sites was determined to have been produced primarily by organic respiration (Wallick, 1983; Wood and Petraitis, 1984; Wood et al., 1993; Keller and Bacon, 1998; Hendry et al., 1999). To the knowledge of the author, only one other $\delta^{13}C_{CO2}$ investigation has been conducted on mine waste materials. The $\delta^{13}C_{CO2}$ measured in a mine waste pile at Key Lake, Saskatchewan (Birkham, 2002) ranged from -26.5 to -7.6 ‰. The $\delta^{13}C_{CO2}$ data indicated that the pore-gas CO_2 in this study was produced primarily from an organic carbon source. The more positive $\delta^{13}C_{CO2}$ results (-7.6 ‰) were attributed to small contributions from an inorganic carbon source (Birkham, 2002). The more positive $\delta^{13}C_{CO2}$ results at SBH suggested that carbonate mineral dissolution may have occurred to a greater extent on SBH than at the Key Lake waste piles.

5.3 South Bison Hill Mid-slope Sites (30-D3-A and 30-D2-A)

The 30-D3-A (mid-slope, 1 m cover) and 30-D2-A (mid-slope, 35 cm cover) moisture content, pore-gas concentrations and stable isotope results are presented in the following section. These results will be compared to the upper-slope and plateau site data to evaluate possible differences in pore-gas or solid sample chemistry related to the effects of slope position and cover treatment.

5.3.2 Moisture Content

The gravimetric moisture contents for the 30-D3-A (1 m cover) and 30-D2-A (0.35 m cover) sites were measured on one occasion (June 2001). The gravimetric moisture content data were converted to volumetric (Equation 5.1) for comparison with the upper slope and plateau sites. The depth profiles of moisture content for the mid-slope sites are presented in Figure 5.18. The moisture contents measured in the peat/mineral mix and till at both sites ranged from 13 to 20 %. In the shale, the moisture content ranged from 17 to 28 % at both sites. These results were comparable with the converted gravimetric moisture content data from the upper slope and plateau sites (Section 5.2.2). At the mid-slope sites, moisture content increased below a depth of 1 m. At 30-D3-A (1 m cover) the moisture content

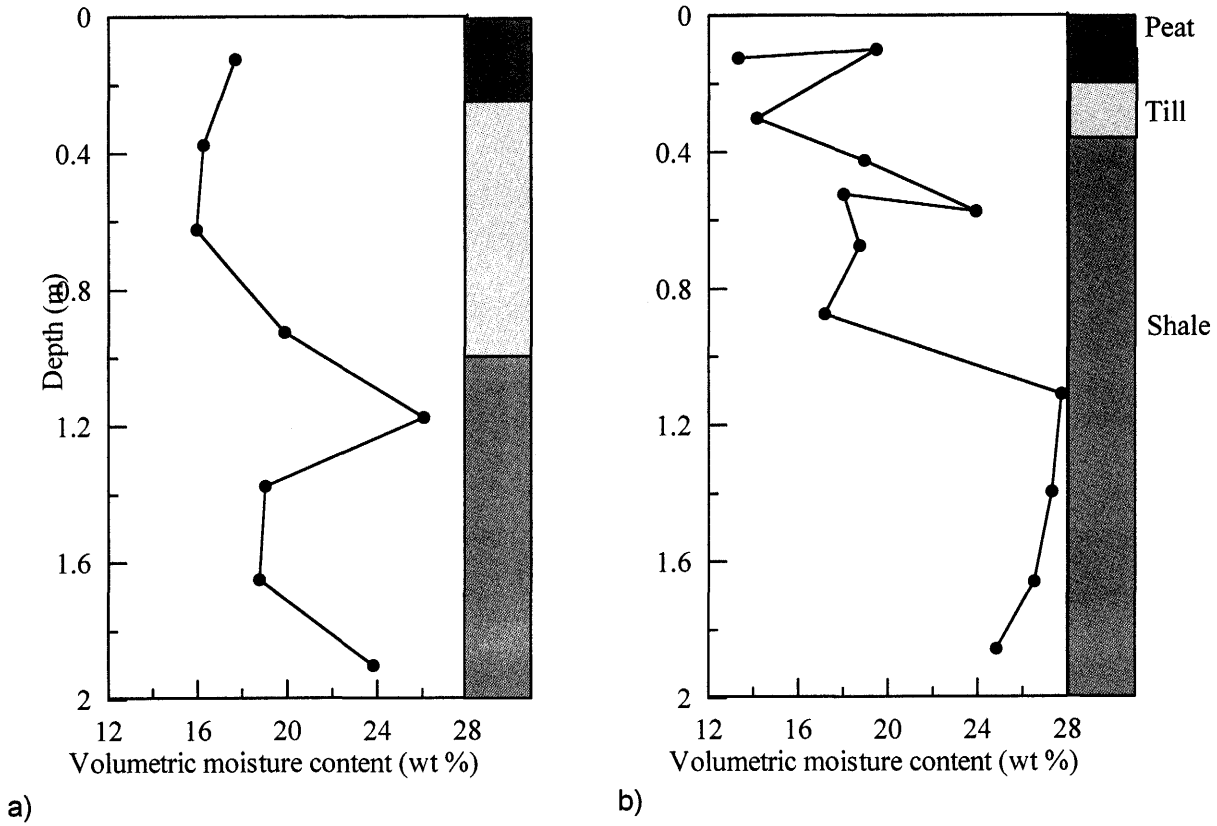

Figure 5.18: South Bison Hill mid-slope site volumetric moisture content profiles. Gravimetric moisture content data was collected in June 2001 and converted to volumetric data for comparison with the upper-slope and plateau sites. a) 30-D3-A (1 m cover). b) 30-D2-A (0.35 m cover)

increased from 18 % at 0.1 m below ground surface to 26 % at 1.2 m. Below 1.2 m, the moisture content in the shale ranged from 19 to 23 %. At 30-D2-A (0.35 m cover) the moisture content increased from 17 % at 0.9 m to 28 % at 1.1 m. Below 1.1 m (1.1 to 1.9 m) the moisture content in the shale remained relatively constant at 26 %. The increase in moisture content at about the one meter depth was similar to trends in the upper slope and plateau moisture content profiles. The results for 30-D2-A suggested that the moisture content increase at 1 m depth was not solely related to cover thickness. At this site, the moisture content was observed to increase approximately 0.6 m below the cover/shale interface.

Volumetric moisture content measurements were collected at the mid-slope sites using a neutron probe (D. Chapman, personal communication) and are presented in Figure 5.19. The neutron probe data indicated that the mean moisture content in the peat/till cover at the mid-slope sites was 21 % (n = 36, s.d. = 1.2). In the shale, the mean moisture content was 28 % (n = 36, s.d. = 3.2). Both sites exhibited an increase in moisture content at the cover/shale interface (0.35 m and 1.0 m respectively). These results were contradictory to the converted gravimetric data for 30-D2-A. However, the converted gravimetric data represented the soil moisture conditions on only one occasion. Because the neutron probe data represented bi-weekly field moisture contents from October 2001 to August 2003, the data was considered an accurate representation of the moisture contents at the mid-slope sites.

5.3.3 Solid Sample Analysis

Solid samples at the mid-slope sites (30-D3-A and 30-D2-A) were collected at the time of gas probe installations (June 2001). Soil samples were transported to the University of Saskatchewan where they were oven-dried, ground, and analyzed for total S, TIC and TOC (refer to Section 4.3.2 for detailed sampling procedures).

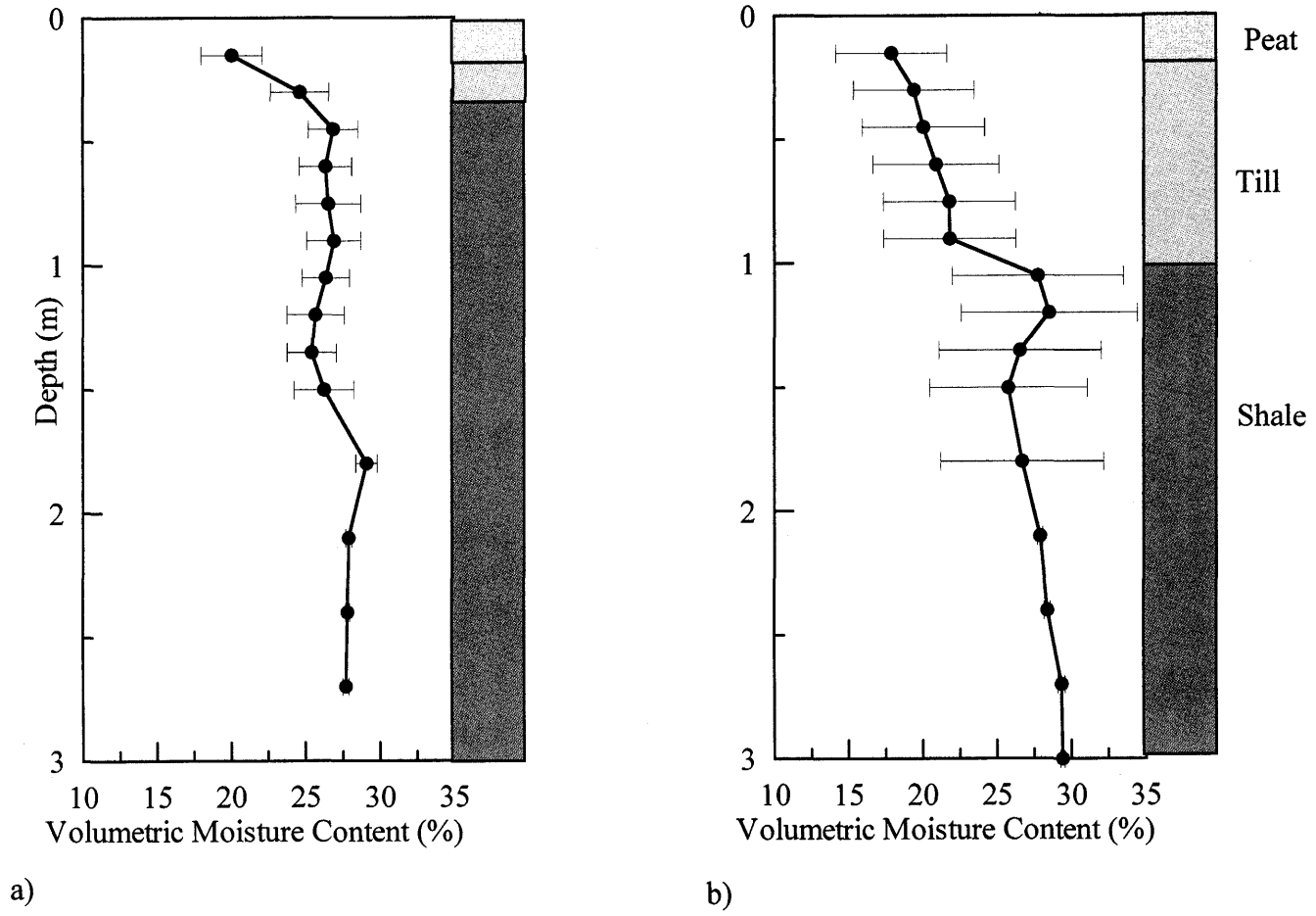

Figure 5.19: Volumetric moisture content data from neutron probe measurements collected between September 2001 and August 2003 (data provided by Denise Chapman). a) Volumetric moisture profile at the D2 (0.35 m) cover. b) Volumetric moisture profile at the D3 (1.0 m) cover.

5.3.3.1 Sulphur

The depth profiles of total S concentration at the mid-slope sites are presented in Figure 5.20. At both sites the total S concentration ranged from 0.22 to 2.3 g/kg in the peat/till cover and from 4.3 to 7.7 g/kg in the shale. These results were similar to the total S concentrations measured in the shale at the upper slope (30-D3-B) and the plateau (30-D3-C) sites (Figure 5.5). No difference in the total S concentration profiles as a result of slope position or cover treatment was observed.

5.3.3.2 Carbon

The TIC and TOC concentration profiles with depth for the mid-slope sites are presented in Figure 5.21. The TIC concentrations in the peat/till cover and the shale at both sites ranged from 0.5 to 0.8 wt %. The TIC concentrations remained relatively constant throughout the soil profiles at both sites. The TOC concentrations ranged from 0.6 to 2.6 wt % in the peat/till cover and from 0.9 to 1.5 wt % in the shale. TOC concentrations in the shale were greater than TOC concentrations in the till. The TIC and TOC concentration profiles for both mid-slope sites were similar to those of the upper slope and plateau sites.

5.3.4 Pore gas O_2, CO_2 and CH_4 Concentrations

The gas probes at 30-D3-A (1 m cover) and 30-D2-A (0.35 m cover) were installed in November 2000 and June 2001 respectively (for specific sampling dates and gas concentrations refer to Appendix E). The pore-gas O_2 and CO_2 profiles with depth for the mid-slope sites are presented in Figures 5.22 and 5.23. Pore-gas CH_4 was not detected at the mid-slope sites throughout the sampling program. At both sites the O_2 concentration decreased from atmospheric at ground surface (20.9 %) to values ranging from 1 to 10 % at 4 m depth. Thus, a decreasing O_2 concentration gradient was observed to exist between ground surface and 3 m depth at both sites. Exceptions to these data were the O_2 concentrations measured in the 3.05 and 4.05 m gas probes at 30-D3-A.on August 26, 2002. The O_2 concentrations on August 26 measured 17 and 20 % respectively. The

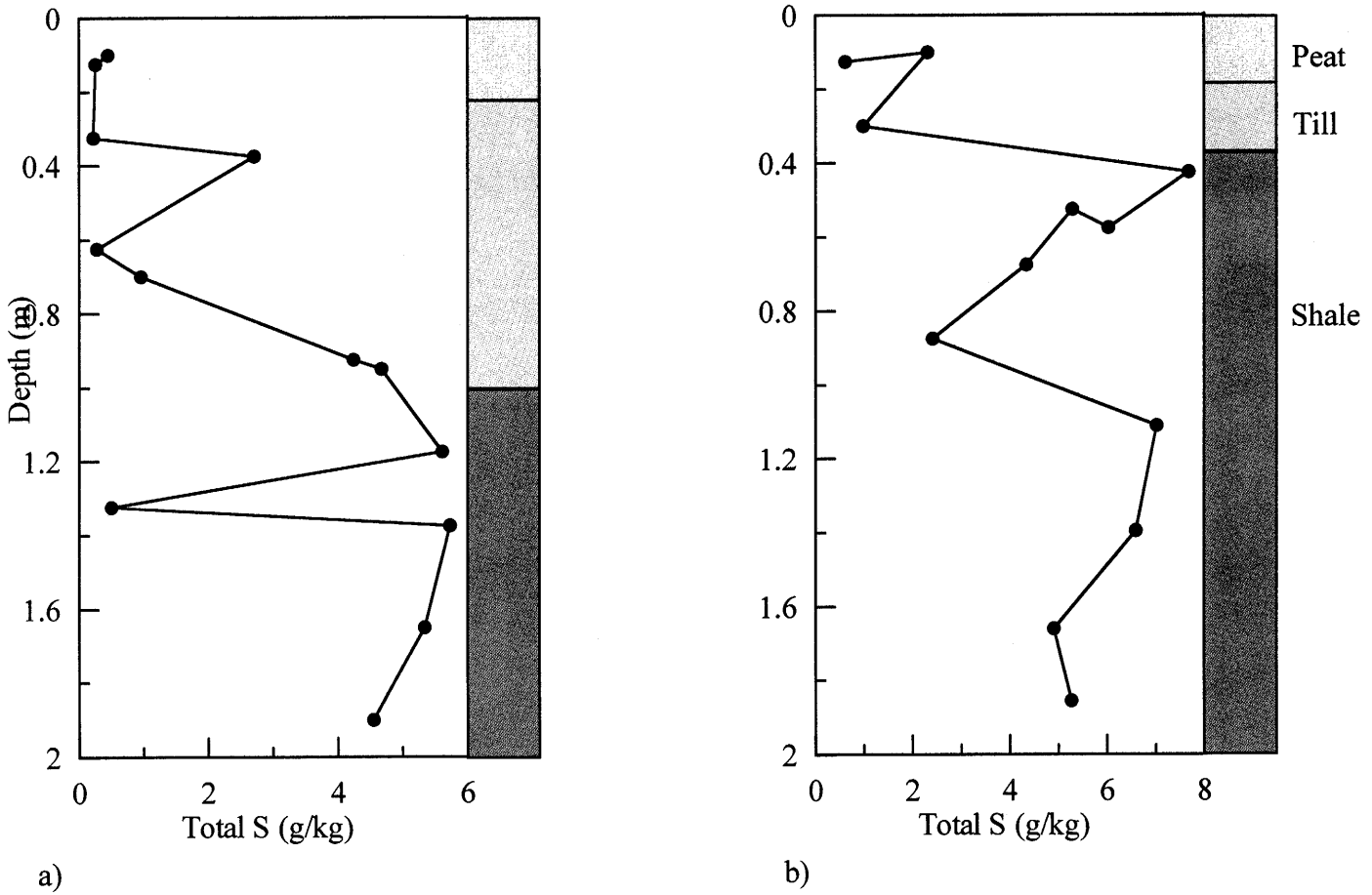

Figure 5.20: South Bison Hill mid-slope sites. Total S concentration with depth profiles. Total S concentration was measured on soil samples collected in June 2001.
a) 30-D3-A (1 m cover) b) 30-D2-A (0.35 m cover).

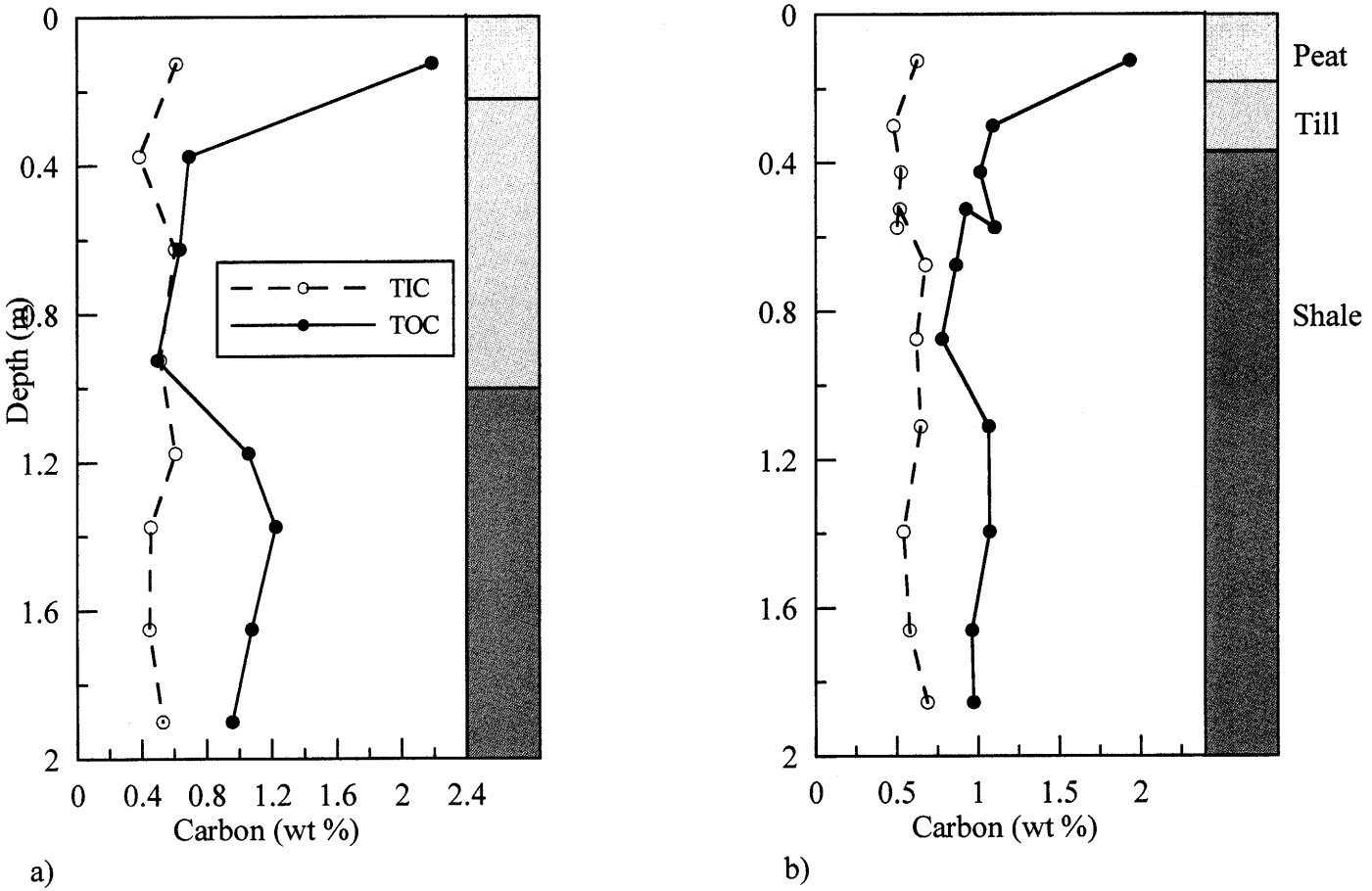

Figure 5.21: South Bison Hill mid-slope site TIC and TOC concentrations with depth. TIC and TOC concentrations were measured on soil samples collected in June, 2001. a) 30-D3-A (1 m cover) b) 30-D2-A (0.35 m cover).

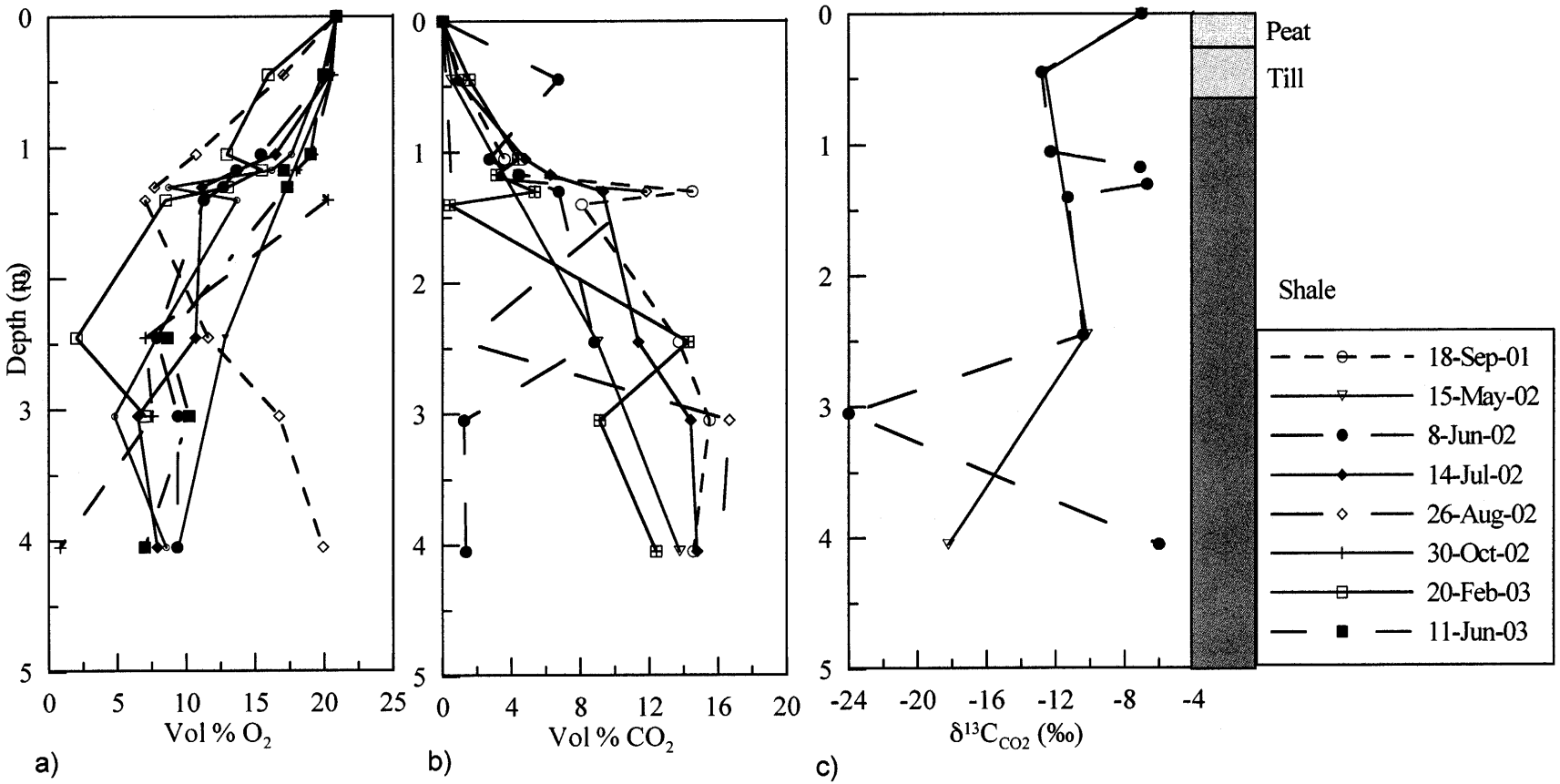

Figure 5.22: 30-D3-A (mid-slope, 1 m cover) pore-gas concentration profiles with depth for each sampling occasion. a) O_2 concentration profile showing a decrease in O_2 with depth. b) CO_2 concentration profile showingan increase in CO_2 with depth. c) $\delta^{13}C_{CO2}$ profile with depth.

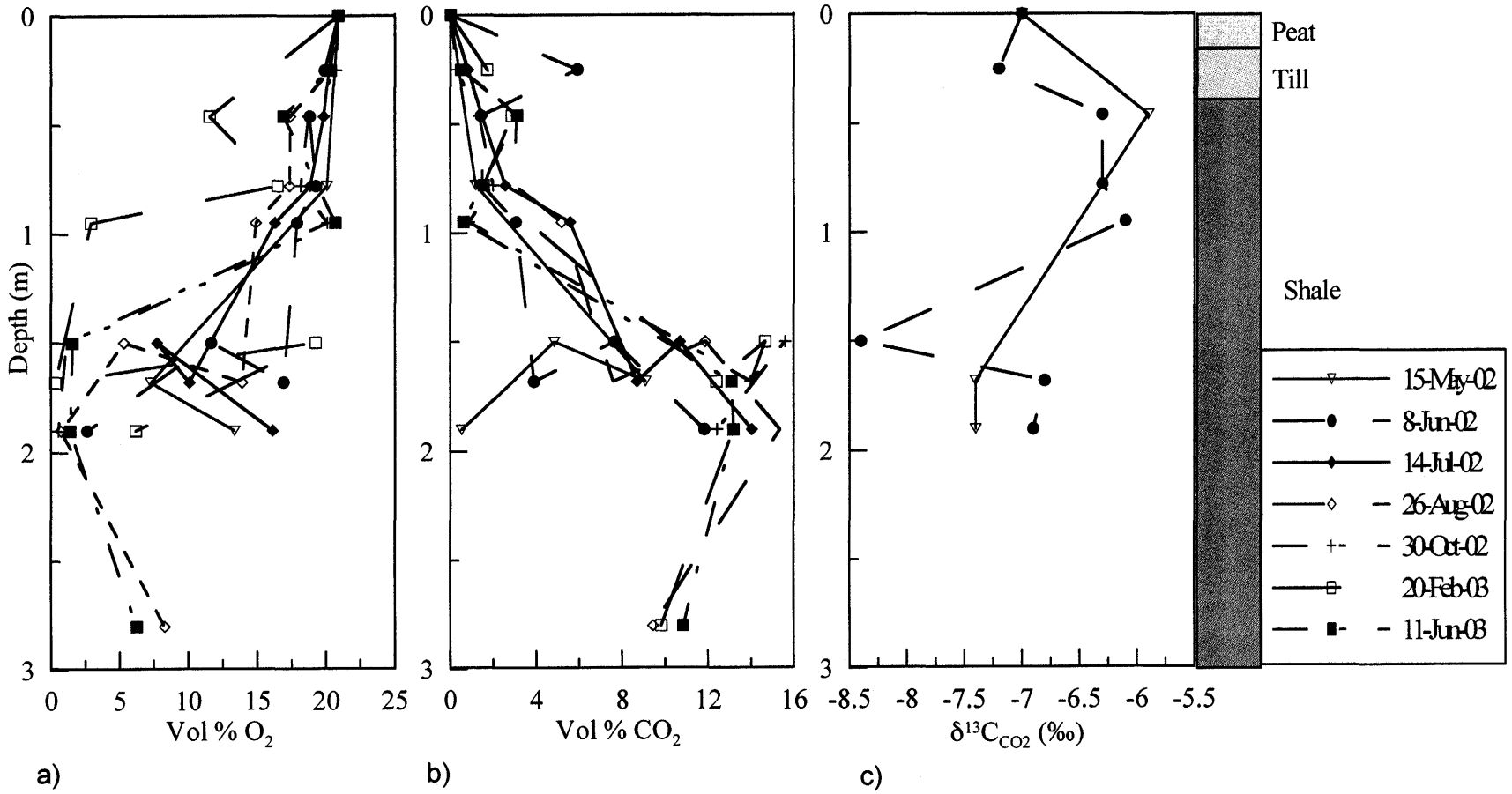

Figure 5.23: 30-D2-A (mid-slope, 1 m cover) pore-gas concentration profiles with depth for each sampling occasion. a) O_2 concentration profile showing a decrease in O_2 with depth. b) CO_2 concentration profile showing an increase in CO_2 with depth. b) $\delta^{13}C_{CO2}$ profiles with depth.

anomalous O_2 concentrations measured on this occasion were attributed to atmospheric contamination during sampling. The CO_2 concentration increased from atmospheric at ground surface (0.04 %) to values between 10 and 16 % at 4 m depth. Exceptions to these data were the CO_2 concentrations measured at the 3.05 and 4.05 m gas probes on May 15 2002 at 30-D3-A and at the 1.9 m gas probe at 30-D2-A. On this sampling occasion, the CO_2 concentrations were <2 %. These anomalous CO_2 concentrations were attributed to atmospheric contamination. The CO_2 concentration profile indicated that an increasing CO_2 concentration gradient was present between ground surface and 3 m depth on all sampling occasions.

The depth profile of O_2 concentrations for the mid-slope sites showed that the average O_2 concentrations at 3 m below ground surface (approximately 8 %) were greater than those measured at the same depth on the upper slope. At the upper slope site, the mean O_2 concentration was 4 % at 3 m depth. The difference in O_2 concentrations at 3 m may have been a result of varying degrees of soil compaction and soil heterogeneity. The CO_2 concentrations measured at the mid-slope sites were comparable to those measured on the upper slope. Both the O_2 and CO_2 concentrations measured at the mid-slope sites were within the range of concentrations reported in other unsaturated soil investigations (Section 5.2.5.1). The shape of the O_2 and CO_2 concentration profiles at the mid-slope sites were similar to those of the upper slope and plateau sites. At all instrumented sites on SBH, O_2 and CO_2 concentration gradients were measured from ground surface to approximately 3 m depth. Below 3 m, the O_2 and CO_2 concentrations at these sites remained relatively constant with depth (to 25 m below ground surface). These results suggested that O_2 and CO_2 diffusion in and out of the soil media was not affected by cover thickness or slope position. A possible explanation for this result may be the existence of freeze-thaw fractures in the shallow soil profile (0 to 3 m). It was possible that fractures created by freeze-thaw cycles in the soil surface extend to a common depth throughout the SBH overburden pile. The temperature data indicated that sub-surface temperature varied between 0 and 5 m depth. Below 5 m, the temperature remained constant. These results suggested that the depth of fracturing as a result of freeze-thaw cycles was approximately 5

m. The O_2 and CO_2 diffusion wad observed to occur to a similar depth of approximately 5 m within the profile despite slightly differing soil physical properties.

The absence of pore-gas CH_4 at the mid-slope sites was in contrast to the pore-gas chemistry results from the upper slope and plateau sites. At these sites, CH_4 (< 80 ppm) was detected in the 3 and 4.5 m gas probes. The absence of CH_4 at the mid-slope sites was attributed to the greater O_2 concentrations at the 3 m gas probes relative to the upper slope site. In the presence of significant O_2 concentrations, the CH_4 may have oxidized to CO_2 and therefore was not detected (Whiticar et al., 1986).

The O_2 and CO_2 concentrations were plotted against time (in months) from the installation date to estimate the time required for gas probes to reach steady-state. The pore-gas concentrations versus time plots were also used for identifying temporal variations and pore-gas relationships. The O_2 and CO_2 concentration versus time plots are presented in Figures 5.24 and 5.25. For simplicity, the 0.55, 1.05 and 4.05 m gas probes at 30-D3-A (1 m cover) and the 0.45, 0.78, and 1.9 m gas probes at the 30-D2-A (0.35 m cover) were considered representative of each site. At the 1 m cover site, the 0.45 m gas probe reached steady-state much more quickly than the deeper probes. This result was attributed to the already near-atmospheric gas concentrations present at 0.45 m depth. At this probe, the CO_2 concentrations were observed to increase slightly in June of each sampling season (2001 to 2003). These results suggested that the CO_2 concentration in the 0.45 m gas probe was affected by seasonal variations.

Corresponding seasonal variations in O_2 concentrations were not observed. At the 1.05 m probe, the time profile showed that the O_2 concentration decreased until approximately September 2001. After September, the O_2 concentrations were variable throughout the remainder of the sampling program. The CO_2 concentrations followed a similar, but inversely correlated, trend. Similar to the 0.45 m gas probe, slightly elevated CO_2 concentrations were measured in June of each summer sampling season. These results suggested that the CO_2 concentration in the 1.05 m gas probe varied seasonally. The concentration versus time profile for the 4.05 m gas probe showed that O_2 concentration

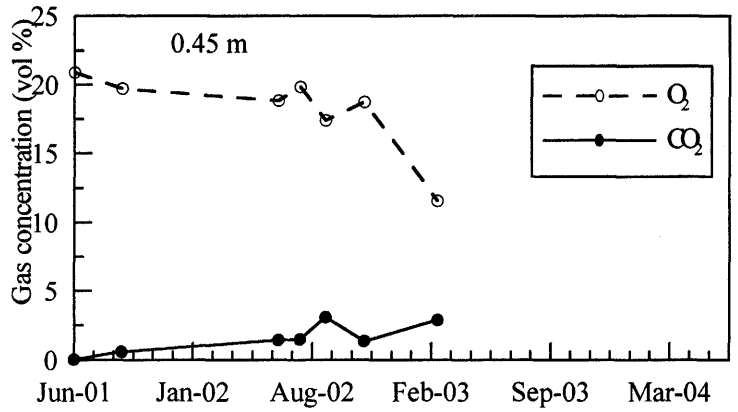

a)

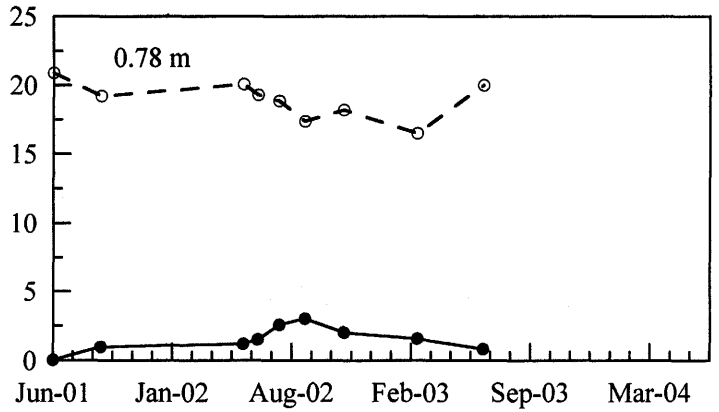

b)

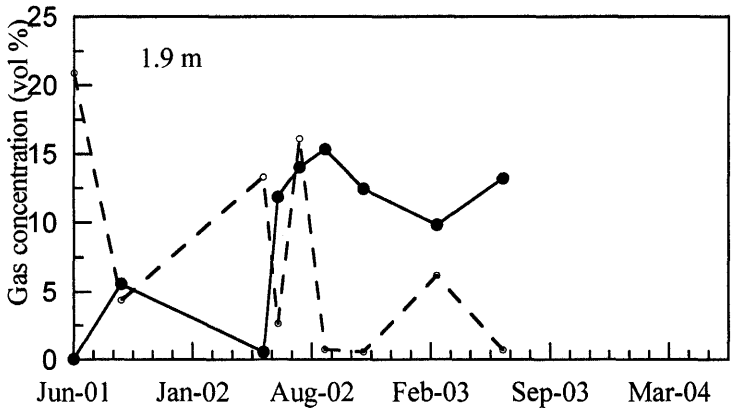

c)

Figure 5.24: 30-D3-A (mid- slope) pore-gas concentrations profiles versus time at the 0.45, 0.78 and 1.9 m deep gas probes. The O_2 and CO_2 concentrations reached steady-state after September, 2001.
a) 0.45 m gas probe. b) 0.78 m gas probe. c) 1.9 m gas probe.

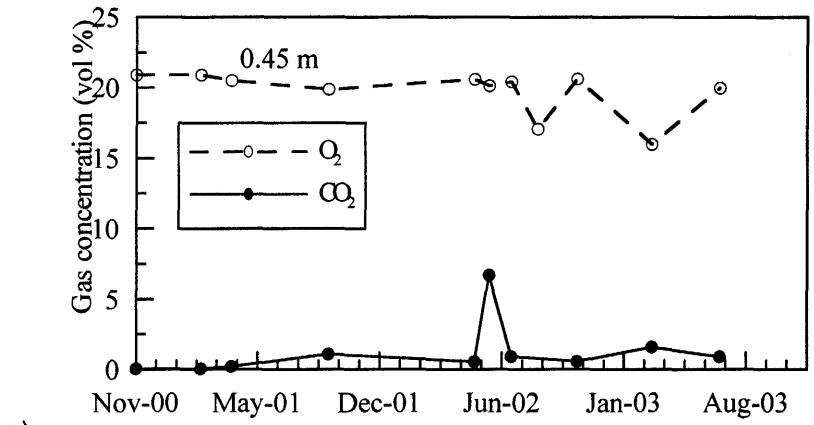

a)

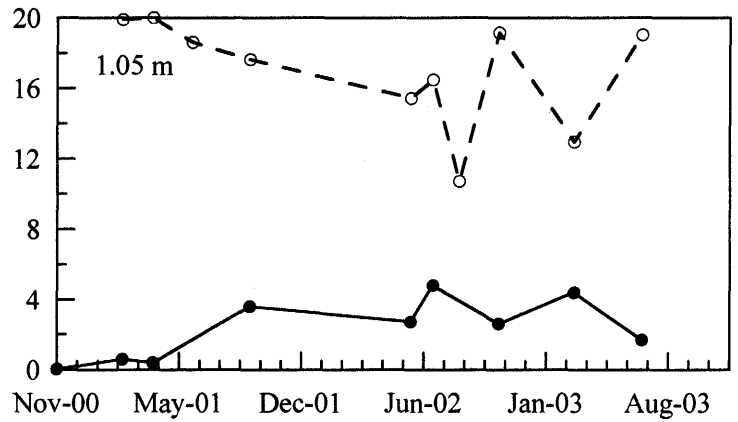

b)

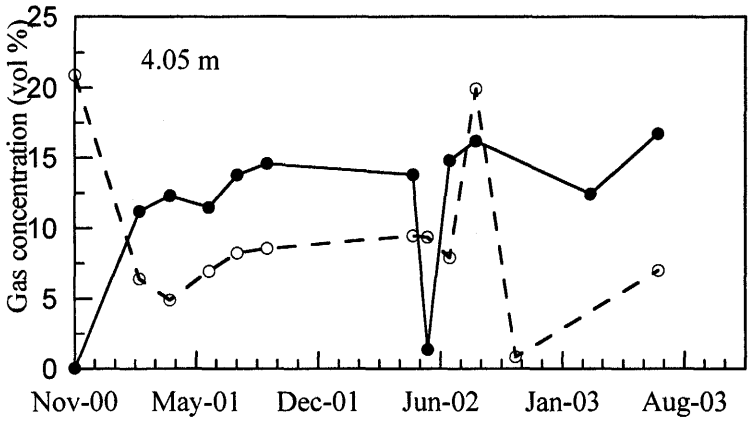

c)

Figure 5.25: 30-D3-A (mid-slope, 1m cover) pore-gas concentration versus time profiles for the 0.45, 1.05 and 4.05 m deep gas probes. The O_2 and CO_2 concentrations reached steady-state after September 2001. a) 0.45 m gas probe. b) 1.05 m gas probe. c) 4.05 m gas probe.

decreased until April 2001. The CO_2 concentration increased until the same sampling occasion. Seasonal variations in the pore-gas chemistry at this probe were not observed.

At the 0.35 m cover, O_2 concentrations at a depth of 0.45 m decreased from installation (June 2001) until approximately June 2002. The CO_2 concentration increased until the same sampling occasion. Similar results were observed at the 0.78 m gas probe. These results suggested that the pore-gas chemistry in the 0.45 and 0.78 m gas probes required approximately one year to reach steady-state. The CO_2 concentration in both shallow gas probes was observed to increase in the summer months of 2002. A corresponding decrease in O_2 concentration was observed in both gas probes. These results suggested that the O_2 and CO_2 concentrations in these gas probes varied seasonally. At the 1.9 m gas probe, the O_2 concentration decreased from installation (June 2001) to approximately September 2001. The CO_2 concentration increased until the same sampling period. After September, the O_2 and CO_2 concentrations were extremely variable throughout the sampling program. Seasonal trends were not observed. These results were similar to those of the upper slope site, where seasonal trends were observed only in the shallow gas probes (0.55 and 1.05 m). The time required for the gas probes to reach steady-state at the mid-slope sites (about 320 and 340 days respectively) was similar to the time required for the upper slope and plateau sites.

5.3.5 $\delta^{13}C_{CO2}$

$\delta^{13}C_{CO2}$ was measured on pore-gas samples collected from the mid-slope sites throughout the sampling program. For specific dates and sampling results refer to Appendix D. As noted in Section 5.3.4, approximately one year was required for the pore-gas chemistry to reach steady-state after gas probe installation. Therefore, the $\delta^{13}C_{CO2}$ data collected prior to September 2001 (30-D3-A) and June 2002 (30-D2-A) were not included in the calculation of mean $\delta^{13}C_{CO2}$ values. However, it was important to note that $\delta^{13}C_{CO2}$ in the complete data set were not observed to vary seasonally. The $\delta^{13}C_{CO2}$ results for 30-D3-A (1 m cover) and 30-D2-A, 0.35 m cover) are presented in Figures 5.22 and 5.23. The $\delta^{13}C_{CO2}$ at the 1 m cover site ranged from -7 to -12 ‰, with the exception of the 3 m gas probe. The

$\delta^{13}C_{CO2}$ measured at 3 m was -24 ‰. The $\delta^{13}C_{CO2}$ measured prior to the pore-gas chemistry reaching steady-state at the 3 m gas probe indicated a $\delta^{13}C_{CO2}$ of -10 ‰. Therefore, an error in sample analysis may have resulted in the anomalously negative $\delta^{13}C_{CO2}$ value. The $\delta^{13}C_{CO2}$ at the 0.35 m cover site was constant with depth in the profile at approximately -7 ‰. The slightly more negative $\delta^{13}C_{CO2}$ measured at the 1 m cover (relative to the 0.35 m cover) suggested that a greater fraction of pore-gas CO_2 was produced from organic respiration at this site. This result suggested that the 1 m thick cover resulted in increased organic respiration. The $\delta^{13}C_{CO2}$ data indicated that pore-gas CO_2 was produced primarily from an inorganic source at both mid-slope sites.

The $\delta^{13}C_{CO2}$ profile for the upper slope site (30-D3-B, 1 m cover) indicated that $\delta^{13}C_{CO2}$ was constant at approximately -4 ‰ throughout the profile (Section 5.2.4.7). At the SBH plateau, $\delta^{13}C_{CO2}$ ranged from +1 to -7 ‰. The $\delta^{13}C_{CO2}$ profiles for both 30-D3-A (mid-slope, 1 m cover) and 30-D2-A (mid-slope, 0.35 m cover) were within the range of $\delta^{13}C_{CO2}$ data for the upper slope and plateau sites.

5.4 Rate of Salt Release in the SBH Overburden Pile

Calculating the rate of salt production within the SBH overburden pile was undertaken to evaluate the risk of soil salinization where salt release reactions were occurring. The calculation of salt production rates was required to provide necessary data for the evaluation of the ability of SBH soil to sustain native reforestation over the long-term. The results of solid sample analyses (see Section 5.2.3) suggested that the reduced S forms present within SBH were being oxidized to soluble S within the upper 2.5 to 4 m of the shale. The pore-gas chemistry presented for the upper slope and plateau sites (Section 5.2.5) further suggested that O_2 consumption and CO_2 production within the waste pile were occurring to a greater extent than could be explained by organic respiration alone. In addition, the $\delta^{13}C_{CO2}$ results (Section 5.2.5.6) indicated that the pore-gas CO_2 was produced primarily from an inorganic carbon source and suggested that carbonate mineral dissolution was occurring in response to acid produced by sulphide mineral oxidation.

The rate calculations were conducted using data collected at the upper slope and plateau sites. The diffusive flux through the till was estimated from the O_2 concentration profiles and Fick's first law. The diffusive flux calculations were done using the more detailed, upper-slope O_2 concentration profile. The calculation provided an estimate of the O_2 diffusion rate into the shale at the till/shale interface. The rate of O_2 diffusion into the shale was considered equal to the rate of O_2 consumption occurring within the shale. The rate of salt release within the shale was estimated stoichiometrically based on the O_2 consumption rate. Salt balance calculations were performed using the solids sample chemistry from the anaerobic samples (collected at the SBH plateau in August 2002) to estimate the rate of salt-release in the top 3 m of the soil profile. Finally, the estimated rate of salt release was compared to the salt release rates determined from solid sample analysis.

5.5 Analytical Modelling of Pore-gas O_2 and CO_2 Concentrations

Fick's first law was used to estimate the O_2 flux through the till and equated to the rate of sulphide oxidation at the till/shale interface. It was assumed that O_2 consumption within the peat/mineral mix layer (0 to 0.20 m) was negligible. This assumption was evidenced by the lack of decrease in O_2 concentration through this zone. In addition, the peat/mineral mix contained very low concentrations of total S and TIC (Section 5.2.3). As a result, the top of the model was set at 0.20 m below ground surface and that the O_2 concentration was atmospheric at 0.20 m depth. This model assumed that the porosity and moisture content within the till were constant with depth and that O_2 flux was occurring under steady-state conditions. It was recognized that the physical properties of the till were variable with depth and that all O_2 consumption was not occurring at the till/shale interface. The O_2 consumption by microbial respiration in the till was considered negligible with respect to the O_2 consumed by sulphide mineral oxidation. However, a detailed, transient-state model to determine O_2 consumption and CO_2 production rates was beyond the scope of this study. The simple, analytical solution provided a first estimate of the O_2 consumption rate, with the understanding that in-depth modelling of O_2 and CO_2 concentrations may be required in the future.

The calculation required input parameters of effective diffusion coefficient (D_e), temperature, and air-filled porosity. The mean subsurface temperature measured at the SBH plateau as well as the mean annual air temperature measured between 1999 and 2003 (D. Chapman, personal communication) was calculated to be 2 °C. The porosity in the till was estimated from dry bulk density measurements (Boese, 2003) to range from 37 to 64 %. The moisture content for the shallow till was estimated from the converted gravimetric data (Section 5.2.2) to range from 20 to 43 % by volume. The D_e for O_2 (Equation 2.15) was calculated to range from 0.06 m^2/day to 0.55 m^2/day based on the range of porosity and moisture content values.

The initial molar concentration of O_2 was calculated from atmospheric concentrations (20.9 % O_2) using the Ideal Gas Law (Equation 3.9). It was 9.33 moles/m^3 O_2. The mean O_2 concentration at the till/shale interface was 14.3 %. The thickness of the till at the upper slope site was 0.8 m.

The rate of O_2 flux ranged from 0.03 moles O_2/m^2/day for till at 73 % saturation to 0.16 moles O_2/m^2/day at 51 % saturation, with a mean flux of 0.07 moles O_2/m^2/day. Equation (2.1) indicates that for every mole of O_2 consumed by sulphide mineral oxidation, 0.6 moles of SO_4^{2-} are produced. For the estimated sulphide oxidation rate, the rate of SO_4 production would range from 1 x 10^{-3} to 8 x 10^{-3} g SO_4/m^2/day. The solid sample analysis indicated that the mean reduced S concentration in the top 1.5 m of the shale was 4 g/kg, while the mean reduced S concentration between 5 and 25 m depth was 6.4 g/kg. The results from pore-gas chemistry suggested that the primary zone of oxidation at SBH was in the top 2 m of the shale. Assuming that the reduced S concentration was constant with depth at the time of waste pile construction, the top 2 m of the shale would contain approximately 295 moles/m^3 of reduced S. At the estimated rate of oxidation, it would take between 10 and 50 years (mean = 22 years) to oxidize the entire mass of reduced S in the shallow shale zone.

The results from solid sample analysis suggested that approximately 2 g/kg reduced S had been oxidized between the time of pile construction and the time of analysis (6 years), if the reduced S concentration was constant with depth at the time of construction. Using the solid sample results, the rate of SO_4^{2-} production was approximately 2.7 x 10^{-3} g/kg/day. At this rate, it would take approximately 20 years to completely oxidize the reduced S concentration in the top 2 m of shale. These results suggested that the rate of sulphide oxidation estimated from solid sample analysis is comparable to the mean oxidation rate estimated using Fick's law of diffusion.

Comparison of the O_2 flux with rates reported in literature for mine waste piles was difficult. O_2 consumption rates have been found to be strongly dependent on sulphide concentration, moisture content and grain size (Hollings et al., 2000; Eberling et al., 1993; Eberling, 1996). Eberling et al. (1993) reported O_2 flux ranging from 1.5 x 10^{-3} moles O_2/m^2/day in fine-grained, near-saturated soil to 4.3 moles O_2/m^2/day in coarse-grained soil. The broad range in O_2 flux indicated the sensitivity of flux rates to variations in D_e. At a mine tailings area near Sudbury, Ontario, Eberling and Nicholson (1996) measured O_2 consumption rates ranging from 2.7 x 10^{-4} moles O_2/m^2/day in the capillary zone to 0.68 moles O_2/m^2/day at sites where the water table is below the oxidation zone. The O_2 flux was observed to decrease by as much as a factor of 1000 where the fine-grained sand layer (80 %) saturation) was present (Eberling and Nicholson, 1996). The O_2 flux measured at SBH was comparable to those reported in literature. The slowest flux rates reported in literature were measured in fine-grained, near saturated soils containing up to 10 % (by weight) sulphides.

Similar calculations were performed to estimate the rate of CO_2 flux out of the shale at the till/shale interface. The calculation used the mean CO_2 concentration at the till/shale interface as the initial concentration. This was determined from pore-gas chemistry to be 1.79 moles CO_2/m^3. The final CO_2 concentration was the atmospheric concentration of 0.016 moles CO_2/m^3. The CO_2 flux through the till ranged from 7.8 x 10^{-3} to 0.27 moles CO_2/m^2/day, with a mean of 0.08 moles CO_2/m^2/day. Equation (2.4) indicates that for every mole of $CaCO_3$ dissolved, one mole of CO_2 and one mole of Ca^{2+} are produced.

Therefore, the rate of Ca^{2+} production was estimated to range from 0.67 to 3.0 g $Ca^{2+}/m^2/day$, with a mean production rate of 1.5 $g/m^2/day$. Results from TIC analysis on solid samples indicated that the shale contained an average of 108 moles $CaCO_3/m^3$ shale. At the estimated rate of $CaCO_3$ dissolution, it would take between 2 and 76 years (mean = 7 years) to dissolve the entire $CaCO_3$ concentration in the top 2 m of shale, depending on the moisture content and air-filled porosity of the shale. These results suggested that at CO_2 production rates ranging between the maximum and mean, the shale may not contain the necessary carbonate concentration to neutralize the acid produced from sulphide mineral oxidation. At a CO_2 flux of 0.06 $moles/m^2/day$ or less, the shale contained the necessary carbonate minerals to neutralize the acid produced.

CO_2 flux at other mine waste piles was not reported in literature. However, it is well understood that the rate of CO_2 production is strongly dependent on moisture content and temperature (Wood et al., 1993; Wood and Petraitis, 1984; Keller and Bacon, 1998, Hendry et al., 1999). CO_2 flux from soil to the atmosphere under steady-state conditions was measured by Kabwe et al. (2001) in a laboratory experiment. The mean CO_2 flux value in the dynamic closed chamber system using the concentration gradient method ranged from 3.6×10^{-2} to 0.16 moles $CO_2/m^2/day$, depending on the temperature and the size of the system. The lower temperature system (5°C) produced a lower CO_2 flux than the higher temperature (21°C) system. De Jong and Scharppert (1972) reported an average CO_2 flux of 0.55 moles CO_2/m^2day during the summer in native prairie grassland and Clark and Kemper (1967) reported fluxes measured on bare soils ranging from 5.2×10^{-2} to 0.55 moles $CO_2/m^2\backslash day$. The CO_2 flux estimated using the concentration gradient method at SBH yielded rates comparable to those reported in literature. The broad variation in CO_2 flux in this and other studies indicated the sensitivity of CO_2 flux calculations to D_e.

5.6 Summary and Conclusions

In situ measurements of pore-gas O_2, CO_2 and CH_4 concentrations were used in conjunction with soil moisture content, temperature and solid sample chemistry to estimate the types and rates of geochemical reactions occurring within the South Bison Hill

overburden pile. The results of the study showed that the pore-gas chemistry and moisture content profile at the undisturbed control site was different than that of the South Bison Hill overburden pile. At the control site, the minimum pore-gas O_2 concentration was 19.4 %. The maximum CO_2 concentration was 0.4 %. The O_2 consumption and CO_2 production occurring at this site was attributed to microbial and root respiration. This conclusion was further supported by the $\delta^{13}C_{CO2}$ results. The O_2 and CO_2 concentrations were observed to vary seasonally, with the maximum concentrations for both species measured in July and August. Pore-gas CH_4 was not detected at this site. The volumetric moisture content profile for Control-1, determined from converting gravimetric measurements, showed that the moisture content was constant throughout the soil profile at 24 %.

At SBH, the O_2 concentrations were observed to decrease from 20.9 % at ground surface to a mean value of 3.5 % at 3 m depth. The CO_2 concentrations increased from 0.036 % to a mean of 9 % over the same depth. Below 3 m, the O_2 and CO_2 concentration profiles remained relatively constant at 2 % O_2 and 4 % CO_2 with depth (to 25 m). Seasonal variation in O_2 and CO_2 concentrations were only observed in the gas probes located between ground surface and 1 m depth. The pore-gas concentration profiles at SBH suggested that the change in O_2 and CO_2 concentrations between ground surface and 3 m depth were too great to be attributed solely to organic respiration. These results were supported by $\delta^{13}C_{CO2}$ analysis. The $\delta^{13}C_{CO2}$ profiles for all instrumented sites on SBH suggested that the pore-gas CO_2 was derived primarily from an inorganic source. Pore-gas CH_4 was measured at the upper slope and plateau sites. The profiles of pore-gas concentrations versus time suggested that CH_4 was oxidized when O_2 concentrations exceeded 2 %. The greatest CH_4 concentrations correlated with low O_2 concentrations, suggesting that pore-gas CH_4 was likely produced at the water table and diffused upward until it was oxidized in the presence of O_2.

The converted gravimetric moisture content profile at SBH showed the presence of two different moisture content zones. Between ground surface and 2.5 m depth, the moisture content ranged from 23 to 31 %. These results indicated that the till and upper 1.5 m of

shale were at or near saturation. Below 2.5 m, the moisture content ranged from 24 to 29 %, indicating that the shale was about 80 % saturated. Saturated or near-saturated conditions in the shallow profile (0 to 2.5 m) were confirmed by visual observation by the presence of standing water in shallow water wells installed at the till/shale interface (1.0 m depth).

The estimated rate of O_2 and CO_2 flux through the till is strongly dependent on the moisture content. Accurate, detailed moisture content measurements through the shallow profile (0 to 5 m) are required to obtain a reasonable estimate of gas flux through the till. The moisture content investigations in this study showed that there are advantages and disadvantages to the Diviner 2000, neutron probe moisture measurement and gravimetric moisture content measurements. The Diviner 2000 moisture probe must be properly calibrated for the soil type being investigated in order to achieve accurate moisture values. Without proper calibration, moisture data must be regarded as relative data. Proper calibration of the Diviner probe for SBH overburden was a time-consuming process beyond the scope of this investigation. The Diviner probe also presented limitations with respect to its small measurement volume and sensitivity to salinity. These limitations were observed in the SBH saline sodic media. The neutron probe method provided a detailed volumetric moisture content profile over 25 m. The neutron probe is not measurements are not affected by salinity, and the larger sphere of influence produced a smoother moisture profile that was less affected by poor tube contact with the soil than the Diviner measurements. However, the less effective (but stronger) steel access tube required and the difficulty of ensuring a tight fit between the tube and the shale over a 25 m profile reduced the reliability of the neutron probe data in this study. The gravimetric moisture content measurements presented a one-time profile of moisture content and did not yield insight into the moisture content changes with time. In addition, the gravimetric moisture content measurements presented limited detail when measuring moisture contents over a 25 m profile. Although the gravimetric moisture content measurement method presented limitations in detail, this method was determined to be the most accurate representation of field moisture conditions in this study.

The results from solids chemistry suggested that there were differences in soil chemistry between the shallow (0 and 5 m depth) and deep zones (5 to 25 m). The exact depth of the shallow zone varied somewhat between soil analyses; however, it was estimated to extend to approximately 5 m depth. The total S results indicated that the greatest total S concentration was measured at 3 m below ground surface. Soluble S results showed the greatest soluble S concentration occurring at 1.4 m depth. Overall, the S results indicated that the reduced form of S dominated the soil profile. EMPA determined that pyrite was the primary sulphide mineral present in the till and shale. In addition, EMPA showed that iron oxide minerals co-existed with pyrite in solid till and shale samples collected between ground surface and 2 m depth. Combined, these results suggested that an oxidizing environment was present within the top 5 m of the profile.

The TIC and TOC results did not indicate significant variations between the shallow and deep zones in the profile. Both TIC and TOC concentrations measured in the till and the shale were within the range of concentrations reported in literature. Acid-base accounting for the SBH shale showed that although the NNP of the SBH shale was within the indeterminate range (-20 to +20), the acid-generating potential of the shale potentially exceeded the neutralization potential (mean NNP = -6.5).

The soluble and exchangeable ion results for the SBH profile showed greater TDS, soluble Na^+ and soluble Ca^{2+} concentrations at 1.4 and 2.5 m than at other depths in the profile. The exchangeable ion results indicated that between 1 and 5 m depth the dominant exchangeable cation varied between Na^+ and Ca^{2+}. Below 5 m, Na^+ was the dominant exchangeable cation. These results suggested that carbonate mineral dissolution had occurred within the top 2 m of the shale (1 to 3 m depth). The greater concentration of soluble Na^+ and Ca^{2+} ions present between 1 and 3 m depth may have resulted in ion exchange on the clay mineral surfaces. This would result in the variable exchangeable ion concentrations observed at shallow depths in the profile.

The chemical analysis of two separate sets of solid samples was useful for understanding the changes in solids chemistry as a result of storage and handling techniques. The two

sets of solid samples were transported, stored and dried under both atmospheric (the first set of samples) and anoxic (the second set of samples) conditions. The results indicated that for the most accurate field representation of soluble ion concentrations, soil samples should be transported, stored and dried in anoxic conditions. Sulphide oxidation and carbonate mineral dissolution was observed to occur in samples that are stored wet under atmospheric conditions. These results were in accordance with a previous study.

The solid sample results compared well with the pore-gas chemistry and stable isotope results. Both data sets suggested that the primary zone where geochemical reactions were occurring was between ground surface and 5 m depth. The results suggested that sulphide mineral oxidation was consuming O_2 and producing soluble S in the top 4 m of the shale. In response to the acid produced from oxidation, carbonate mineral dissolution reactions produced CO_2 in concentrations as high as 9 % and releasing Ca^{2+} ions. As a result, elevated Na^+ and Ca^{2+} ions were observed within the top 5 m of shale. Ion exchange between Na^+ and Ca^{2+} ions on the clay surfaces appeared to have occurred as a result of the increased soluble Ca^{2+} ion concentration at shallow depths in the shale.

The depth at which sulphide mineral oxidation and carbonate mineral dissolution reactions were occurring (1 to 5 m) correlated with the depth at which saturated or near-saturated conditions were measured to exist (1 to 2.5 m). These results suggested that the saturated or near-saturated conditions in the shale may have prevented the zone of oxidation from extending to greater depths. Near-saturated conditions greatly reduce the rate of O_2 diffusion into the shale thus reducing the sulphide mineral oxidation rate. In addition, the temperature data showed that sub-surface temperature varied to approximately 5 m depth. These results suggested that fractures produced as a result of freeze-thaw cycles may be present between ground surface and 5 m depth. The fractures may have increased the likelihood of O_2 diffusion through the zone of elevated saturation to the base of the fracturing (5 m), thus allowing sulphide mineral oxidation and salt release to occur in the top 4 m of the shale.

The rate at which the sulphide mineral oxidation (O_2 consumption) and carbonate mineral dissolution (CO_2 production) reactions were occurring was estimated using both mass balance calculations and one-dimensional, steady-state, analytical modelling. These methods assumed that all O_2 consumption and CO_2 production was a result of sulphide mineral oxidation and carbonate mineral dissolution. It was recognized that some O_2 consumption/CO_2 production as a result of microbial and root respiration was occurring, as evidenced by seasonal pore-gas O_2 and CO_2 variations in the shallow gas probes on SBH. However, the contribution of O_2 consumption and CO_2 production by microbial and root respiration was considered negligible compared to the contributions from sulphide mineral oxidation and carbonate mineral dissolution. The SO_4^{2-} production rate determined for the shale using mass balance calculations from the time of pile construction until the present (2.7×10^{-3} g/kg/day SO_4^{2-}) was comparable to the SO_4^{2-} production rate determined from modelling the O_2 flux through the till (1×10^{-3} to 1×10^{-8} g SO_4^{2-}/m^2/day). At these rates, it would take between approximately 10 and 50 years to oxidize the entire reduced S concentration in the top 2 m of the shale. It is important to note that the estimated flux rates are strongly dependent on moisture content, and may change significantly with changes in moisture content. The flux rates calculated in this study were based on a range of both porosity and moisture content values. The calculation of flux rates for individual sampling occasions may have been useful if representative detailed shallow moisture content data had been collected on the same occasions as time of pore-gas sampling. These results may have yielded a more in-depth understanding of the relationship between flux, pore-gas concentration and moisture content. However, the limited shallow moisture content data and limitations encountered with moisture content measurements prevented this analysis.

The O_2 flux through the till ranged from 0.03 to 0.16 moles O_2/m^3/day and the CO_2 flux ranged from 0.017 to 0.078 moles CO_2/m^3/day. The O_2 and CO_2 flux rates through the till were in keeping with those reported for other mine waste piles and soil-gas investigations reported in literature. The rate of carbonate mineral dissolution was estimated to range from 1.5 to 7.0 g $CaCO_3/m^2$/day, with a corresponding Ca^{2+} production rate ranging from 0.67 to 3.0 g/m^2/day. At this rate, it would take between 8 and 36 years to completely

oxidize the inorganic carbon present in the top 2 m of the shale. These results suggested that at the mean moisture contents measured in the top 5 m of the shale, the geochemical reactions would probably not cause a negative effect on the shale within the top 5 m of the soil profile.

In summary, this research has presented evidence that sulphide mineral oxidation and carbonate mineral dissolution are the primary geochemical reactions occurring within an unsaturated, saline-sodic waste pile. Although the saline-sodic shale of which the overburden waste pile is composed placed it at risk for both acidification and salinization, this research suggests that, at present, these conditions are not of concern. The low sulphur concentrations present in the shale, combined with the presence of near-saturated conditions in the shallow shale zone have resulted in oxidation reaction rates that are slow enough to be neutralized by the existing inorganic carbon concentrations.

5.7 Recommendations for future research

Suggestions for further research to improve the findings of this study include a detailed investigation of the moisture content conditions within the top 5 m of the overburden. It would be useful to understand the long-term persistence of the saturated zone below the cover/shale interface (1.5 to 3.0 m depth) to evaluate the potential for moisture conditions to change with time. A change in moisture conditions will affect the predicted O_2 consumption and CO_2 production rates and possibly cause the depth of the oxidation front to migrate with time. In addition, an evaluation of the presence and importance of advective gas migration through the overburden pile is considered beneficial. The presence of advective gas migration could influence the quantification of reaction rates in the waste pile. Previous studies on mine waste piles have indicated that advective transport can occur within waste piles as a result of pressure and temperature gradients. Lastly, in-depth numerical modelling is required to obtain a more accurate estimate of reaction rates within the waste pile.

This study has identified the primary geochemical reactions occurring within the overburden pile and the depths at which these reactions are occurring. The study has also provided an estimation of sulphate release rates within the pile. Understanding the geochemistry and rate of salt release plays an integral role in understanding the overall salt balance on the overburden pile. By knowing the rate and location of SO_4 and Ca production, and by investigating the detailed salt distribution over the shallow zone (0 to 3 m depth), it is possible to understand the direction of salt movement in the pile with time. As the shale has a very low hydraulic conductivity, it would be unlikely that the salts would travel down through the shale zone. Rather, the salts may diffuse upward through the cover along a concentration gradient. Therefore, it would be useful to investigate the salt distribution through the cover and shallow shale zone to determine the salt movement since the time of pile construction. It would also be useful to understand the water balance on the waste pile (i.e. precipitation, evaporation, and runoff) and how the water balance affects salt movement. The estimated upward diffusion rate of salts through the cover and the overall sulphide oxidation/carbonate dissolution rates can be combined with the water balance of the pile to estimate the loss of salts in runoff and the effects of evaporation and precipitation on salt distribution. In particular, a detailed study of water flow through the peat/till cover would add insight into the movement and flushing of salts in the cover. To characterize and quantify the fundamental processes controlling salt balance and landscape evolution on the waste pile, many aspects of salt and water balance need to be investigated. The calculated rate of salt production through sulphide oxidation and carbonate dissolution determined in this study can be used in conjunction with an understanding of the salt distribution through the cover, the water flow through the till and the relation of salt balance to water balance. The combined investigations will lead to an evaluation of the overall performance of the cover treatments and design of the overburden waste pile over time.

6 References

Aggarwal, P.K., Fuller, M.E., Gurgas, M.M., Manning, J.F., Dillon, M.A., 1997. Use of stable oxygen and carbon isotope analyses for monitoring the pathways and rates of intrinsic and enhanced in situ biodegradation. *Environmental Science and Technology*, 31:590-596.

Aggarwal, P.K., Dillon, M.A. 1998. Stable isotope composition of molecular oxygen in soil gas and groundwater; a potentially robust tracer for diffusion and oxygen consumption processes. *Geochimica et Cosmochimica Acta*, 62:4, 577-584.

Amundson, R., Stern, L., Baisden, T., Wang, Y., 1998. The isotopic composition of soil and soil respired CO_2. *Geoderma* 82:83-114.

Anderson, Sogaard, Larson, Flemming, Postma, Dieke, 2001. Pyrite oxidation in usaturated aquifer sediments, reaction stoichiometry and rate of reaction. *Environmental Science and Technology*, 35:20, 4074-4079.

Bardsley, C.E., Lancaster, J.D., 1965. Sulphur in Methods of Soil Analysis Part 2: Chemical and Microbiological Properties, Black, C.A. ed., American Society of Agronomy, Wisconsin, USA, 1102-1116.

Bennet, J.W., Comarmond, M.J., Jeffrey, J.J., 2000. Comparison of sulphidic oxidation rates measured in the laboratory and in the field. ICARD 2000 Proceedings, Denver, Colorado. The Society for Mining, Metallurgy, and Exploration Inc., 171-180.

Birkham, 2002. Characterizing geochemical reactions in waste-rock piles at the Key Lake mine using gaseous oxygen and carbon dioxide. M.Sc. Thesis, Department of Geological Sciences, University of Saskatchewan.

Birkham, T., Hendry, M.J., Wassenaar, L.I., Mendoza, C.A., Lee, E.S., 2003. Characterizing geochemical reactions in unsaturated mine waste-rock piles using gaseous O_2, CO_2, $^{12}CO_2$, and $^{13}CO_2$. *Environmental Science and Technology*,

Boese, C.D., 2003. The design and installation of a field instrumentation program for the evaluation of soil-atmosphere fluxes in a vegetated cover over saline/sodic shale overburden. M.Sc. Thesis, University of Saskatchewan.

Bresler, E., McNeal, B.L., Carter, D.L., 1982. Saline and Sodic Soils: Principles, Dynamics, Modeling, Advanced Series in Agricultural Science. Springer-Verlang Berlin Heildelberg New York.

Cerling, T. E., 1984. Stable isotopic composition of modern soil carbonate and its relationship to climate. *Earth and planetary Science letters*, 71:229-240.

Cerling, T.E., Solomon, D.K., Quade, J., Bowman, J.R., 1991. On the isotopic composition of carbon in soil carbon dioxide. *Geochimica et Cosmochimica Acta*, 55:3403-3405.

Clark, I., and Fritz, P., 1997. Environmental Isotopes in Hydrogeology. CRC Press, Lewis Publishers, Boca Raton FL, USA.

Coplen, 2002. Compilation of minimum and maximum isotope ratios of selected elements in naturally occurring terrestrial materials and reagents. U.S. Geological Survey Water Resources Investigations Report 01-4222.

Craig, H., 1953. The geochemistry of the stable carbon istopes. *Geochimica et Cosmochimica Acta*, 3:53-92.

Crill, P.M., 1991. Seasonal patterns of methane uptake and carbon dioxide release by a temperate woodland soil. *Global Biochemical Cycles*, 5:4, 319-334.

Curtin, D., Steppuhn, H., Selles, F., 1994. Structural stability of chernozemic soils as affected by exchangeable sodium and electrolyte concentration. *Canadian Journal of Soil Science*, 74:157-164.

Curtin, D., Mermut, A.R., 1985. Nature and behaviour of montmorillonite in an acid inland marine shale from east central Saskatchewan. *Soil Science Society of America Journal*, 49:250-255.

Donahue, R.L., Miller, R.W., Shickluna, J.C., 1983. Soils: An introduction to soils and plant growth. Prentice-Hall Inc., New Jersey, USA.

Dixon, J.B., Weed, S.B., 1989. Minerals in Soil Environments. Soil Science Society of America, Madison, Wisconsin.

Dusseault, M.B., Scafe, D.W., Scott, J.D., 1989. Oil sands mine waste management: clay mineralogy, moisture transfer and disposal technology. *AOSTRA Journal of Research*, 5:303-319.

Eberling, B., Damgaard, L.R., 2001. Microscale measurements of oxygen diffusion and consumption in subaqeous sulphide tailings. *Geochimica et Cosmochimica Acta*, 65:12, 1897-1905.

Eberling, B, Nicholson, R.V., David, D.J., 1993. Field evaluation of sulphide oxidation rates. *Nordic Hydrology*, 24:323-338.

Eberling, B., Nicholson, R.V., 1996. Field determination of sulphide oxidation rates in mine tailings. *Water Resources Research* 32:6, 1773-1784.

Fetter, C.W., 1993. Contaminant Hydrolgeology, 2nd ed. Prentice Hall, NJ, USA

Fredlund, D.G., Rahardjo, H., 1993. Soil Mechanics for Unsaturated Soils. John Wiley and Sons Inc., USA.

Freney, J.R., 1958. Determination of water-soluble sulphate in soils. *Soil Science*, 86:241-244.

Fuller, E.N., Schettler, P.D., Giddings, J.C., 1966. A new method for prediction of binary gas-phase diffusion coefficients. *Industrial and Engineering Chemistry*, 58:5, 19-27.

Garrels, R.M., Thompson, M.E., 1960. Oxidation of pyrite by iron sulphide solutions. *American Journal of Science*, 258: 57-67.

Gaston, L.A., Selim, H.M., Walthall, P.M., 1993. Predicting cation transport in smectitic soils. *Soil Science Society of America Journal*, 57:307-310.

Gelinas, P., Lefebvre,R., Choquette, M., 1992. Monitoring of acid mine drainage in a waste rock dump, in Environmental issues and waste management in energy and minerals production, Singhal et al. (eds.), Balkema, Rotterdam, pp 742-756.

Gerke, H.H., Molson, J.W., Frind, E.O., 1998. Modelling the effect of chemical heterogeneity on acidification and solute leaching in overburden mine spoils. *Journal of Hydrology*, 209:166-185.

Germain, M.D., Tasse, N., Bergeron, M., 1994. Limit to self-neutralization in acid mine tailings. *in* Environmental Geochemistry of Sulphide Oxidation, Alpers C.N., Blowes, D.W (eds.). American Chemical Society, Washington DC, pp 365-379.

Guy, R.D., Fogel, M.L., Berry, J.A., 1993. Photosynthetic fractionation of the stable isotopes of oxygen and carbon. *Plant Physiology*, 101:37-47.

Happell, J.D., Chanton, J.P., Showers, W.S., 1994. The influence of methane on the stable isotopic composition of methane emitted from Florida swamp forests. *Geochimica et Cosmochimica Acta*, 58:20, 4377-4388.

Harries, J.R., Ritchie, I.M., 1981. The use of temperature profiles to estimate the pyritic oxidation rate in a waste rock dump from an opencut mine. *Water, Air and Soil Pollution*, 15: 405-423.

Harries, J.R., Ritchie, I.M., 1985. Pore gas composition in waste rock dumps undergoing pyritic oxidation. *Soil Science*, 140:2, 143-152.

Hendry, M.J., Buckland, G.D., 1990. Causes of soil salinization: 1. A basin in Southern Alberta, Canada. *Groundwater*, 28:3, 385-393.

Hendry, M.J., Lawrence, J.R., Zanyk B.N., and Kirkland R., 1993. Microbial production of CO_2 in unsaturated geologic media in a mesoscale model. *Water Resources Research* 29 (4) 973-984.

Hendry, M.J., Mendoza, C.A., Kirkland, R.A., and Lawrence, J.R., 1999. Quantification of transient CO2 production in a sandy unsaturated zone. *Water Resources Research*, 35:7, 2189-2198.

Hendry, M.J., Wassenaar, L.I., Birkham, T.K., 2002. Microbial respiration and diffusive transport of O_2, $^{16}O_2$ and $^{18}O^{16}O$ in unsaturated soils – a mesocosm experiment. *Geochimica et Cosmochimica Acta*, 66:19, 3367-3374.

Hendry, J.P., 2002. Geochemical trends and palaeohydrological significance of shallow burial calcite and ankerite cements in Middle Jurassic strata on the East Midlands Shelf (onshore UK). *Sedimentary Geology* 151, 149-176.

Henry, J.L., Bullock, P.R., Hogg, T.J., Luba, L.D., 1985. Groundwater discharge from glacial and bedrock aquifers as a soil salinization factor in Saskatchewan. *Canadian Journal of Soil Science*, 65:749-768.

Hoag, R.B., Webber, G.R., 1976. Significance for mineral exploration of sulphate concentrations in groundwaters *in* Geochemical Exploration, CIM bulletin, 1976.

Hollings, P, Hendry, M.J., Kirkland, R.A., 2000. Quantification of oxygen consumption rates for gneissic waste rock piles, Key Lake Uranium Mine, northern Saskatchewan, Canada: Application for the kinetic cell technique, *ICARD Proceedings, 2000.*

Hunt, J.M., 1991. Petroleum geochemistry and geology, 2nd Edition. W.H. Freeman and Company, New York, USA.

Jaynes, D.B., Rogowski, A.S., 1983. Applicability of Fick's Law to gas diffusion. *Soil Science Society of America Journal*, 47:425-430.

Jaynes, D.B., Pionke, H.M., Rogowski, A.S., 1984. Acid mine drainage from a reclaimed coal strip mine I: Model Development. *Water Resources Research, 20:2, 233-242.*

Jurinak, J.J., Amrhein, C., Wagenet, R.J., 1984. Sodic hazard: The effect of SAR and salinity in soils and overburden materials. *Soil Science*, 137:3, 152-159.

Keller, C.K., Bacon, D.H., 1998. Soil respiration and georespiration distinguished by transport analyses of vadose CO2, 13CO2 and 14CO2. *Global Biogeochemical Cycles*, 12:2, 361-373.

Keller, C.K., 1985. Hydrogeology of the glacial till confining the Dalmeny aquifer near Martensville, Saskatchewan. Final Report No. 406-03, Saskatchewan Research Council, Saskatoon, Saskatchewan.

Kiddon, J., Bender, M.L., Orchardo, J., 1993. Isotopic fractionation of oxygen by respiring marine organisms. *Global Biogeochemical Cycles*, 7:3, 679-694.

Loeppert, R.H., Suarez, D.L., 1996. Carbonate and Gypsum in Methods of Soil Analysis Part III: Chemical Methods, Sparks, D.L. (ed.), Soil Science Society of America, Madison, Wisconsin, USA.

Lord, E.R.F., Isaac, B.A.A., 1989. Geotechnical investigations of dredged overburden at the Syncrude oil sands mine in Northern Alberta, Canada. *Canadian Geotechnical Journal*, 26:132-153.

Mason, B., Moore, C.B., 1982. Principles of Geochemistry. John Wiley & Sons, Toronto.

Massmann, J., Farrier, D.F., 1992. Effects of Atmospheric pressures on gas transport in the vadose zone. *Water Resources Research*, 28:3, 777-791.

Menzies, N.W., Mulligan, D.R., 2000. Vegetation dieback on clay-capped pyritic mine waste. *Journal of Environmental Quality*, 29:437-442.

Mermut, A.R., 2000. Chemistry and clay mineralogy of selected sediments from the Syncrude mine sites. Syncrude Canada contract report for Gord McKenna.

Mermut, A.R., Arshad, M.A., 1987. Significance of sulphide oxidation in soil salinization in Southeastern Saskatchewan, Canada. *Soil Science Society of America Journal*, 51:247-251.

Miller, J.J., Pawluck, S., Beke, G.J., 1993. Soil salinization at a side-hill seep and closed basin in Southern Alberta. *Canadian Journal of Soil Science*, 73:209-222.

Millington, R.J., Quirk, J.P., 1961. Permeability of porous solids. *Faraday Society Transactions*, 57:1200-1207.

Mitchell, J.K., 1979. Fundamentals of Soil Behaviour. John Wiley and Sons Inc.

Moran, S.R., Trudell, M.R., Macyk, T.M., Cheel, D.B., 1990. Plains hydrology and reclamation project: summary report. Alberta Land Conservation and Reclamation council, (RRTAC) Report 90-6.

Morin, Kevin A., 1990. Problems and proposed solutions in predicting acid drainage with acid-base accounting, *in* Acid Mine Drainage: Designing for Closure, Gadsby, J. Malick, J., Day, S., (eds.). BiTech Publishers Ltd., B.C., pp 93-109.

Moses, C.O., Nordstrom, D.K., Herman, J.S. and Mills, A.L., 1987. Aqueous pyrite oxidation by dissolved oxygen and by ferric iron. *Geochimica et Cosmochimica Acta*, 51:1561-1567.

Nicholson, R.V., Gillam, R.W., Cherry, J.A., Reardon, E.J., 1989. Reduction of acid generation in mine tailings through the use of moisture-retaining cover layers as oxygen barriers. *Canadian Geotechnical Journal*, 26:1-8.

Oster, J.D., 1982. Gypsum usage in irrigated agriculture: a review. Fertillizer Research, 3:73-79.

Pantelis, G., Ritchie, A.I.M, 1991. Macroscopic transport mechanisms as a rate-limiting factor in dump leaching of pyritic ores. *Applied Mathematical Modelling*, 1991, 15:136-143.

Papendick, R.I., Runkles, J.R., 1965. Transient-state oxygen diffusion in soil: I. The case when rate of oxygen consumption is constant. *Soil Science* 100:4, 251-261.

Pearson, G.A., Bernstein, L., 1958. Influence of exchangeable sodium on yield and chemical composition of plants: II. Wheat, barley, oats, rice, tall fescure, and tall wheategrass. *Soil Science*, 86:254-261.

Pratt, P.F., Whitig, L.D., Grover, B.L., 1962. Effect of pH on the sodium-calcium exchange equilibria in soils. Soil Science Society Proceedings, 227-230.

Pugh, C.E., Hossner, L.R., Dixon, J.B., 1984. Oxidation rate of iron sulfides as affected by surface area, morphology, oxygen concentration, and autrophic bacteria. *Soil Science*, 137:5, 309-314.

Pye, K and Miller, J.A., 1990. Chemical and biochemical weathering of pyritic mudrocks in a shale embankment. *Journal of Engineering Geology*, 23:365-381.

Quadir, M., Qureshi, R.H., Ahmad, N., 1996. Reclamation of a saline-sodic soil by gypsum and *Leptochloa fusca*. *Geoderma*, 74:207-217.

Reardon, E.J., Allison, G.B., and Fritz, P., 1979. Seasonal chemical and isotopic variations of soil CO_2 at Trout Creek, Ontario. *Journal of Hydrology* 43, 355-371.

Reardon, E.J., Moddle, P.M., 1985. Gas diffusion coefficient measurements on uranium mill tailings: Implications to cover layer design. *Geoderma* 2, 111-131.

Regier, H.F., 1973. Oil sand overburden characterization within the mine area of Syncrude lease no. 17 for reclamation of spent oil sand. M.Sc. Thesis, Department of Soil Science, University of Alberta.

Revesz, K., Coplen, T.B., Baedecker, M.J., Glynn, P.D., 1995. Methane production and consumption monitored by stable H and C isotope ratios at a crude oil spill site, Bemidiji, Minnesota. *Applied Geochemistry*, 10:505-516.

Rhoades, J.D., 1996. Salinity: Electrical conductivity and total dissolved solids *in* Methods of Soil Analysis Part 3: Chemical Methods, Bartels, J.M., Bigham, J.M., eds. Soil Science Society of America, USA, pp 417-436.

Roberts, J.A., Daniels, W.L., Bell, J.C., Burger, J.A., 1988. Early stages of mine soil genesis in a southwest Virginia spoil lithosequence. *Soil Science Society of America Journal*, 52:716-723.

Schoell, M., 1980. The hydrogen and carbon composition of methane from natural gases of various origins. *Geochimica et Cosmochimica Acta*, 44:649-661.

Shainberg, J., Letey, J., 1984. Response of soils to sodic and saline conditions. *Hilgardia*, 52:2, 1-55.

Singer, P.C. and Stumm, W, 1970. Acidic mine drainage: the rate determining step. *Science*, 167:1121-1123.

Smith, B.N. and Epstein, S., 1971. Two categories of $^{13}C/^{12}C$ ratios for higher plants. *Plant Physiology*, 47:380-384.

Speck, P.J.H.R., de Graff, J.W.M., Nieuwenhuis, J.D., Zijlstra, J.J.P., 1998. Optimizing the process of sulphuric acid injection into limestones. *Journal of Geochemical Exploration,* 62:331-335.

Sparks, D.R., 1995. Environmental Soil Chemistry. Academic Press, San Diego, USA.

Sposito, G., Mattigod, S.V., 1979. Ideal behaviour in Na+ trace metal cation exchange on camp berteau montmorillonite. *Clays and Clay Minerals* 27:2, 125-128

Steffen, Robertson, Kirsten, 1989. Draft Acid Rock Drainage Technical Guide, vol 1. British Columbia acid mine drainage task force report.

Stott, D.F., Aitken, J.D., 1993. Interior platform, western basins and eastern cordillera; geological exploration of the interior plains. In Sedimentary Cover of the Craton in Canada, pages 15-30. Geological Survey of Canada, Ottawa, ON, 1993.

Sposito, G., Mattigod, S.V., 1977. On the chemical foundation of the sodium absorption ratio. *Soil Science Society of America Journal*, 41:2, 323-329.

Taylor, B.E, Wheeler, M.C., Nordstrom, D.K., 1984. Stable isotope geochemistry of acid mine drainage: experimental oxidation of pyrite. *Geochimica et Cosmochimica Acta*, 48:2662-2678.

Syncrude WWW document, Oil Sands: Who we are and why we are here. URL: http://www.syncrude.com/who_we_are/01_02.html

Syncrude 2001 annual report. www document. URL: http://www.syncrude.com

Trumbore, S.E., Davidson, E.A., de Camargo P.B., Nepstad D.C. and Martineli L. A., 1995. Belowground cycling of carbon in forests and pastures of Eastern Amazonia. *Global Biogeochemical Cycles* 9 (4), 515-528.

U.S. Salinity Laboratory Staff, 1954. Diagnosis and Improvement of Saline and Alkali Soils. Agriculture handbook no. 60, United States Department of Agriculture, Washington D.C..

Van Stempvoort, D.R., Hendry, M.J., Schoenau, J.J., Krouse, H.R., 1994. Sources and dynamics of sulphur in weathered till, western glaciated plains of North America. *Chemical Geology* 111:35-56.

Wallace, A., Wallace, G.A., 1992. Factors influencing the oxidation of pyrite in soil. *Journal of Plant Nutrition*, 15:1579-1587.

Wallick E.I., 1983. Gas composition in the unsaturated zone as an index of geochemical equilibrium in reclaimed landscapes. In Assessment of Reclamation Potential and Hydrologic Impact of Large-Scale Surface Mining of Coal in Plains Areas of Alberta: Summary Report of Activities 1982-1983. Vol. Appendix H. Alberta Chapter C.L.R.A., Reclamation Conference, 24-25, February, 1983.

Whiticar, M.J., Faber, E., Schoell, M., 1986a. Biogenic methane formation in marine and freshwater environments: CO2 reduction vs. acetate fermentation – isotopic evidence. *Geochimica et Cosmochimica Acta*, 50:693-709.

Whiticar, M.J., Faber, E., 1986. Methane oxidation in sediment and water column environments – isotopic evidence. *Organic Geochemistry*, 10:759-768.

Wilken, R.T., Barnes, H.L., Brantley, S.L., 1996. The size distribution of framboidal pyrite in modern sediments: An indicator of redox conditions. *Geochimica et Cosmochimica Acta*, 60: 3897-3912.

Wilken, R.T., Barnes, H.L., 1997. Formation processes of framboidal pyrite. *Geochimica et Cosmochimica Acta,* 61:323-339.

Whiticar, M.J., Faber, E. and Schoell, M., 1986. Biogenic methane production in marine and freshwater environments: CO2 reduction vs. acetate fermentation – isotopic evidence. *Geochimica et Cosmochimica Acta*, 50:693-709.

Winfrey, M.R. and Ward, D.M., 1983. Substrates for sulphate reduction and methane production in intertidal sediments. *Applied and Environmental Microbiology*, 45:1, 193-199.

Wolt, Jeffery D., 1994. Soil Solution Chemistry. John Wiley and Sons Inc., New York, U.S.A.

Wood, B.D., Keller, K.C., and Johnstone, D.L., 1993. In situ measurement of microbial activity and controls on microbial CO2 production in the unsaturated zone. *Water Resources Reasearch* 29 (3), 647-659.

Wood, W.W. and Petraitis, M.J., 1984. Origin and Distribution of Carbon Dioxide in the Unsaturated Zone of the Southern High Plains of Texas. *Water Resources Research* 20:9, 1193-1208.

Wrightman, D.M. and Pemberton, S.G., 1997. The lower Cretaceous (Aptian) McMurray Formation: An overview of the Fort McMurray area, northeastern Alberta, *in* Petroleum Geology of the Cretaceous Manville Group, Western Canada. Pemberton, S.G and James, D.P., eds., Canadian Society of Petroleum Geologists, Calgary, AB, 1997.